La collana della Scuola di Alta Formazione Dottorale accoglie le migliori tesi di dottorato dell'Università degli Studi di Bergamo, insignite della dignità di stampa e sottoposte a procedura di *blind peer review*.

The equilibrium of self-balanced masonry shells during their construction is the focus of this research. Investigation of historical self-balanced technologies, i.e., based on techniques that allow building shells without supports, is the foundation of the study. A two-step approach to assess the equilibrium of masonry structures during their construction is derived. This considers the essential building factors and can be applied to different self-supporting technologies. Amongst all the historical technologies studied, the cross-herringbone technique has been closely investigated. The two-step approach formulated is now implemented to assess the self-balanced state of two case studies that were built adopting this technology.

Vittorio Paris is a Researcher at the School of Engineering and Applied Science, University of Bergamo. He is also a member of the Form Finding Lab at Princeton University. In 2019, he earned his PhD with a thesis titled: 'On the equilibrium of self-balanced shells under construction – Crossherringbone technology', at the Doctorate School of Engineering and Applied Science of the University of Bergamo. His research involves various aspects of masonry structures in the context of limit analyses and discrete element modelling (DEM), but his main focus is on the Herringbone technology, widely used in the Renaissance to build self-balanced domes, now a lost knowledge.

ISBN: 978-88-97413-52-3
DOI: 10.6092/978-88-97413-52-3

Vittorio Paris

EQUILIBRIUM OF SELF-BALANCED SHELLS

33

Collana della Scuola di Alta Formazione Dottorale
- 33 -

Vittorio Paris

EQUILIBRIUM OF SELF-BALANCED SHELLS
Cross-herringbone technology

UNIVERSITÀ DEGLI STUDI DI BERGAMO

2021

Collana della Scuola di Alta Formazione Dottorale

Diretta da Paolo Cesaretti

Ogni volume è sottoposto a *blind peer review*.

ISSN: 2611-9927

Sito web: https://aisberg.unibg.it/handle/10446/130100

Vittorio Paris

EQUILIBRIUM OF SELF-BALANCED SHELLS
Cross-herringbone technology

Università degli Studi di Bergamo

2021

Equilibrium of self-balanced shells. Cross-herringbone technology
/ Vittorio Paris. – Bergamo :
Università degli Studi di Bergamo, 2021.
(Collana della Scuola di Alta Formazione Dottorale; 33)

ISBN: 978-88-97413-52-3
DOI: 10.6092/978-88-97413-52-3

Progetto grafico: Servizi Editoriali – Università degli Studi di Bergamo
© 2018 Università degli Studi di Bergamo
via Salvecchio, 19
24129 Bergamo
Cod. Fiscale 80004350163
P. IVA 01612800167

https://aisberg.unibg.it/handle/10446/200415

Acknowledgements

This document bears witness to the progress that I made in these years of study, very intense yet exciting years, that were full of unexpected events and challenges that, to be honest, more than once, seemed like enormous obstacles. However, despite the difficulties, Prof. Attilio Pizzigoni has always wisely guided me by demonstrating his attention towards me, committing himself beyond his professorship obligations. Thank you very much for this. I would also like to thank Professor Sigrid Adriaenssens, for supporting me and helping me during my time in Princeton. I should also thank her for advising me wisely and showing great patience while we await the first set of results of this research.

I would like to say a few words of thanks for all those people who have chosen to work with passion, and I would particularly like to thank Professor Santiago Fernandez Huerta and Professor Maurizio Angelillo.

I further extend my thanks to Professor Giuseppe Ruscica, Professor Giulio Mirabella Roberti, Carlo Olivieri, Isabella Elia, and Diego Pezzoli.

I want to thank Itasca C.G. who granted free use of the 3DEC software under the Education Partnership Program, fundamental for the analyses performed, and thanks also to Rhima Gazal for its availability in tutoring me. I desire express my gratitude to Monsignor Vittorio Lanzani, Mr. Carlo Colonna and to all archivists of the Fabbrica di San Pietro for having allowed access to the marvelous domes of the San Peter Catedral.

I do not want to forget Nicola and Nandini for the endless discussions (at all hours of the day and night) which have certainly provided a fundamental contribution to writing and editing the document presented here.

Thank you to those who despite not understanding anything about my research, listened to me. Among them I am particularly grateful to Mattia Agazzi and all the guys at FabLab Bergamo.

Foreword

A starry sky

The theoretical history of architecture defines the relationship between the disciplines of architecture and engineering based on the Vitruvian triad: firmitas, utilitas, venustas (stability, utility, beauty). It is a definition that recognises the disciplinary complexity of each, maintaining the rule of diversity that runs between engineering, construction, and architecture. Beyond this aporia is the constructive imagination which rather links in a conscious cognitive process, the twin disciplines of design: engineering and architecture. All of these are indeed based on an analogous act of knowledge, on a common thought generator of form, whether structural, functional or symbolic.

The marvel begins with the gesture of a man who lays one stone atop another. It is an elementary act that transforms the amorphous and inert material into a sign of life, that produces a simulacrum animated by the tensions between opposing forces and composes them in their equilibrium. This active human presence, the force makes of all this a cognitive process, in a sense a game, is poetic, *poiesis*, the art of doing. Paul Valery speaks of the same when, in dialogues with Eupalinos. He tells about how Amphion built the walls of Thebes by moving stones using the power of music.

There is no grander gesture than to raise a monolith in front of the Ocean. It however is known to serves no purpose, but one cannot deny the social and imaginative impact of this extended efforts.

Nothing is more moving than reading the lightness of the heavens in stone, in an absolute and simple form such as that of the Florentine Cupola, which one would almost imagine to be of unknown author. As if it had been created by the automa of Heron, or held up by nothing at all as in the Stereotomies of Philibert De L'Orme.

An ancient narrative that tells of stones finding their equilibrium in the wonder of reason: from Brunelleschi's dome to the mechanical arms of modern-day robotics where technology is performative of space and its social use.

It is in the continuity of the eternal dialectic of the creative practise that our current research takes place, to fix that mirroring between modern and ancient of which Heidegger speaks: "the grand tradition advances towards us as the future".

With these studies we aim to approach moments in history when the sole form of technology available to man was the abstract rationality of geometry. Much of modern science, in an effort to reach ever more efficient production goals, has abandoned those ancient paths. All this done in the name of an experimental truth built on theoretical models that have yielded great results such as the mechanical theories of elasticity and of plasticity. That geometrical theory which until the dawn of modern times served as the foundation of all mechanical science today seems distant and rightly surpassed as a tool

of the past. But the past is also constituted by what is still present, for our eyes to examine as proof of what has “already been”. Thus, it possesses a potential that cannot be ignored. The presence of the future and that of the past are hence co-located within the same polarity, inside which true innovation may develop: the creative architectural kind as well as the art of building for need. What we as designers, architects and builders can learn from the past is the knowledge of a structural equilibrium of form based on the geometry of materials and of their reciprocal measurements in three-dimensional space which we call “stereotomy”. Thus, we find ourselves operating in a field that seems very far from contemporary urgencies, in a world of inelastic inelastic materials and outside of the most recent theories of plasticity. But we also find ourselves, as if by magic, in that axiomatic field that seemed to have disappeared centuries ago, and that we now see reappearing, driven by the strength of the analytical minds of the great contemporary scientists like Jacques Heyman. New possibilities open, both in the use of more sustainable building materials like brick and earth, as well as more sophisticated and suggestive options like ceramics and glass. It is a search for balance not just of forces but also of forms. A research that includes themes and concepts from “stereotomy” and from static graphics, from that science that still lives, and has archetypal models that are at once structural paradigms and architectonic prototypes, physical ideas and conceptual visions and their composites at the heart of its fundamental conception

This is why it is so convincing to start once more from the “herringbone” so much loved by Brunelleschi and perfected by Sangallo, or by the Leonardian “plate-bande” that was already in use in the temples of the Egyptian pharoahs, or the “plate-vault” that was the totalising experience of Philibert De l’Orme and then of all of the great French architects of the post-renaissance centuries including masters such as Mansard, Blondel, Bullet, Rondelet and Sufflot.

Perhaps the most intriguing aspect of studies such as these undertaken in V. Paris’ PhD thesis is in fact that rethinking of a future dimension determined by building techniques abandoned by mechanical science. Today we see the renewed need to study the behaviour of structural elements simply compressed, rigid, able to self-balance due to their own geometry and to reciprocal adherence. These new structural issues emerge from building procedures prospected in a world where construction practices seem to require more and more automation via robotic arms which, by nature, can only be operated in conditions of continuity in form and at equilibrium, and above all during the intermediate phases of the construction process.

Attilio Pizzigoni

Dedication

To my family. To my mother Silvana and my father Ferruccio. To my brother Cristian. I thank you all for your love.

Table of contents

Introduction

In this dissertation, an approach to evaluate the self-balanced state of masonry shells during the construction phase is proposed. The approach illustrated in the following chapters has been implemented to assess the equilibrium of domes built with the use of the cross-herringbone spiralling technique. The dissertation proposes an approach to evaluate the state of masonry shells during their construction. The approach illustrated here aims at assessing the equilibrium of the domes that are built with the use of the cross-herringbone spiralling technique.

Design and technology

In recent decades, masonry shells have been the subject of considerable studies. In particular, the development of computational technologies and digital fabrication tools, have influenced the direction of research in this field. A witness to this development is the Armadillo Vault pavilion project [1], where the extreme geometry has been designed using a digital Graphic Static software, and has been fabricated through the aid of computer numerical control tools. Even from the perspective of the structural behaviour, it can be said that considerable progress has been made. The formulation of plastic theory for masonry structures [2] formed the basis for this thriving research [3] [4] [5] in the last fifty years. According to this theory, the geometry of a masonry structure is a crucial factor for assuring its equilibrium, and from the simple study of this geometry, it is possible to determine the state of the masonry structure.

This relation, was well known by the Byzantine builders, they believed that the stability, geometry were the two of three fundamental elements deeply connected for understanding the masonry structures [6] [7]. The third fundamental element is the construction factor [6] [7], in sense of the technology point of view, and as shown through this document, this factor can influence the geometry and the stability as well. Despite that, much of the research developed over the last decades points to the development of advanced construction systems [8] [9] that does not necessarily consider this relation.

Nevertheless, the new digital fabrication technologies and the use of robotic systems (such as robotic arms, drones, etc.) can with no doubt open new possibilities re-inventing and re-discovering historical or new building techniques. In this direction must also be considered the reduce the costs of construction of masonry structures [10], particularly with reference to the relative costs of fabrication and formwork. Again, the questions that researchers encounter in the context of productivity and

economic efficiency of curved spatial structures are not new, and they highlight the connection among stability, geometry, and construction.

Nevertheless, limited research is dedicated to defining an approach for evaluating the equilibrium of these structures under construction. This evaluation is now going to be the focus of the current research.

Statement of the problem

The economic factor in terms of productivity is the main issue faced in the construction field [11]. Starting from the study of existing and historical techniques, the development of efficient and sustainable construction technologies should be one of the main scopes of current day research in the field of masonry structures. To achieve this goal, a theory to evaluate the state of equilibrium of structures during their construction must be developed. Specifically applied for masonry buildings, the developed approach must be able to consider the peculiarity of masonry mechanical behaviours.

Outline of chapters

The research outlined in this document is organized broadly into three parts. In **Part I** there are chapter 1. and chapter 2., that give an overview of the principal historical self-balanced technologies and an introduction to the theory and methods adopted for assessing the equilibrium of masonry structures.

Part II constitutes chapters 3., 4. and 5., with chapters 3. describing the characteristics of the cross-herringbone spiralling pattern a self-supporting technology developed by the Sangallo architects. The two step approach for evaluating masonry structures during their construction is illustrated in chapter 4., meanwhile, an exhaustive formulation on how the two step approach can be applied to evaluate the equilibrium of a dome is describe in chapter 5. The conclusions are illustrated in **Part III,** constituted by chapter 6. At the end three appendixes are reported.

Three appendixes follow the conclusions: Appendix A reports a list of domes, where the herringbone or cross-herringbone spiralling technology may have been used. Appendix B and Appendix C, provide the results of limit state analysis, and the results of discrete element method conducted. The analysis conducted are relative to the two masonry domes built using the cross-herringbone spiralling pattern, introduced, and detailed out in chapter 5.

Part I: State of the Art

1. Self-balanced vaulting technologies

Arches, vaults, and domes are surely among of the most significant expressions of civilisation. These structural systems have numerous applications, varying from providing shelter, defining a space, and in the creation of monuments. These structures can define architectural forms and at the same time can resist loads efficiently [12]. However, for their construction, they require a significant investment in terms of resources in the form of centering or formwork, and this can take up to around 20-30% of the entire project cost [13] [14].

Every culture has sought building methods and techniques primarily based on the principles of efficiency. In this process, they have also explored technologies that allow to build arches, vaults, and domes without the need for any formwork or shoring. As a witness to this, several efficient technologies have been developed throughout history [15] [16]. Unfortunately, over the last centuries, most of this traditional knowledge has been lost.

The literature refers to these efficient vaulting technologies, through the adoption of various terms: self-centering [17], self-supporting [18] or self-balancing [19]. Self-supporting and self-centering are terms related to the construction aspect but with a slight difference in their meanings: not all self-supporting technologies are self-centering; but all self-centering technologies are self-supporting. The self-supporting techniques do not require the use of formwork, and in the self-centering ones, even the use of centering is not needed. The term self-balancing, on the contrary, is related to the static aspects. Self-balancing indicates the ability of a structure to find a balanced state without any support during all its construction phases. Therefore, in this document, the author refers to the following terms: self-supporting, self-centering or self-balancing, depending on the aspect analysed: construction or structural.

This chapter is dedicated solely to the description of the most relevant historical self-supporting and self-centering technologies: the Pitched vaulting technique in chapter 1.1, the Clay tube vaulting technique is described in chapter 1.2, the Tile vaulting technique in chapter 1.3, and the herringbone vaulting technique is presented in chapter 1.4. A wider literature on various other self-supporting or self-centering technologies is available; nevertheless, the current research does not include all of them. An example of such other technologies is the armchair voussoirs technique [20] [21] applied in the Roman Empire to build self-supporting structures, or the nuraghe vaulting technique [22].

The chosen technologies are representative of all self-supporting techniques; for each technique, a historical and critical overview is presented, highlighting its main characteristics and the construction principles behind.

1.1 Pitched vault

1.1.1 Notes on the history of pitched vault

The pitched vaulting technique, also called the "Nubian" technique, is the first or among the first self-centering methods that was developed. The origin of this technology dates back to the same period of the origin of the arch, with evidence of its existence from as early as the 21st century BCE [23] [24] [25]. The pitched vaulting technique is still in use in a few parts of North Africa or Asia [26].

Traces of these kinds of structures can be found on three continents: Asia (Middle East), North Africa and Europe, which suggests that this construction technology spread through the Mediterranean Sea and the cultures surrounding it [7] [16] [20] [27]. Several sources document the use of the pitched vaulting technique: such as domes at Taq-I Kisra (Sassanid Empire, around the 6th century, ancient city of Ctesiphon, Iraq) [16] or the Byzantine domes [28] of the apse hall of the Palace of Byzantine Emperors (Byzantine Empire, ancient Constantinople in modern Istanbul) [7], or also by historical documents such as the A. Choisy's treatise [6].

1.1.2 Principles of pitched vaulting technique

To understand how the pitched vaulting technique allows building a structure without centering, it is essential to first visualize a barrel vault under construction. Traditionally to build this kind of vault, the bricks are laid as shown in figure 1 a), thus, it is essential the use of auxiliary structures to prevent sliding. A peculiar pattern characterizes the barrel vaults built with the pitched vaulting technique, figure 1 a): the bricks are laid radially to form arches placed in inclined planes, and laid one next to another with the new arch resting over the previous one [29].

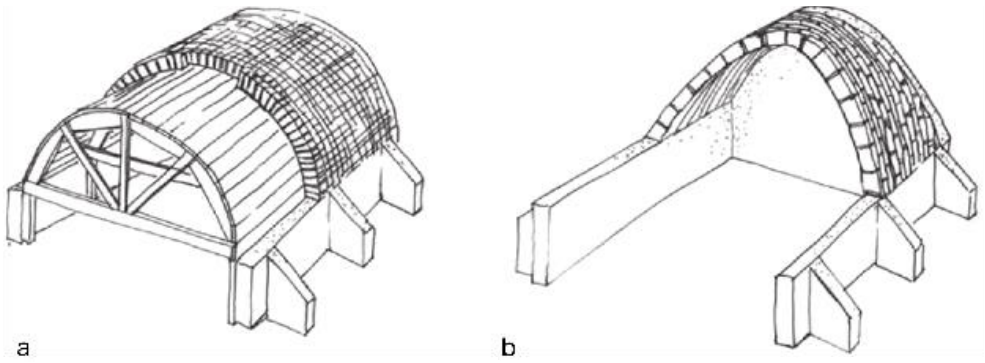

Figure 1: Barrel vault and pitched vault under construction. Drawing by J. F. D. Dahmen [16].

Referring to figure 2, it is possible to visualize the initial stages of the construction method: the first arch is placed against a boundary wall, which has a crucial role in supporting the barrel vault during its construction. The first bricks are laid inclined to push against the wall. Once the first arch is complete, the next one can be laid. Following this construction sequence, the new brick course is

placed over the previous one, allowing each brick to interact with the previous arch. These contacts prevent the slippage of bricks during the construction.

Figure 2: Pitched vault under construction. Photography by Adobe alliance.

As mentioned, the arches formed in this system are not laid in vertical planes and they can display different inclinations; some examples of the variations are shown in figure 3 [7] [27]. Similar to the laying plane, the shape of arches is not uniquely defined, but past research, studies, and evidences from archaeological remains testify that the main geometry adopted is parabolic arch [20] [30].

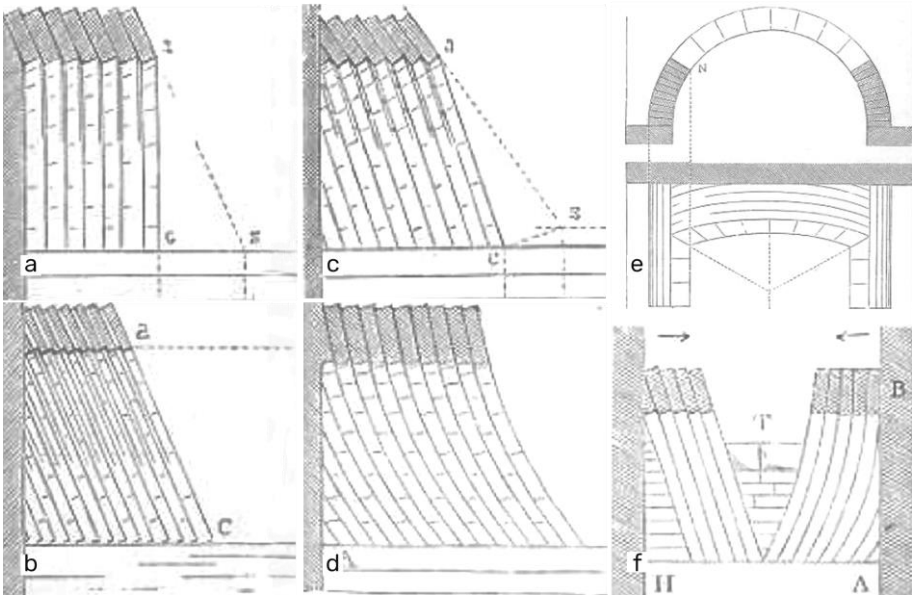

Figure 3: Pitched vaulting technique, different schemes to lay the bricks. a), b), c) and d) are a lateral view of barrel vaults each one shows a different scheme and inclination of arch. e) and f) represent a combined method [6]. Drawing of A. Choisy.

During construction, once the first arch is completed, the geometry of all the subsequent arches is defined, thus no tracing tools are required (even tools such as a light centering). The equilibrium of the pitched vault is guided by the arch's stability and by the stability of the supporting wall; both of these depend essentially on their geometries [2].

1.1.3 Geometries of the pitched vault

Certainly, the geometry most suitable for pitched vault self-centering technology is the barrel vault, due to its similarity to the shape of the arch. However, it can be applied to build domes with different geometries such as hemispherical domes, cross vaults, dominical vaults and many other complex shells [27]. To build such structures, it is necessary to design the orientation of mortar joints, see figure 4.

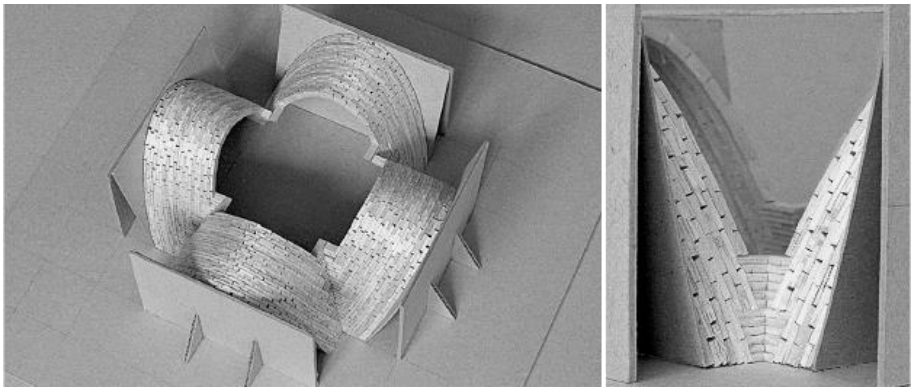

Figure 4: Pitched vaulting technique. Scaled model of cross vault under construction: different orientation pattern [27] [31]. Photography by D. Wendland.

1.2 Clay tubes vault

1.2.1 Notes on the history of Clay tube vault

Several building technologies flourished during the Roman Empire, and among them there is the clay tube vaulting technique which origins can be traced back to the 4th century BCE [32] [33]. Over the next centuries this technique was applied primarily in the African Proconsularis (Tunisia, Libya, Algeria and Morocco) and then through the European continent, especially in Italy, France, Spain and Britain [20] [24] [33]. Even after the fall of the Roman Empire, this technique was used until the 7th century CE by civilizations in North Africa, such as the Vandals, the Byzantines and the Arabs [34]. Nowadays, these tubes vaults and domes are used as a low-cost alternative in India [20].

The first application for this technology can be associated with a pre-existing building technique used for clay kilns [35], originally as a shelter for covered grain storage spaces, where the fireproof properties of clay protected the supply from fire-related dangers [20].

1.2.2 Principles of Clay tube vaulting technique

Several archaeological campaigns dedicated to trace the origin of the clay tube technique [33] [24] reveal different shapes and sizes of the clay tubes. In fact, it was observed that until the 2nd century CE the shape of the clay tubes changed constantly, and the technique underwent numerous refinements and variations. These construction elements unearthed are hollow clay cylinders with a

small nozzle. Their sizes varied with the period and the context in which they were manufactured. Broadly estimating, they have a length of less than 20 cm and a diameter between 6-10 cm [20].

The shape and size seem to be a product of fine research: the smaller dimensions of the clay tubes guarantee lightness, allowing the mason to place them easily. The shape allows the tubes to be stacked, in a manner that the nozzle is inserted within the hollow end of the next tube. During construction, gypsum mortar is placed between the two interacting parts: the nozzle of the first one and the inner surface of the second one [34], allowing it to be partially filled before inserting it into the previous one.

Unlike the pitched vaulting technique, see chapter 1.1, in the clay tube vaulting technique, as shown in figure 5, the arches are oriented in vertical planes and do not push against any retaining wall or structural support [32].

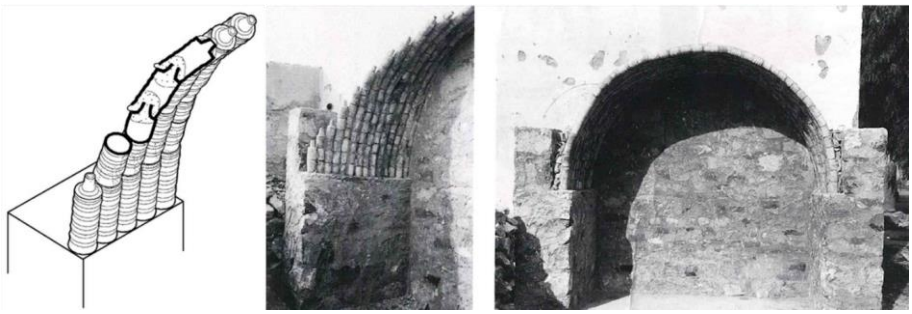

Figure 5: Tube vaulting technique, (left detail) under construction, the clay tubes and gypsum mortar Drawing of L. C. Lancaster [20]. Reconstruction of a barrel vault (center and right), Chemtou (Tunisia) [34].

The use of gypsum-based mortar and the tube's stereotomy do not make the construction sequence fundamental: unlike the pitched vault, here it is not necessary to complete the previous arch before being able to proceed with the subsequent one. Therefore, this process of constructing the tubes vaults allows creating self-supporting structures without the use of centering.

1.2.3 Geometries of clay tube vault

The tube vaulting technique allows building even complex geometries, such as hemispherical domes, cross vaults, pavilion domes, squinch domes, etc. For building these, the study of the orientation pattern of tubes is needed. Figure 6 presents few examples where it is interesting to observe the cases with various orientation patterns that can be permitted in revolution geometries. [34].

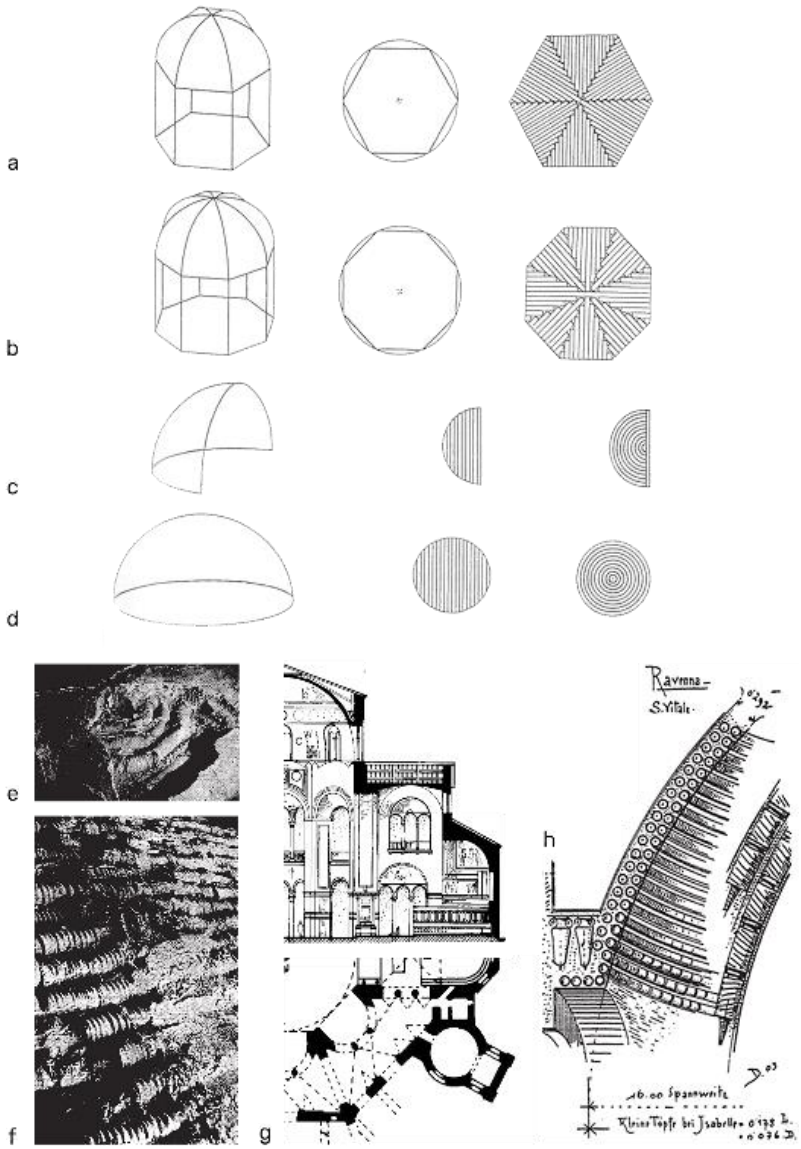

Figure 6: a), b), c), d) orientation pattern of clay tubes. For cases c) and d) two different patterns can be adopted [34]. e), f), g), h) San Vitale Basilica (Ravenna, Italy). e) and f) are details of the dome, which was built with the tube vaulting technique. e) Detail near the crown, the tubes are laid to form rings. f) Detail near the base of the dome, as well as e) the tubes form rings [36] [37]. g) Section and plan view of San Vitale in Ravenna. h) Detail of a section of San Vitale dome, the horizontal orientation of the tubes [38].

1.3 Tiling vault

1.3.1 Notes on the history of tile vault

Tile vaulting is a popular self-supporting technology that was developed in Spain around 13-14th CE [39]. This technology is based on the use of fast setting mortars and light tiles.

Although extensive literature on the tile vaulting technique reports its evolution and application [40] [41], the origin of this technology is not clear. It is reasonable to think that the encounter between Islamic and Romanesque cultures has favoured the birth of this construction system. This interaction

that took place in the Spanish peninsula, where, the scarcity of wood along with the wide use of tiles and gypsum in construction [41], overlapped with the advanced building knowledge of Byzantine and Islamic builders [15], must have fostered the perfect environment to develop the tile vaulting technique.

A report of the complete historiography and evolution of the historical self-supporting techniques is not the purpose of the current study [41], although it is fundamental to list the milestones in its evolution. In the case of the tile vaulting technique, these milestones are broadly related to the aspects of efficiency and strength of the vaults. In fact, the early known applications were recorded between the 12th-13th century, where tile vaulting technique was applied for the construction of secondary structures such as stairs [39] or for filling space between ribs vaults [42] (span: 1.3 -1.5 m). In the following centuries, the knowledge of this construction method grew, leading to a widespread application for building domes and vaults without any support. Along the 16th century, the method was systematically applied along the Spanish eastern coast [15], especially in the area of Catalonia, Valencia and Extremadura. During the 19th and by the beginning of the 20th century, architects like Guastavino played a significant role in taking this technique to America [43]. Here, tile vaulting technique was a widely adopted self-supporting system [44], allowing the construction of vaults with larger spans, of about 15 m. This construction method was learnt and applied in the 18th century Europe, not only within Spain, but also in regions of Italy [15] and France [45]. In the current day, this technique is primarily used in the context of developing countries [26] [46].

1.3.2 Principles of tile vaulting technique

To build a tile vault, it is essential to use material with defined characteristics and to follow a precise construction sequence [47]. The first operation needed, as shown in figure 7 a) [48], is to place a light centering, which is necessary only for tracing the form of the structure.

Following this, thin tiles with a thickness less than 4 cm are laid according to a designed construction sequence, for example, figure 7 b). Generally, tile vaults are composed of 2-3 layers of tiles, which are laid using two different types of mortar. The inner shell is placed by using gypsum mortar (plaster of Paris) or fast-setting cements. This then supports the following layers and acts as a formwork during the construction process. The other two tile layers can be laid with any kind of mortar because they are already supported [50]. To avoid any overlap in the joints, the orientation of the tiles must be changed between layers. This is typically done by rotating the layer by 45° with respect to its adjacent ones. [51] figure 7 c). The use of a fast-setting mortar alone does not provide all the resources needed to prevent sliding or overturning of the structure during the construction phases.

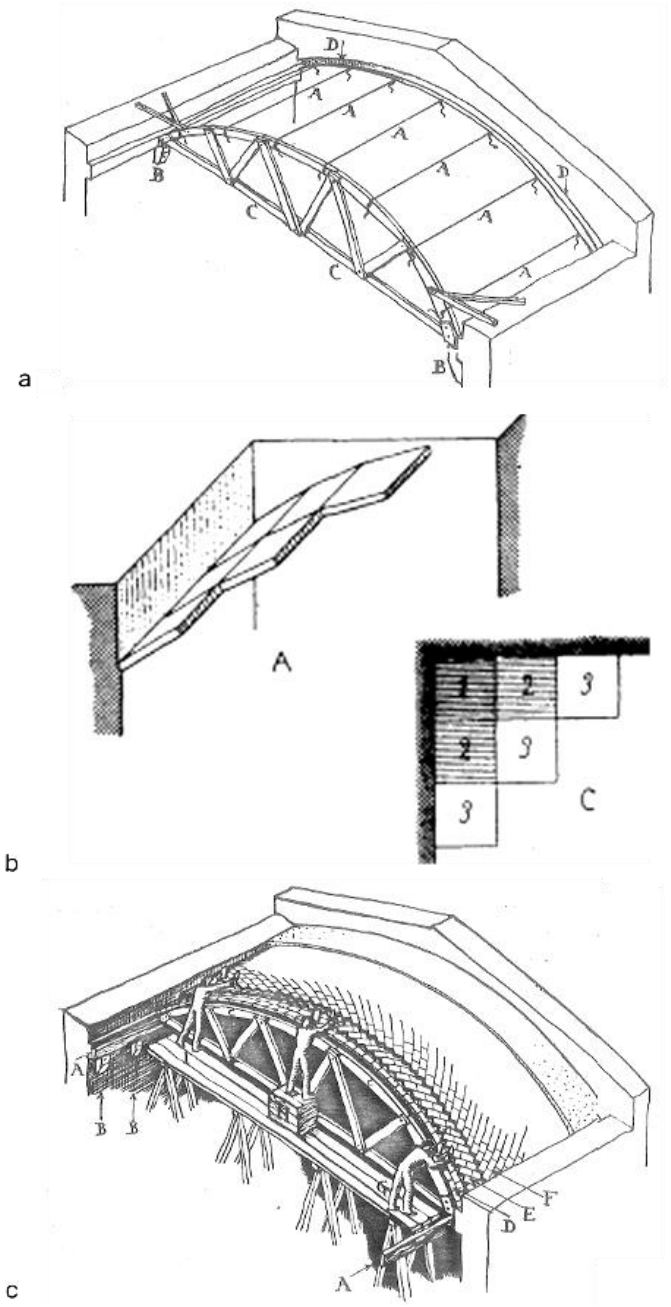

Figure 7: Tile vault under construction. a) Centering [48]. b) The construction sequence [49]. c) A portion of tile vault under construction [48]. Drawing of (from top to bottom) L. B. Moya, A.Choisy, L B. Moya.

Indeed, tile vaulting technique allows to build structures without any support only if all these factors are respected: the construction sequence, the geometrical stiffness derived from the curved geometry [27], and even the lightness and strength of the tiles and the fast-setting property of the binder [44].

1.3.3 Geometries of tile vault

The peculiar construction technique of the tile vaulting permits the construction of almost any kind of compressed shell: from staircases [44] to barrel vaults. As displayed in figure 8, contemporary projects [46] [52] explore the full potential of this technique [51].

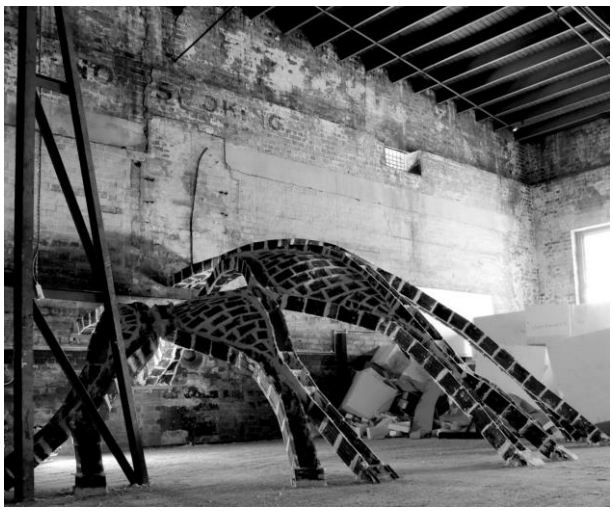

Figure 8: Complex ribbed vaults. Masterclass - Ribbed Catalan. Photography by M. Ford [52]

1.4 Herringbone vaulting technique

1.4.1 Notes on the history of Herringbone vaulting

The herringbone tile vaulting technique was used to build the dome of Santa Maria del Fiore (1418-1471) [53] [54], and, probably, for such application this secret building process has fascinated researchers for around six hundred years [55] [56] [57].

The origins of the herringbone construction technology have been obscured by the fame of the dome of Santa Maria del Fiore. It is unreasonable to think that Filippo di Ser Brunellesco Lapi (1377-1446 [58]), commonly known by the name Brunelleschi, built his masterpiece without having a full knowledge of the herringbone technology.

Some researchers also believe that this technique is derived from the Opus spicatum [59], a Roman technique, shown in figure 9 a), used to build walls, where the pattern appears to be similar to that of the Brunelleschi's herringbone.

Other researchers trace its origins to the east [60] [61] [62], and second that through the cultural contact between Florentine, Byzantine and Arab cultures, it was imported and applied. There are numerous testimonies as an evidence of this cultural interaction: the council of Florence (1055) chaired by Victor II [63] or the commercial agreements between Tuscans and Arab kingdoms [64]. Furthermore, the influence of Arab and Byzantine cultures on Florentine architecture begins at least a century before the construction of Santa Maria del Fiore's dome [64].

Even after considering all these theories, it is not easy to point out what are the exact origins of the herringbone spiralling technology, or even how Brunelleschi gathered his knowledge on this construction system.

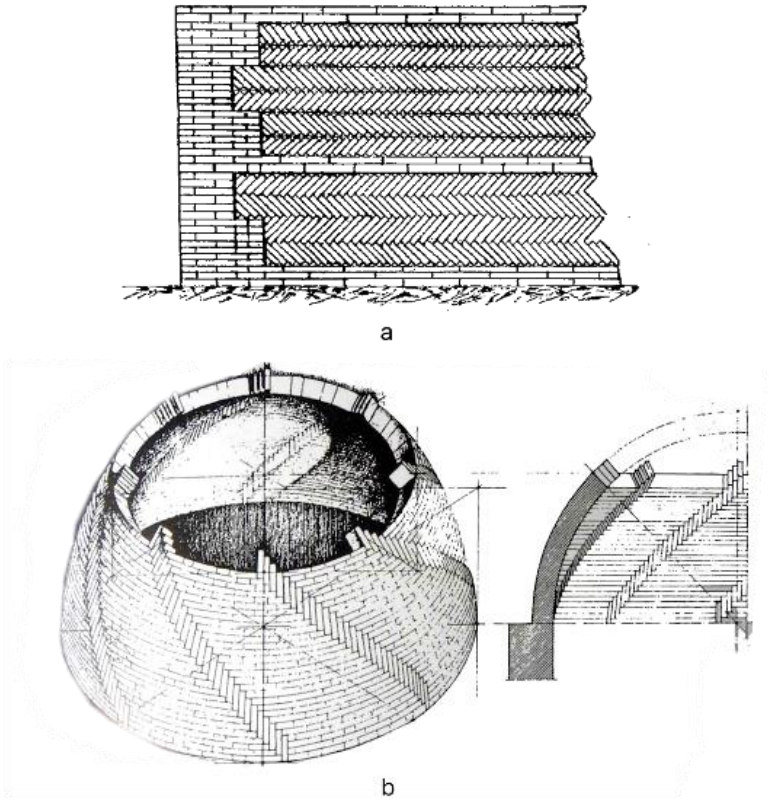

Figure 9: Herringbone spiralling pattern. a) Opus spicatum. Drawing of C. G. de Montauzan [65] b) Revolution dome and herringbone spiralling pattern, the vertical bricks are highlighted. Drawing of F. Gurrieri [66].

The first traces of the herringbone vaulting technique are related to the Venetian master masons, along the 11th century, where they used it in areas around Venice [60]. In the same period, the Seljuks applied it to build mosques [61] and figure 10 shows the dome of Northern Prayer Hall (completed in 1088) of the Isfahan Friday Mosque (Isfahan, Iran). Other Iranian structures also show the use of herringbone such as the Ardestan Friday Mosque (completed in 1158, Ardesan, Iran), displayed in figure 11. Despite that, the invention of this technology could be even much ancient as it is interwoven with the history of traditional Iranian wind towers (the Bādgir) and the traditional Iranian water cisterns (the Ab Anbar) whose origins even date back to the 1st millennia BCE, figure 12 [68]. In Italy, the herringbone spiralling technique was used systematically by Florentine Sangallo architects [62] (Appendix A) up until the second half of the 16th century. Sangallo perfected this building technology developing the cross-herringbone spiralling technique [69]. It also seems that the application of this technique ends with the Sangallo architects. However, the specific reasons why the use of this technique ceased after the 16th century, is unknown.

Figure 10: Northern Prayer Hall (completed in 1088 CE) of the Isfahan Friday Mosque (Isfahan, Iran). Photography by R. Piperno.

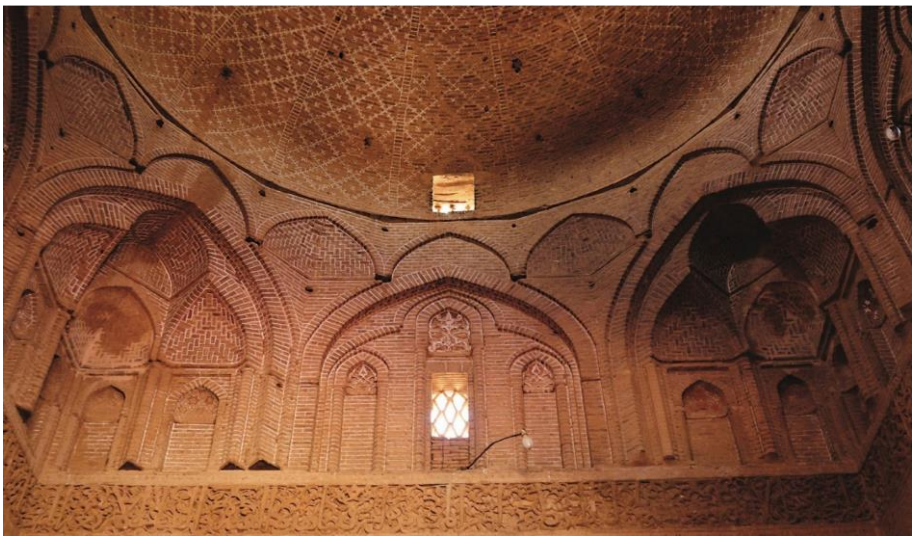

Figure 11: Ardestan Friday Mosque (completed in 1158 CE, Ardesan, Iran). Photography by Selcuklu Belediyesi [67]**.**

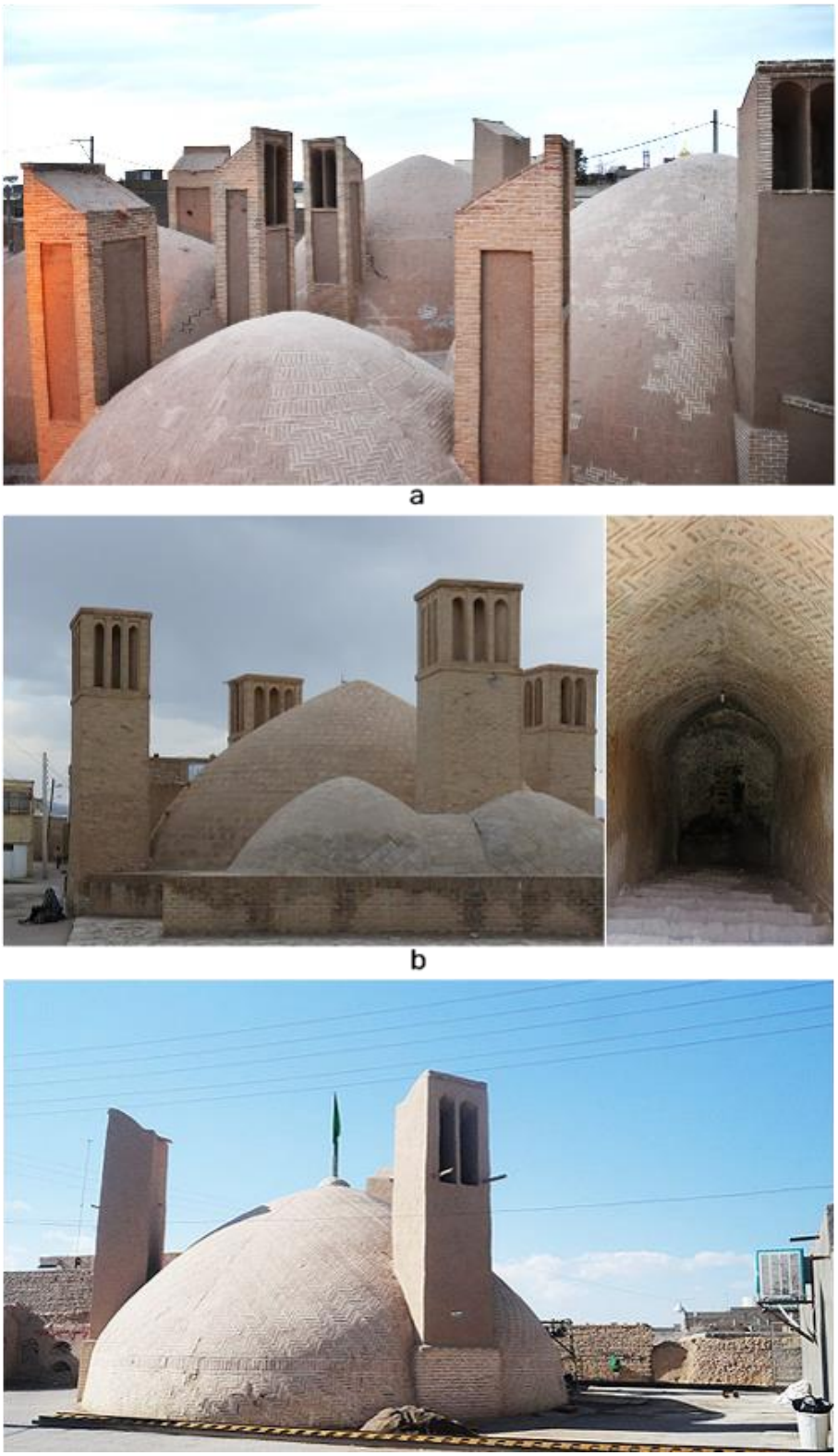

Figure 12: a) Traditional Iranian water cisterns (date unknown, Ardakan, Iran) Photography by unknown. b) water cisterns facility of Ardestan Friday Mosque (completed in 1158 CE, Ardesan, Iran). Photography by R. Piperno. c) Traditional water cisterns (date unknown, Ardakan, Iran) Photography by unknown.

1.4.2 Principles of herringbone vaulting technique

To understand how the herringbone spiralling technique allows building structures without support it is necessary to examine its typical masonry pattern: as shown in figure 9 b). The herringbone spiralling pattern consists of an arrangement of horizontal brick courses interrupted by vertical bricks, which from now on, in this document, will be referred to as herringbone bricks. The herringbone bricks are laid at regular intervals and within the same courses of the horizontal bricks.

The herringbone bricks belonging to different courses describe a peculiar curved trajectory: the loxodrome called also rhumb line [70] [71][72]. The loxodromic curves are a class of mathematical curves with the following properties: they are continuous, and they are developed on the entire surface of the structures. This geometrical continuity highlights the role of the herringbone pattern by linking the courses together.

Figure 9 b) shows an incomplete dome with a herringbone spiralling pattern, and by assuming to build using the completed course, i.e., placing bricks of a new course only when the previous one is completed, it is possible to understand how the vertical bricks tie two courses together. They belong to a closed course which is a balanced structure and stable; therefore, the vertical bricks are fixed and capable of acting as constraints for the construction of the next course. Under construction, the herringbone spiralling technique allows the formation of resistant substructures, see chapters 3.3 and 5.3.2, whose role is to prevent slippage and overturning.

1.4.3 Geometries of herringbone vault

The herringbone spiralling technique has been applied mainly to hemispherical or pavilion domes; however, as illustrated in figure 11 and 12 b) with appropriate measures, other complex geometries can also be catered to.

2. Notes on masonry mechanics

The following chapters 2.1, 2.2 and 2.3 illustrate the mechanical assumptions and the essential characteristics of the theory and tools adopted to pursue the research presented in this document.

2.1 Notes of the history on the theory of arch and vaults

The history of the structural theory of arches, vaults and domes is vast and well known, as presented by the literature [73] [74] [75]. Hence, this research, only provides a brief overview on the origins of the contemporary structural approaches. The knowledge of the of the History of approaches and theories formulated in the past is relevant to avoid repetition of errors and to critically approach the inquiry.

The earliest scientific research published on an arch is written by R. Hooke (1670). He understood the link between the geometry of the catenary and the resistance capacity of the arch, figure 13 [76]. About three decades years later, D. Gregory (1697) reached the same conclusion, with an additional condition: the sufficient condition to guarantee equilibrium.

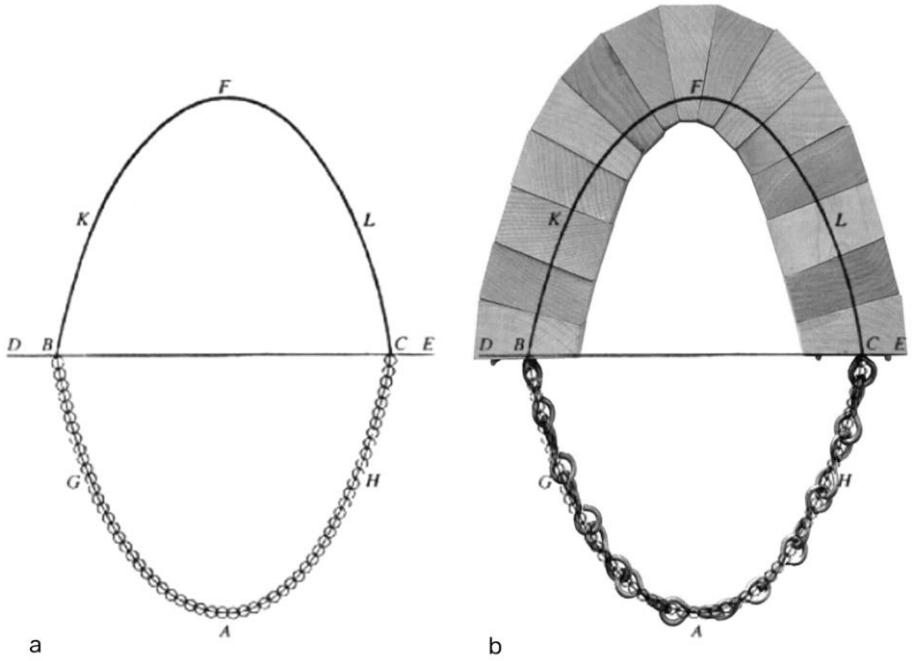

Figure 13: a) Poleni's drawing of Hooke's analogy. b) Over position of: The Catenary and The Arch by R. Pedreschi and Poleni's. Drawing of Hooke's analogy

Simultaneously in France, by pursuing the medieval tradition, initially P. de La Hire (1695) [77] [78] and then later B. F. de Belidor (1739) [79] analysed the kinematics of the arch as a system of macroblocks. Today, a similar approach is adopted through DEM [80], see chapter 2.3. In the same

century, in France itself, although with some inaccuracies and without much mathematical rigour, A. Couplet (1730) in his second memoir [81] preceded the hypotheses fundamental for what it is called today: the limit analysis [2]. From the observation of the real structures, Couplet understood that the collapse of arches commonly occurs due to the formation of a kinematic mechanism. He illustrated this through the dual nature of structural analysis: the static approach aimed at determining equilibrium and the kinematic approach, whose purpose is to analyse the possible mechanisms. Couplet's work, as well as that one of de La Hire and Belidor, was revisited and reformulated by C. A. de Coulomb (1773) [78], who introduced, the new concept of the upper and the lower limit of thrust and described the nature of crushing phenomena [76]. Only 50 years later, through the research of the T. Young (1817) [74] [82], the two approaches (static and kinematic) were connected by the introduction of the concept of the curve of pressure.

The curve of pressure is a specific curve related to an arch, through which the real state of the structure can be described. The curve of pressure is the locus of the application points of the resultant internal forces. In addition, to assessing the stability of the arch investigated, these resultants do not necessarily act orthogonal to the arch's masonry joints, but at the limit, in the hypothesis of finite friction, they must be contained within the friction cone. Furthermore, to reflect the real mechanical behaviour of masonry, i.e., really low tensile strength, the curve of pressure must be entirely contained within the arch's thickness [83]. Determining the curve of pressure was the primary subject for research in the first half of the 19th century [84] [85].

At the same time, other researchers such as: C. Navier (1826), JV Poncelet (1852), H. Bresser (1852), W. J. M. Rankine (1860), E. Winkler (1879) and A. Castigliano (1879) [74] investigated on the possible applications of the theory of elasticity for the analysis of arches and vaults. The elastic theory permitted the description of the correct curve of pressure of the ideal arch, however for analysing real structures, several coefficients needed to be approximated. According to Winkler, these coefficients called perturbations, justify the differences between the determined elastic curve and the behaviour of the real arch [86]. Due to the considerable computational complexity and the shortcoming in the developments in static-graphical tools at that time, the application of the elastic arc theory was limited [2].

In the second half of the 19th century, the development of graphic statics tools permitted this analysis on vaults and domes. In particular, as shown in figure 14, H. T. Eddy (1878) determined a method to evaluate the state of shells of revolution [87]. Despite that, the first studies for estimating the state of masonry domes date back to the 18th century by P. Bouguer (1734) [88]. These analyses assimilate the dome's behaviour as several arches placed next to another, and, in fact, A. F. Frezier (1737) introduced the Slicing Technique [89], an essential approach for estimate the vault's and dome's state,

neglecting their spatial behaviour. Later, G. Ungewitter (1892) placed a milestone with the publication of the manual for static study of vaults [90] based solely on graphic static tools.

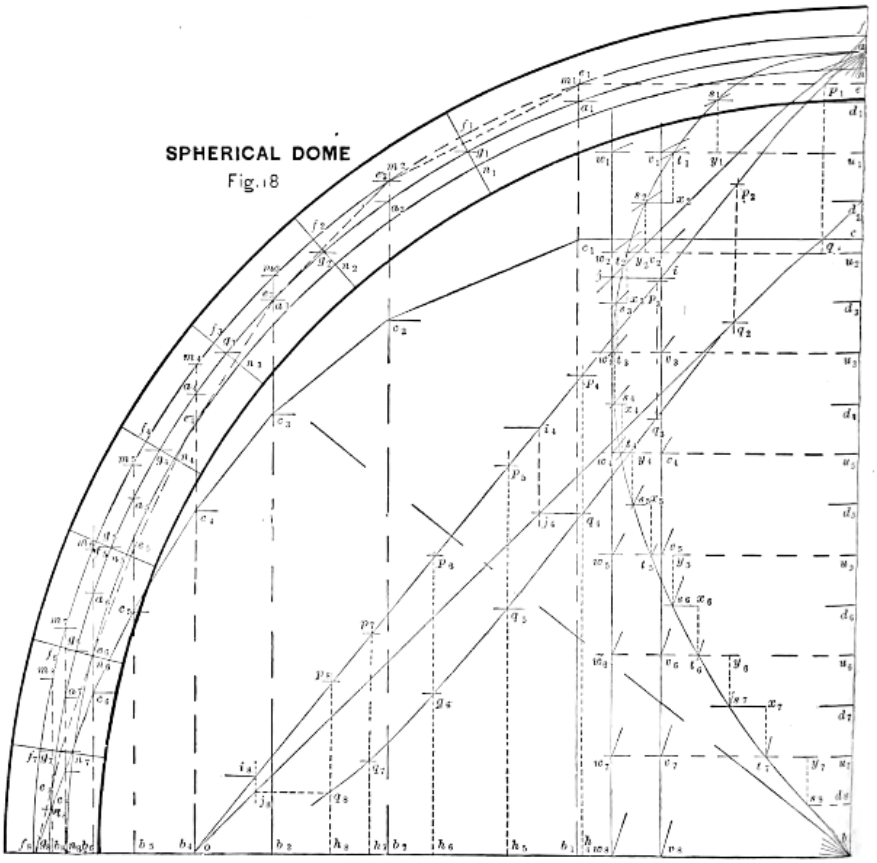

Figure 14: Eddy's method, analysis of hemispherical domes. Drawing of H.T. Eddy [87]**.**

Despite the difficulties and the inaccuracies, the theory of the elastic arch was considered the most correct until the second half of the 20th century when D.C. Drucker (1952) [91], A. Kooharian (1953) [92] and W. Prager (1959) [93], formulated the theory of plasticity and Limit Analysis for perfectly plastic solids. Following their studies, J. Heyman (1966) presented his structural theory for masonry [2]. He revisited the traditional methods of analysis of masonry constructions (Hooke, Gregory, Couplet, Coulomb) in the framework of the plastic theory [2]. Thus, through Heyman's formulations, it is possible now to apply the principle of limit analysis to masonry structures.

Today, although with some variations, the approach of the elastic theory is still predominant. This is mainly due to the development and the diffusion of Finite Element Method (FEM), and other commercial software based on the elastic approach. The commercial tools that permit the evaluation of masonry structures within the framework of limit analysis approach have not yet been developed [30] [94] [95].

Finally, during the last decade of the 20th century, some researchers adopted methods based on the discretisation of masonry structure as rigid elements [96] [97] [98]. The most widespread of these

approaches is the distinct element method (DEM), also called the discrete method, permits to evaluate masonry structures as a system of distinct blocks [99].
The analyses reported in this document (see Appendix A and B) have been executed adopting DEM and by referring to Heyman's formulation. In fact, among all approaches developed so far, DEM and Heyman's formulation are the most suitable method to evaluate the state of masonry shells under their construction.

2.2 Essential of the *Structural theory for masonry* [2]

The structural theory for masonry formulated by Heyman (1966) [2] provides a method for evaluating masonry structures within the framework of the plastic theory [100]. His formulation is based on three fundamental hypotheses:

I. Sliding failure cannot occur;
II. Masonry has no tensile strength;
III. Masonry has infinite compressive strength;

It is not a coincidence that the hypotheses mentioned were already derived by Couplet in the 18th century; they reflect the behaviour of the real masonry structures. In fact, the collapse of the arch is strictly related to the formation of a sufficient number of hinges, for a kinematic mechanism to occur. This is because, in ordinary structures global collapse mechanisms are not generated by sliding, and the compressive stresses recorded are generally one order lower compared to the strength of masonry [101] [102] [98].
For ordinary conditions and common structures, the Heyman's hypotheses **I.**, **II.** and **III.** are usually respected, thus the lower bound theorem (or static theorem) provides the condition to guarantee the equilibrium of masonry structures. Therefore, to evaluate the stability of an arch, the lower bound theorem can be expressed as follows:

> Under a given set of loads, if at least one line of thrust can be found entirely within the arch's geometry, no kinematic mechanism can exist, and this is an absolute proof that under this set of loads, the structure is stable. Indeed, in this state collapse can never occur.

This form of the lower bound theorem is called master 'safe' theorem. It provides sufficient condition to guarantee the equilibrium of an arch [2]. To trace the line of thrust, several methods can be adopted, most of them based only on the principle of equilibrium. The arch being a structure that is statically indeterminate, it is easy to understand that infinite lines of thrust that can be traced [2]. Theoretically given a set of loads, a range of balanced solutions can be determined, figure 15 reports an example

of it. The range is characterized by two factors: its bounds and the number of solutions contained. The bounds correspond to the minimal line of thrust and the maximal line of thrust.

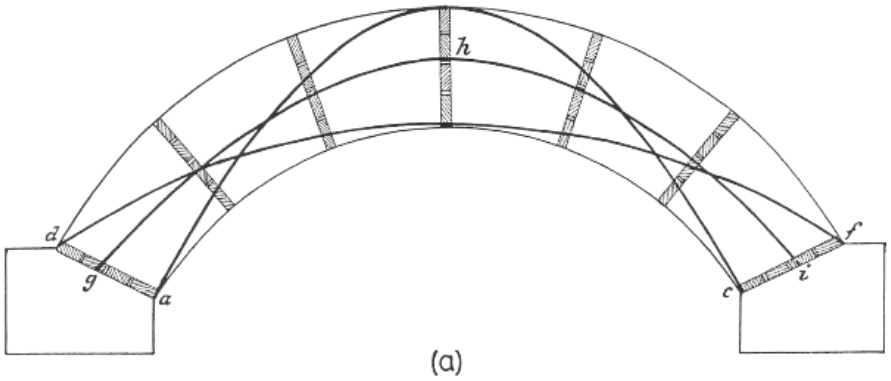

Figure 15: Different lines of thrust for an arch: curve d-f represents the maximum line of thrust; curve a-c the minimum line of thrust. Drawing of W. H. Barlow [103]**.**

The number of solutions contained, instead, depends on several factors, as the arch geometry or the presence of cracks.

In cases, for example, the existence of more than four hinges, the master 'safe' theorem is violated, the range is empty; hence the arch is not stable. To the current day, the literature presents several scientific documents that introduce variations to conditions **I.**, **II.** or **III.**, and are aimed at justifying local phenomena or particular circumstances considered [104] [105] [106].

As detailed in chapter 5.3, in the research here presented, limit analysis is used to evaluate the equilibrium of domes under construction; the master 'safe' theorem was applied to provide the resources to assess the balance without any temporary support.

2.3 Discrete element method

The Distinct Element Method (DEM) was conceived for geo-mechanical analysis, such as caves or mines [96] [97]. However, some researchers have also demonstrated its validity for masonry structures [107] [108] [109].

DEM is a computational method to study the temporal evolution of structures. Through DEM, the masonry is assimilated to a system of discrete bodies consisting of two elements: bodies (the solid elements) and discontinuities (the interfaces) [96] [97]. The bodies can be rigid or deformable; in the second case, DEM and FEM methods are integrated, allowing to estimate stresses and deformations [110]. The discontinuities between the bodies could be described by elements or, in the simplified models by an interface between two bodies. The purpose of DEM is to describe the time evolution of the discrete system, and to perform this, the collisions between the bodies can be detected, and their influence on the evolution of the system itself can be outlined. DEM uses an explicit time-marching scheme to solve the equations of motion directly, thus the determination of the different temporal

states is calculated by the explicit numerical integration of the equations of the motion of rigid bodies in time [99].

The analyses are ruled by several parameters, some related to the blocks, such as the characteristics of the material, and other relevant to the discontinuities for simulating the joints [99]. However, the most decisive factors that influence the analysis are:

- The geometry of the blocks, whose choice must be weighted concerning different factors, including the type of analysis performed [111].
- The coefficients of the discontinuities, they depend on the scale of the model analysed, its geometry, and the failure criteria adopted to describe the joints [112].

Even if several documents propose different approaches on how the parameters should be chosen [113], their determination is related to the goal of the analysis. Thus, before defining any model, it is necessary to identify what the goal of the analysis is, only then the hypothesis can be formulated. The wide spread application of the technique through different fields has led to the development of different DEM methods characterised by notable differences [114] [115]. Within the research conducted, chapter 5.4 describes the method DEM was used to investigate the effect of cross-herringbone spiralling pattern on domes under construction.

Part II: Equilibrium under construction

3. Cross-herringbone vault

The wide literature on the application of herringbone spiralling technology for Brunelleschi's dome: Santa Maria del Fiore in Florence [54] [116], does not provide enough information on how Brunelleschi gained knowledge of this technology, see chapter 1.4.1. Undoubtedly, its application in this dome has influenced its popularity and diffusion. Even as Leon Battista Alberti explicitly writes about this technique in his treatise *De re Aedificatoria* [117], the most significant contribution to the knowledge and conservation of the herringbone spiralling technology is provided by the Florentine family of architects and master masons: the Sangallo.

Despite the diffusion of the technique, today, there are only two historic and scientific documents that describe the herringbone technique. They are preserved in the Uffizi Museum. The first is the drawing 900A (n. 639051) GDSU (Gabinetto dei Disegni e Stampe Uffizi) and the second: the drawing 1330 (n. 594469) GDSU, illustrated in figure 16 and figure 28 respectively. By reading these documents, and by studying the Sangallo's domes which are still standing, such as the dome of Santa Maria in Ciel d'Oro in Montefiascone (Viterbo) or the dome of Simon Mago of San Pietro cathedral in Rome, an attempt to interpret the secret behind this technology is proposed. The domes reported in Appendix A are the proof that the Sangallo architects, especially Antonio the Younger, has contributed to the growth of the herringbone spiralling technology. They do not only systematically apply the herringbone spiralling technique, but they were also able to perfect it. This research conducted by the Sangallo family led them to develop a construction system: the cross-herringbone spiralling technology. Even if such a technique is based on the same principles of Brunelleschi's one, the differences observed are significant. Figure 15 b) illustrates the main variation, the presence of two orders of loxodromic curves, one right-handed oriented and another left-handed oriented.

The cross-herringbone spiralling technique is the last self-balancing technique presented in this document and is perhaps the most modern one. Unlike the Brunelleschi's technique, the cross-herringbone spiralling technology requires a detailed preliminary study that influences the project from the first conceptual phase. The following chapters illustrate the cross-herringbone spiralling technology through its history in chapter 3.1, its geometric characteristics outlined in chapter 3.2, and the principles behind the technology and its structural behaviour in chapter 3.3.

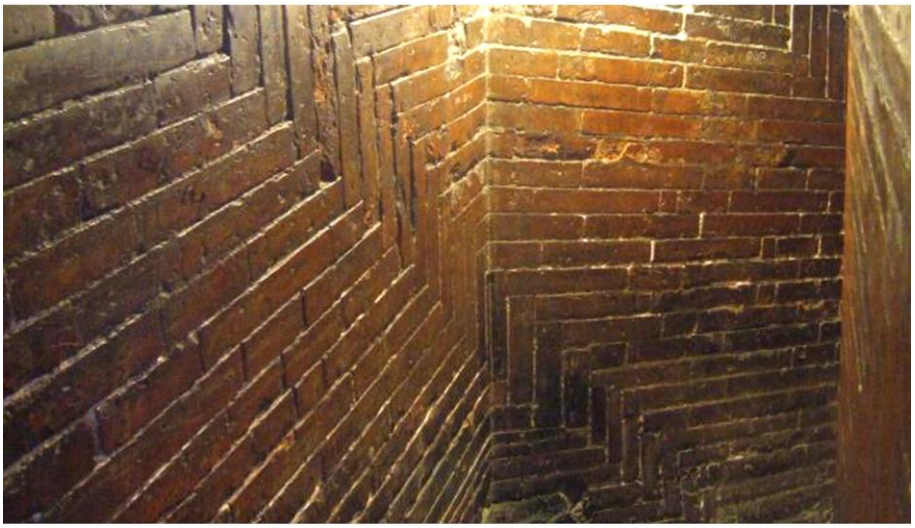

a

b

Figure 16: a) Herringbone spiralling pattern, Santa Maria of Fiore dome in Florence. b) Cross-herringbone spiralling pattern, dome of Simon Mago of San Pietro in Rome.

3.1 Traces of the cross-herringbone spiralling technology

The origins of the cross-herringbone spiralling technique are to be found in the works of architects and master masons of the 15th century. They had perhaps acquired the knowledge behind the herringbone technique at the building site of the Florentine Cathedral and were able to develop as well as master it until they had defined the cross-herringbone spiralling technique. Among the Florentine master masons, who guarded the secret of herringbone and cross-herringbone spiralling techniques, were the Sangallo architects, descendants of Francesco Giamberti (1405-1480 [58]), who was the master mason contemporary to Brunelleschi. Surely Giamberti and Brunelleschi would have known each other, and perhaps Giamberti would have also worked under the leadership of Brunelleschi [118]. His sons: Antonio da Sangallo the Older (1455-1534 [58]) and Giuliano da

Sangallo (1452-1512 [58]) were brilliant architects. They worked alongside Pope Alessandro VI Borgia and Lorenzo il Magnifico respectively, integrating the herringbone technique in the architecture of that time. Despite this, it was Antonio da Sangallo the Younger (1484-1546 [58]), Francesco's nephew, who gave us the most significant amount of evidence and documents on the application of the cross-herringbone spiralling technique.

3.1.1 Development of herringbone and cross-herringbone spiralling technologies

It is common knowledge that Brunelleschi's proposal for building the dome of Santa Maria del Fiore (1418) was said to be questioned by the jury of the Opera del Duomo. As evidence of their perplexity, in the early stages, Lorenzo Ghiberti was chosen as co-director and supervisor for Brunelleschi's work. Ghiberti, who was linked to the traditional approach, had never fully understood the Brunelleschi's approach or even what the herringbone spiralling pattern meant. To testify this, several examples are recorded [118] [119], one for them is where Ghiberti accused Brunelleschi of not respecting the promise made a century before by the master masons to construct a gothic dome, but to build a dome of revolution [120]. The fact that this construction method was not a simple hypothesis is extensively documented in the Florentine Opera's records, e. g. notes of the request of a buy a specific kind of bricks for building the Brunellesch's scale model of the dome, called *Mezzane* are found or by the scale model of the dome itself, which was built to prove the effectiveness of Brunelleschi's proposal [118]. The two elements, first the report of the bill of Mezzane bricks and second the incapacity of the Ghiberti to understand the construction method, are sufficient to prove how innovative the approach that Brunelleschi adopted was. Nevertheless, it is reasonable to think that Brunelleschi already had the knowledge of the herringbone spiralling technology, as he would not have been testing a new technique in a structure with such dimensions and relevance.

The herringbone spiralling technology [62] was practised for many years after Brunelleschi's death, see Appendix A. In fact, during the 16th century, the changed political and economic conditions, with the new weapons available, such as the cannons [121], gave impetus to build several fortresses. Consequently, as testified by the domes still in existence and the historical reports, Sangallo architects used the herringbone to complete domes of these defensive structures [122]. Nowadays, evidences of the use of herringbone and cross-herringbone are readable in many vaults built in the 15th and 16th centuries, such as in the vaults of the Vecchia Fortezza in Livorno (1519) [123], where Antonio da Sangallo the Younger built a hemispherical vault, or in the Sala d'Armi of the Fortezza da Basso in Florence (1534) [121]. The dome of Santa Maria delle Carceri in Prato (1484) and in Basilica della Santa Casa in Loreto in Ancona (1468) also see Giuliano da Sangallo's application of this technology [124]. Figure 17 maps the existing structures where probably the herringbone or cross-herringbone

spiralling technologies was applied by Sangallo architects. As shown in the figure, the buildings are mainly situated in the Tuscany region, the same context where the Sangallo architects practiced.
Inevitably, the use of this technology led to perfecting it, thus, Sangallo probably introduced the use of the cross-herringbone spiralling technique in some of these fortresses. Indeed, the presence of plastered surface in many of these domes does not give a clear picture of the underlying masonry pattern [125].

Figure 17: Distribution of domes built (probably) using herringbone or cross-herringbone spiralling technologies. Complete list reported in Appendix A.

As it can be understood by the restricted area of application of these building systems, their use was kept secret, and was closely guarded; it is not by chance that after the Sangallo architects, the herringbone and cross-herringbone spiralling techniques were lost.
Today, the presence of the cross-herringbone spiralling pattern is certainly proved only through a few constructions, all of them realised by Antonio the Younger. Few examples include the domes of octagonal rooms, called octagons of San Pietro cathedral in Rome, and the dome of Santa Maria in Ciel d'Oro in Montefiascone [126]. These non-plastered domes make the masonry tessellation visible, allowing us to formulate hypotheses on how they were built.

3.1.2 Historical documents of herringbone and cross herringbone

For the purpose of providing a proof, for the existence and the secrecy behind the herringbone and cross herringbone spiralling technologies, in addition to the previously mentioned testimonies, the two drawings: 900A (n. 639051) and 1330 (n. 594469) GDSU, drawings, shown in figure 28 and figure18 need to be investigated thoroughly.

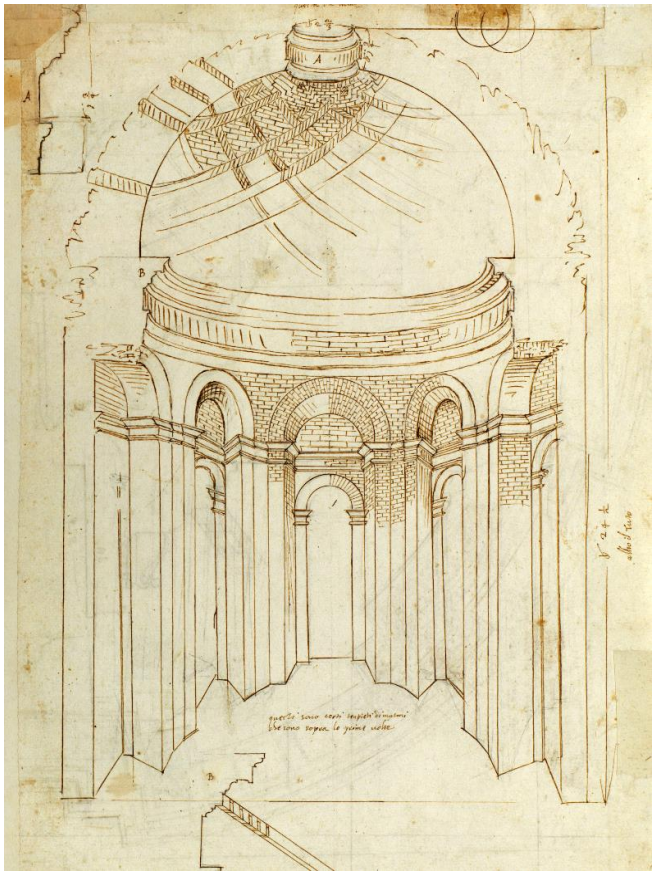

Figure 18: Drawing 1330 (n. 594469) GDSU. View of Simon Mago chapel, the cross-herringbone spiralling pattern is visible.

The drawing 900A is attributed to Antonio da Sangallo [127] the Younger and 1330 to Guido Guidetti [59], who was an architect close to Antonio da Sangallo the Younger. These two drawings constitute further evidence of the existence of the Sangallo's school, where the herringbone spiralling technology was handed down and developed. Despite numerous doubts regarding the origin's effective application of this technology, it is known that, Sangallo architects used it until the first half of the 16th century. Further, besides, as witnessed at the dome of Santa Maria in Ciel d'Oro and at the domes of the octagons, it is indisputable that Antonio da Sangallo the Younger knew and used the cross-herringbone spiralling technique during his Roman permanence under Pope Paolo III.

3.2 Cross-herringbone spiralling pattern

The study of existing structures is the primary source for understanding the behaviour of the structures themselves. In the following chapters 3.2.1, 3.2.2, 3.2.3 and 3.2.4, the geometric characteristics of the cross-herringbone spiralling technology are illustrated. They are derived through a primary study and survey of the domes of Santa Maria in Ciel d'Oro and Simon Mago of San Pietro.

3.2.1 Overall information of cross-herringbone dome

As mentioned in chapter 3.1, Antonio da Sangallo the Younger designed the two domes: Santa Maria in Ciel d'Oro and Simon Mago of San Pietro. These two structures have quite similar histories. Santa Maria in Ciel d'Oro was designed around the year 1526 and completed in 1548 [128]. The construction has been stopped several times for various reasons, including the bubonic plague or the invasion of Lanzichenecchi. The initial idea was to build a monastery for pilgrims, but due to the interruptions only a modestly church, reported in Figure 19 a), was realised. For this project, Antonio da Sangallo the Younger visited the building site only three times, and for the remaining time the works were supervised by his brother Giovanni Battista Fiorentino and by the local master mason. The second structure built using cross-herringbone spiralling pattern is the Simon Mago dome in San Pietro cathedral. This is shown in figure 19 b) c) d) and it cover a small chapel at the first level in San Pietro. The historical documents do not say when its construction precisely started, but there is evidence of Antonio da Sangallo the Younger working at the Fabbrica of San Pietro from 1520 until 1546 [122]. His presence in this building site is testified by numerous documents collected in the Archive of the Fabbrica of San Pietro. Thus, it is reasonable to think that the building of Simon Mago dome was supervised with more accuracy and skill than the Santa Maria in Ciel d'Oro.

The dimensions of the two domes are similar, but one is an octagonal dome and the other a hemispherical one. As shown in detail in figure 20, Simon Mago is a perfect hemispherical dome whose inner radius is 4.83 meters, and the maximum radial deviation is about 1.8 centimetres. The dome presents an oculus of a diameter of 1.82 meters with no other openings. Santa Maria in Ciel d'Oro, represented in figure 21, is an octagonal dome. The eight sails are described geometrically by portions of ellipsoidal cylinders, and the ribs of the sails are defined by circular arches whose radius is about 5.47 meters. The length of the four internal diagonals varies between 10.95 meters and 10.98 meters meanwhile the clear height is 5.31 meter.

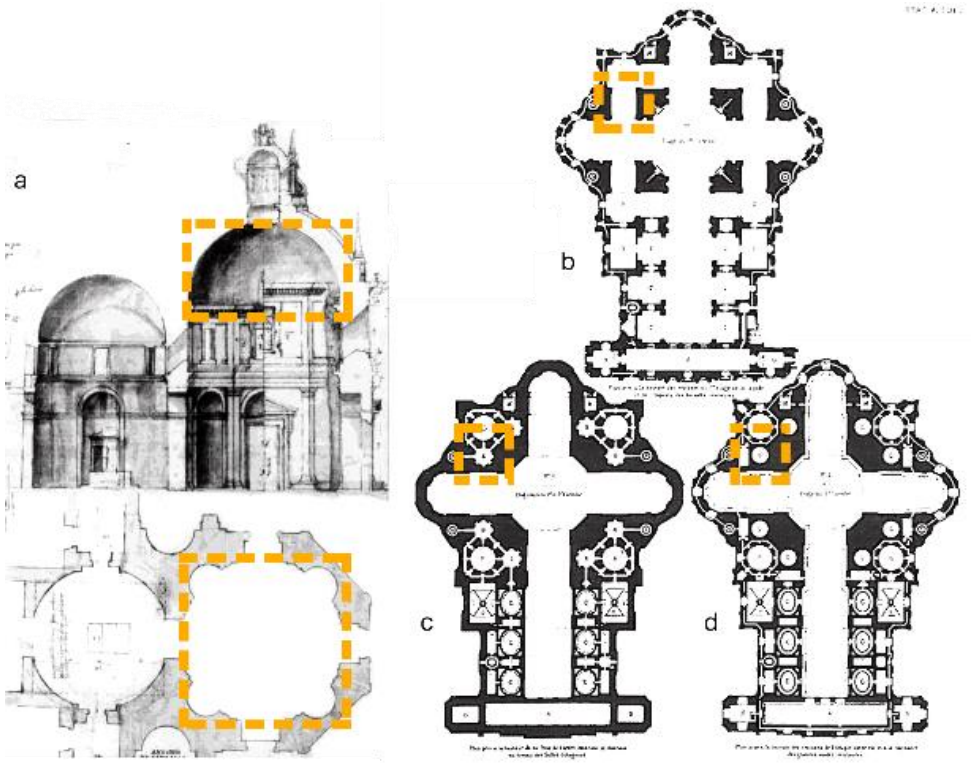

Figure 19: a) The drawing n. 173 Uffizi Museum archive, plan view and vertical section of Santa Maria in Ciel d'Oro. Drawing of Antonio, the Younger. b), c), d) Plans view of San Pietro Cathedral. b) Ground level. c) The first level above the secondary naves. d) View at the base of the dome of octagonal rooms. In all plans view, Simon Mago chapel is highlighted in yellow. Drawing of P. M. Letarouilly [59].

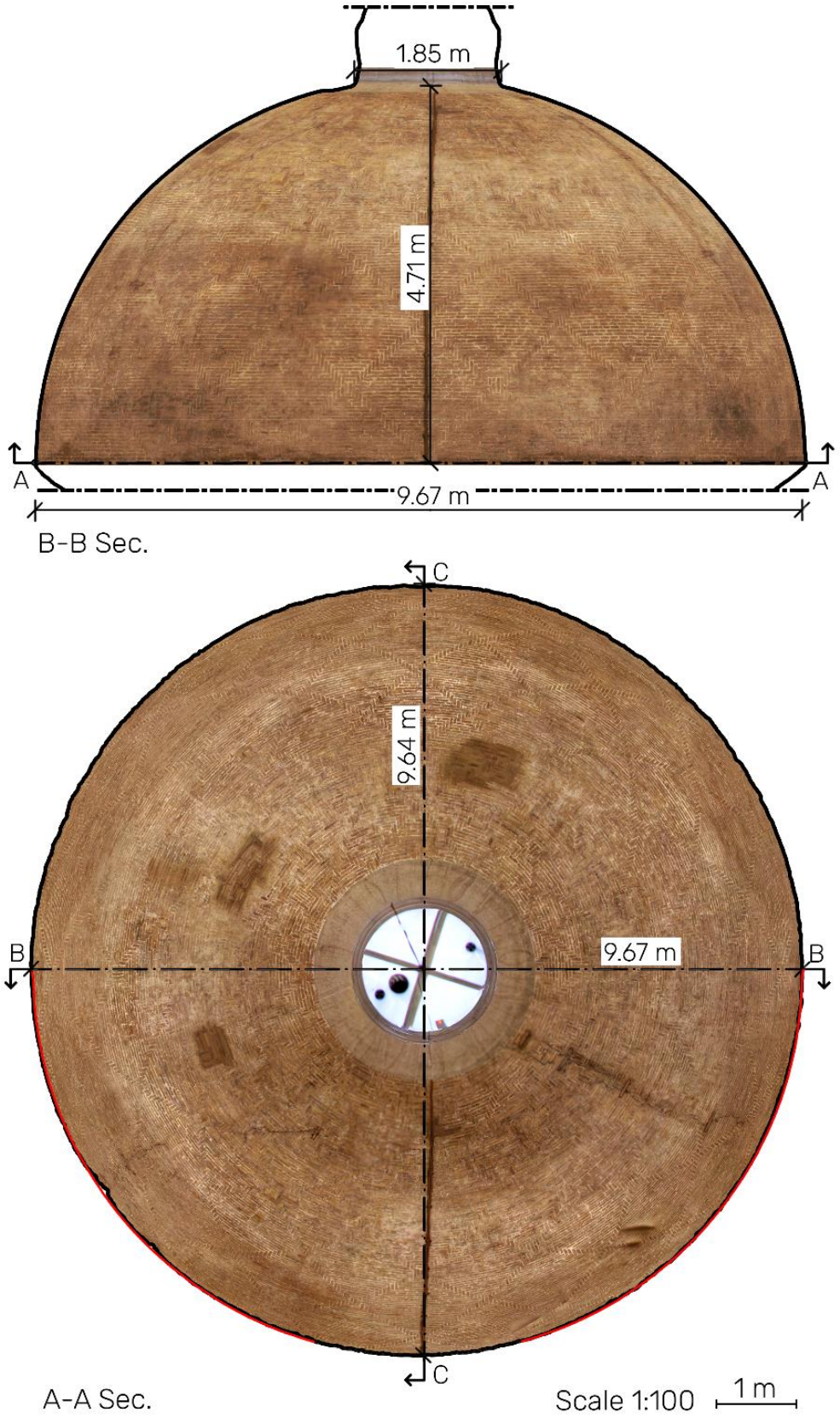

Figure 20: A-A Sec. Plans view (from bottom to top) of Simon Mago dome. B-B Sec. Vertical section.

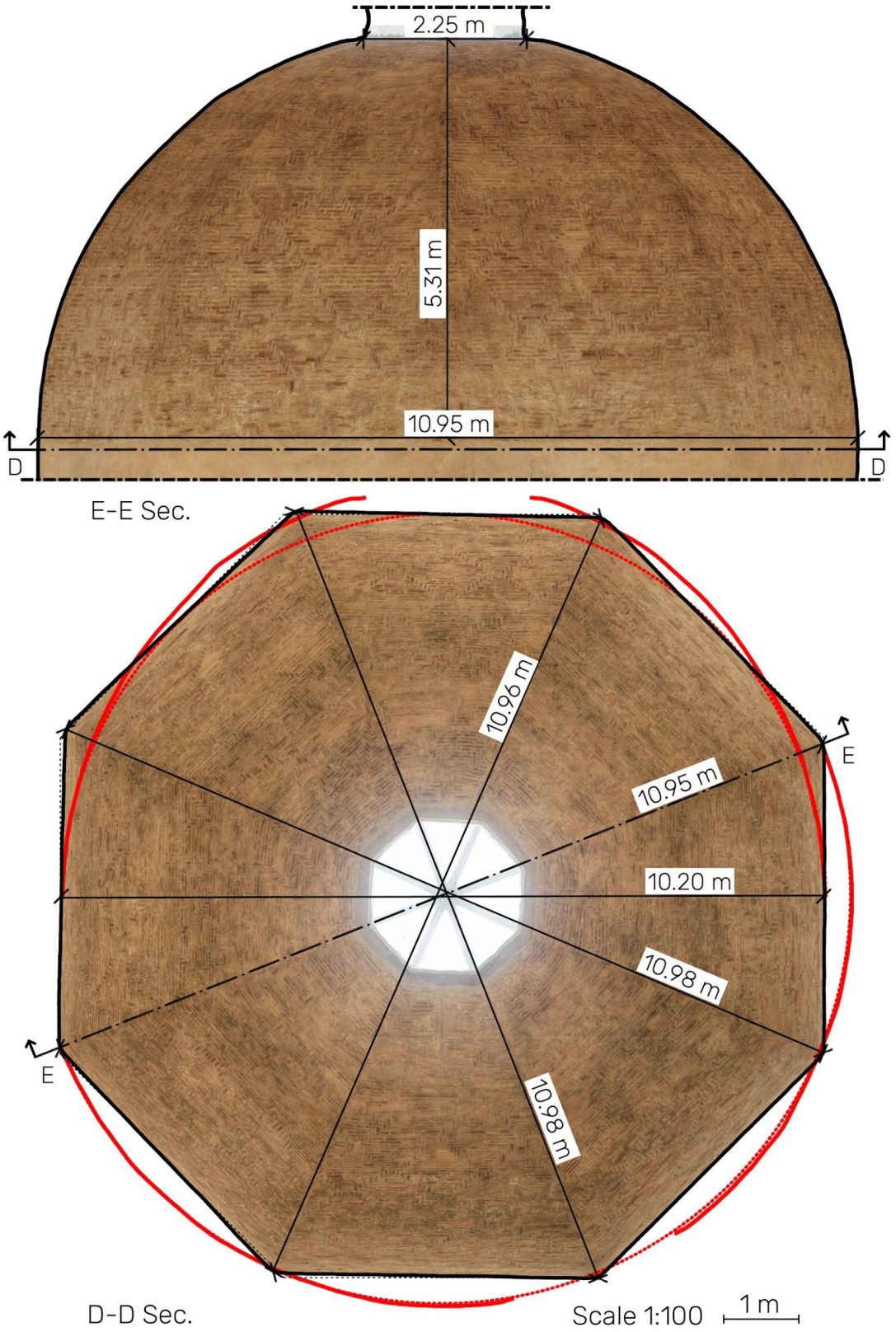

Figure 21: D-D Sec. Plans view (from bottom to top) of Santa Maria in Ciel d'Oro dome. E-E Sec. Vertical section.

3.2.2 Geometry of cross-herringbone spiralling pattern

The cross-herringbone spiralling pattern is a brick tessellation characterised by a double system of herringbone paths: one left-handed spiralling and the other right-handed. Thus, referring to figure 22, at each of these intersections of the two systems of loxodromic curves, nodes are formed. The nodes are materialised by 1, 2 or 3 bricks placed one adjacent to another. The global tessellation, then appears as a complex system of rhombi, each one delimited by loxodromic trajectories and whose dimensions decrease from the bottom to the crown of the dome. The geometry of loxodromic curves that trace rhombi is defined by several factors: the thickness of mortar, the size of bricks and the dome's geometry itself [129].

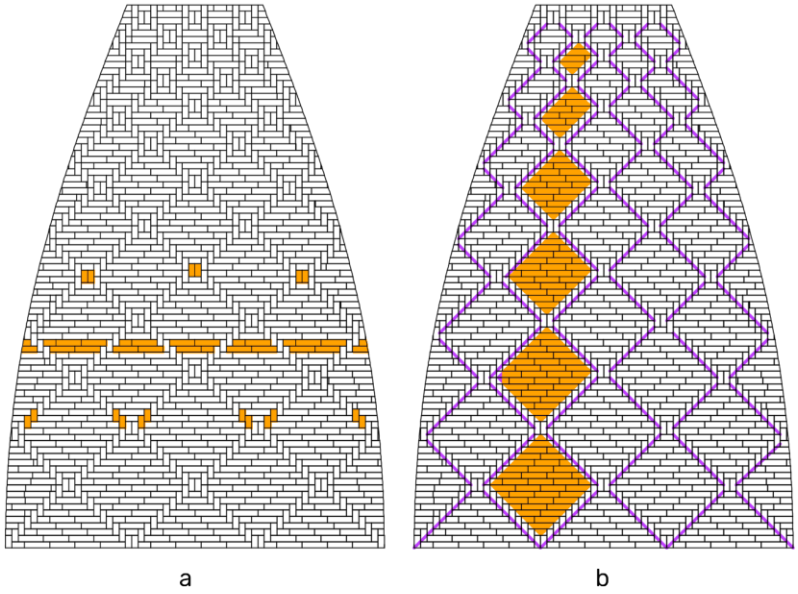

Figure 22: Cross-herringbone spiralling pattern: masonry pattern for a sail of an octagonal dome. a) Elements highlighted: nodes (top), horizontal courses (middle), herringbone bricks (bottom). b) Elements highlighted: left and right-handed loxodromic curves (thick lines) and rhombi (areas filled).

As shown in figure 23 and 24, the intrados of Simon Mago dome exhibits the cross-herringbone tessellation. The geometries of all loxodromic curves (one of them highlighted with continuous purple line) are the same in term or inclination and trajectory. All rhumb lines have the same inclination with respect to the course of horizontal bricks, and all nodes are radially aligned (highlighted with dot orange lines). The dome presents 16 right-handed and 16 left-hand loxodromic paths, hence 32 spirals in total with the two systems of spirals intersecting to form regular rhombi. At the level of the spring of the dome, the spirals are spaced 3 Florentine arms, about 1.80 meters arms apart(1 Florentine arm corresponds to 0.584 meters [126]. Santa Maria in Ciel d'Oro, on the other hand, presents several discontinuities, such gaps, or interruptions of trajectories. The reason for these discontinuities can be found in its history, as reported in chapter 3.2.1, and this probably led to a variation of the masons who works on its construction.

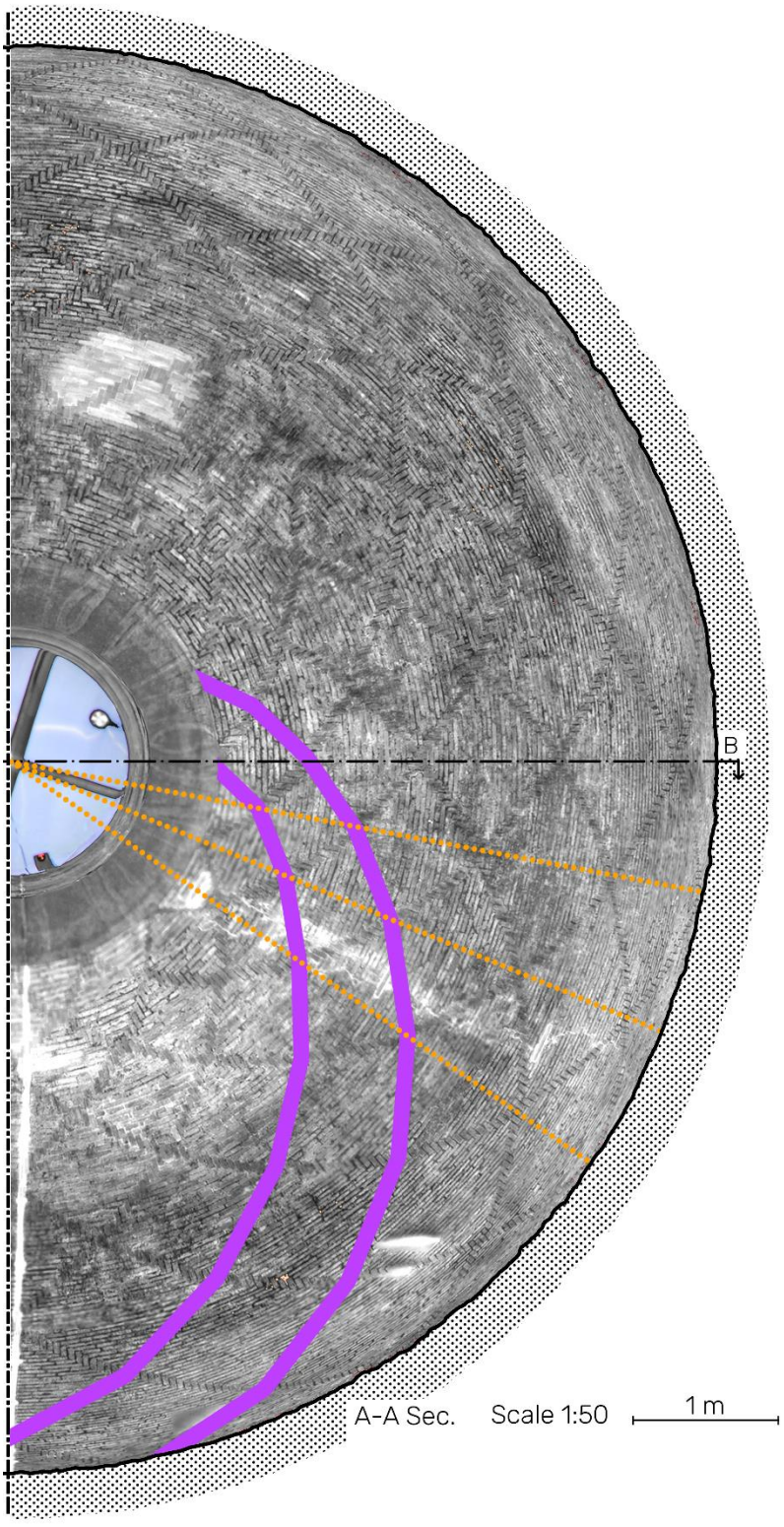

Figure 23: Plan view of Simon Mago dome.

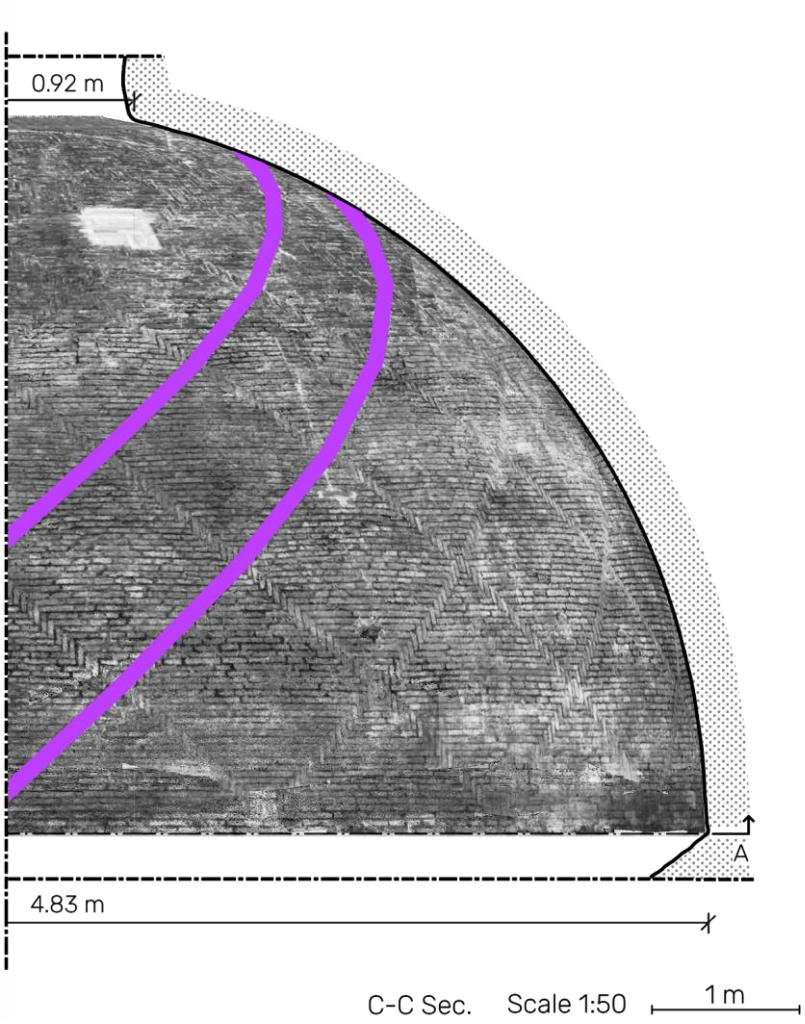

Figure 24: Vertical section of Simon Mago dome.

The new builders employed when the work resumed probably did not know the cross-herringbone spiralling technique and as a result several inaccuracies occured. Furthermore, Antonio da Sangallo the Younger did not supervise the building site assiduously, but he was only present for important construction phases such as the first one required to tracing and correctly starts the construction. In fact, as shown in figure 25, the masonry pattern close to the dome's base is more regular than one at the crown, where the cross-herringbone spiralling pattern is not clearly visible. Despite the discontinuities in the masonry pattern of the Santa Maria in Ciel d'Oro dome, 6 loxodromic curves for each sail, 3 left-handed and 3 right-handed, can be visually identified. Figure 26 displays the sail of Santa Maria in Ciel d'Oro, and here within the sails, the position of the nodes describes a scheme 4 - 3 - 4 - 3 rhombi. The same pattern is visible in the plan view of figure 25, where the rhombi defined through paths lie in the two different sails, are highlighted. At the base of the dome, the distance between two loxodromic curves corresponds approximately to 1.15 m, which is about 2 Florentine arms.

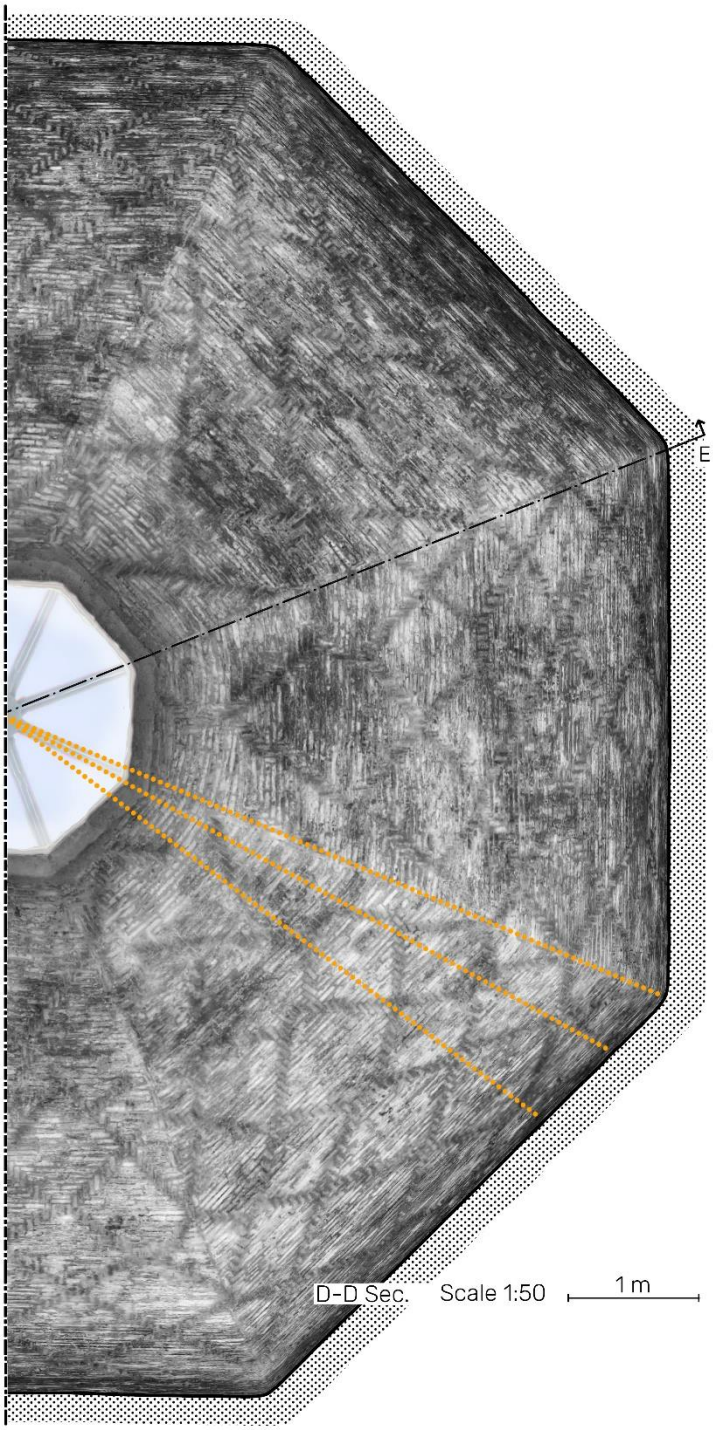

Figure 25: Plan view of Santa Maria in Ciel d'Oro dome.

3.2.3 Brick dimensions

Two different types of bricks were adopted in the two domes presented, as shown in figure 27 a), b) that exposes details of the masonry: the Simon Mago a) and Santa Maria in Ciel d'Oro b). The dimensions of Simon Mago's bricks are 4-13-27 centimetres (height-width-length), while the bricks used at Santa Maria in Ciel d'Oro are 7-14-28 centimetres. The bricks are quite similar, they have

almost the same length, but it is more relevant to express the relationship between the three dimensions referring to height as a unit.

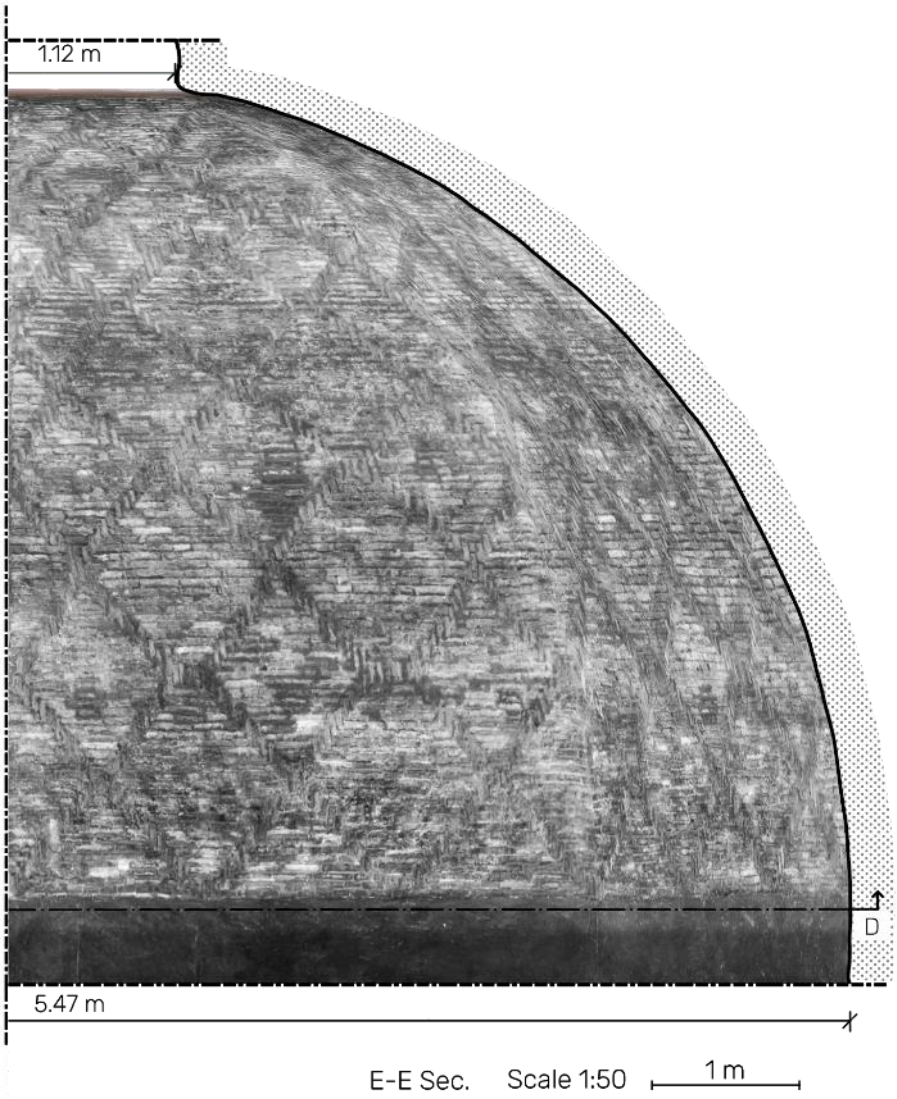

Figure 26: Vertical section of Santa Maria in Ciel d'Oro dome.

Therefore, Simon Mago bricks are described through the relation *1-3-6*, meanwhile Santa Maria in Ciel d'Oro as *1-2-4*. Although the two types of bricks have different ratios, it is possible to identify a common root: *1-1⍺-2⍺.* This ratio assumes relevance in the cross-herringbone technique, because, for a correct construction the ratio between length and width must be 2. With different ratio, e.g., 3 the herringbone bricks cannot be placed in the right texture.

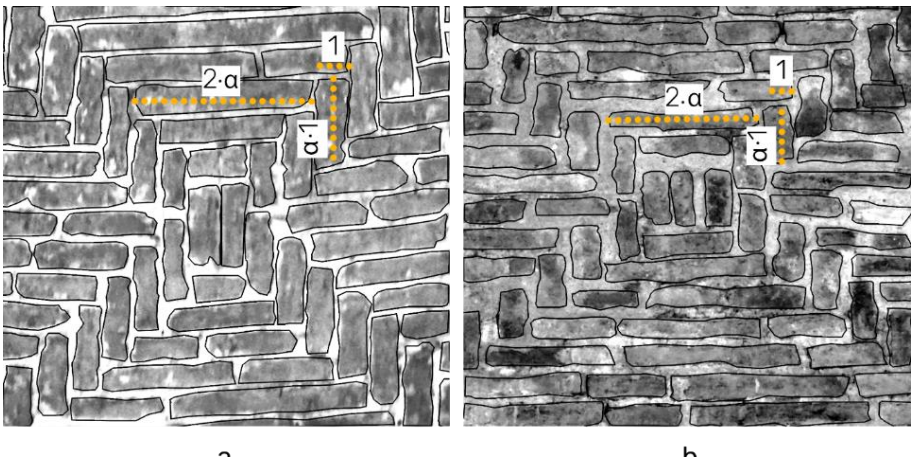

Figure 27: Details of cross-herringbone spiralling pattern in correspondence of nodes. a) Detail of Simon Mago, ratio 1-3-6. b) Detail of Santa Maria in Ciel d'Oro, ratio 1-2-4.

4.2.4 The drawing 900A

The drawing 900A (n. 639051) GDSU, shown in figure 28 and previously mentioned in chapter 3.1, testifies the knowledge of Antonio the Younger of the herringbone spiralling technique. Despite its historical value, this document certainly has more importance from a technological point of view. The document displays one plan view, one vertical section and one caption that says: *'volte tonde di mezzane quali si voltano sanza armadura a Firenze'* that translates it means: hemispherical domes built using *mezzane* bricks without any formwork as done in Florence. The drawing describes the herringbone spiralling technique, which displays several projections of loxodromic curves on the plan view of a hemispherical dome. Although the plan provides some information about the loxodrome trajectory, for the purpose of this research, the vertical section displayed on the right is much more relevant.

Few researchers suggest that this vertical section is associated to the Brunelleschi's dome [53] [127] [130], and according to them it describes a double dome of the Santa Maria del Fiore. However, by closely observing the drawing, it is possibly understanding that rectangular elements drawn can only be bricks. Considering the accuracy of the drawing in the plan view, the vertical section appears to be just an explanatory scheme. It can be hypothesised that the same hand that has designed such an accurate plan could not have drawn so inaccurately when depicting the vertical section. If not just for explanatory purposes, the scale itself of the bricks is a clue. The vertical section reported in figure 29 a) is however associated with the same hemispherical dome seen in the plan view in figure 28. The figures drawn at the inner arch can be assimilated to bricks laid according to a radial alignment. In the central portion of the vertical section, radial elements with double length are illustrated, and with

respect the other bricks drawn they dimensions have the same relationship *1α-2α* illustrated in chapter 3.2.3.

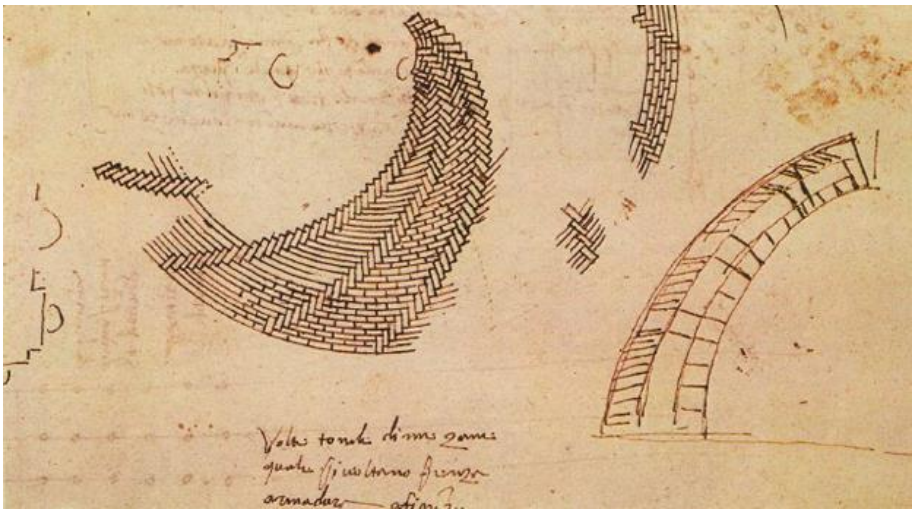

Figure 28: Drawing 900A (n. 639051) GDSU. Drawing by Antonio da Sangallo the Younger.

Therefore, it is possible to understand that these double-width elements describe the herringbone bricks, see figure 29 b). Thus, the plan view and the vertical section illustrate the tessellation of herringbone spiralling pattern for a hemispherical dome. The document explicitly provides some indications on the possible stratigraphy of the domes built with herringbone spiralling technique.

To date, this drawing is the only historical source which provides information on how the herringbone spiralling pattern links the layer in the direction of the thickness of the dome. Only two other sources available today can give some information about the composition of the walls. The first is a historical dome near Brunelleschi's dome, which consists only of one brick layer, thus, from the point of view of the current investigation, this structure has not relevance [131]. The second source is a scale model of the Santa Maria del Fiore dome, called Antonella model, built at the end of the 20th century [116]. This model presents similarities to the hypotheses made but fails to provide any historical information. It is reasonable to assume that the herringbone tessellation links the bricks layers through the thickness of the dome. Referring to figure 29 b), the model of the cross-herringbone spiralling pattern presents the same characteristics of the herringbone spiralling pattern, but the presence of the two systems of loxodromic curves increases the cross connections through the dome's thickness. The cross-herringbone, different from the herringbone pattern, permits to identify volumes completely delimited by herringbone bricks. The analogy between these empty volumes and the empty spaces between the surfaces of the formwork is immediate. Perhaps the stratigraphy of some domes built with cross-herringbone spiralling technique is similar to that of rubble masonry. Unfortunately, no one can affirm how the layering of the dome is. The surveys carried out on such structures were

unable to provide any information about this, but however the vertical section in figure 29 a) shows empty central areas which could be representative of empty volumes.

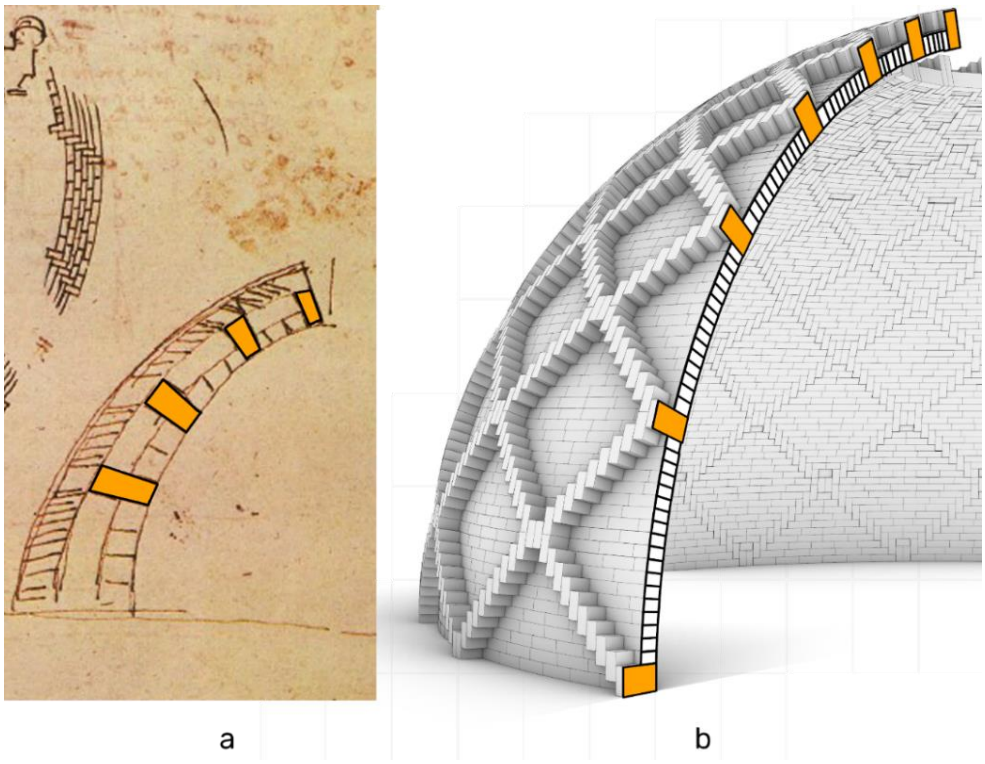

Figure 29: Comparison of drawing 900A (n. 639051) GDSU. Drawing by Antonio da Sangallo the Younger.

The last element displayed on the vertical section is an external layer of bricks, the extrados of the dome. The bricks are not arranged radially but almost lie within horizontal courses. The elements are only sketched, indicating the lack of importance of the external layer with respect to the structure of the herringbone. Hence, considering the purpose of the drawing 900A GDSU: explaining the herringbone spiralling technology, the bricks of the extrados play a marginal role and do not constitute as essential elements needed to reach the self-balance state during the phases of construction.

3.3 Principles of cross-herringbone vaulting technique

As already mentioned in the previous section, the herringbone and the cross-herringbone spiralling techniques are based on the same principles. In this chapter, we refer to the cross-herringbone spiralling technology, but unless otherwise specified, the same concepts also apply to the herringbone one.

The ability to achieve the self-balance state of structures built using the cross-herringbone spiralling technique is affected by their construction process. Even if it is not the specific scope of this chapter (in this respect see for example [69] [119] [126]), some elements of construction technique must be discussed.

To use the cross-herringbone spiralling technique an executive scheme is needed. The goal of this operation is to primarily to identify the position and geometry of the nodes with respect to the whole structure and then to identify the number of herringbone bricks located between two nodes. Possible inaccuracies in the arrangement of these elements could inevitably lead to mistakes that can compromise the self-balancing state of the structure itself. As shown in figure 30 a), Santa Maria in Ciel d'Oro dome exhibits several inaccuracies, probably due to the reasons mentioned in chapter 3.2.1. The realization of an accurate executive scheme is even more significant in double-curved structures such as the domes of revolution. Figure 30 b) shows this scheme for a hemispherical dome. Here, the non-alignments between herringbone bricks belonging to different rhumb lines (highlighted with an orange dotted line) are unquestionable.

Therefore, for the effectiveness of the cross-herringbone technique, executive drawings and the tracing operations are fundamental to guarantee the self-balancing, while, due to the absence of the nodes, they have less importance when adopting the herringbone spiralling technique.

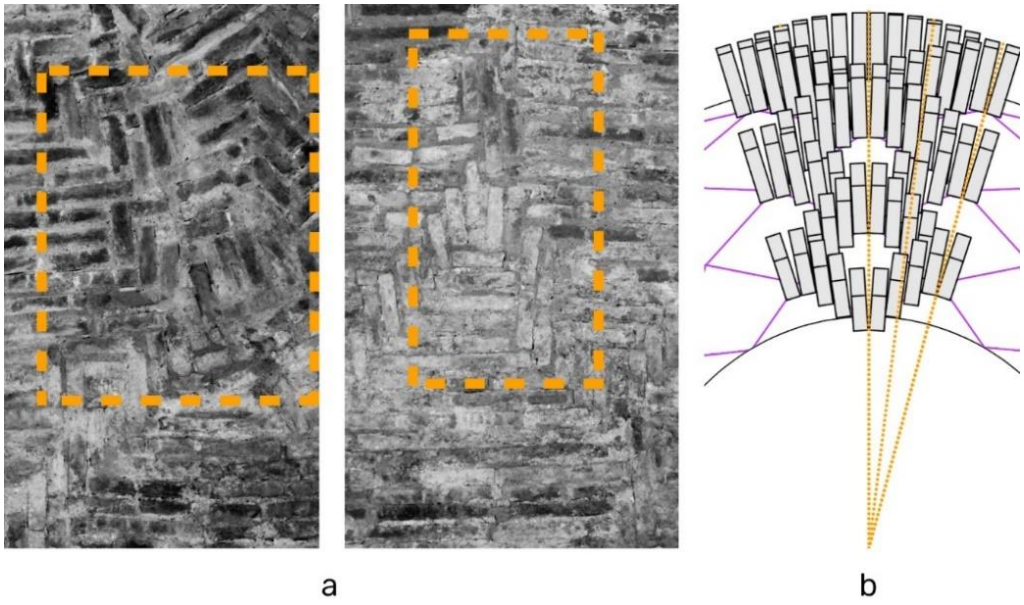

Figure 30: a) Details of nodes of Santa Maria in Ciel d'Oro. b) Scheme of herringbone bricks for a hemispherical dome. The herringbone bricks which belong to different loxodromic curves are not aligned.

The cross-herringbone spiralling technique permits to achieve the self-balanced state in the shells only by building through complete horizontal courses, i.e., during the construction before proceeding the laying of a new bricks course, all lower bricks courses must be completed (condition A.). Condition A. is the first of two requirements necessary to guarantee the effectiveness of the cross-herringbone spiralling technique. For the domes of revolution, during the laying of a brick course, the sliding of the elements can take place only before the course itself is completed. Once closed, it

withstands to compressive forces preventing sliding. Likewise, the cross-herringbone spiralling pattern allows the development of resistant sub-structures that act as a completed bricks course.

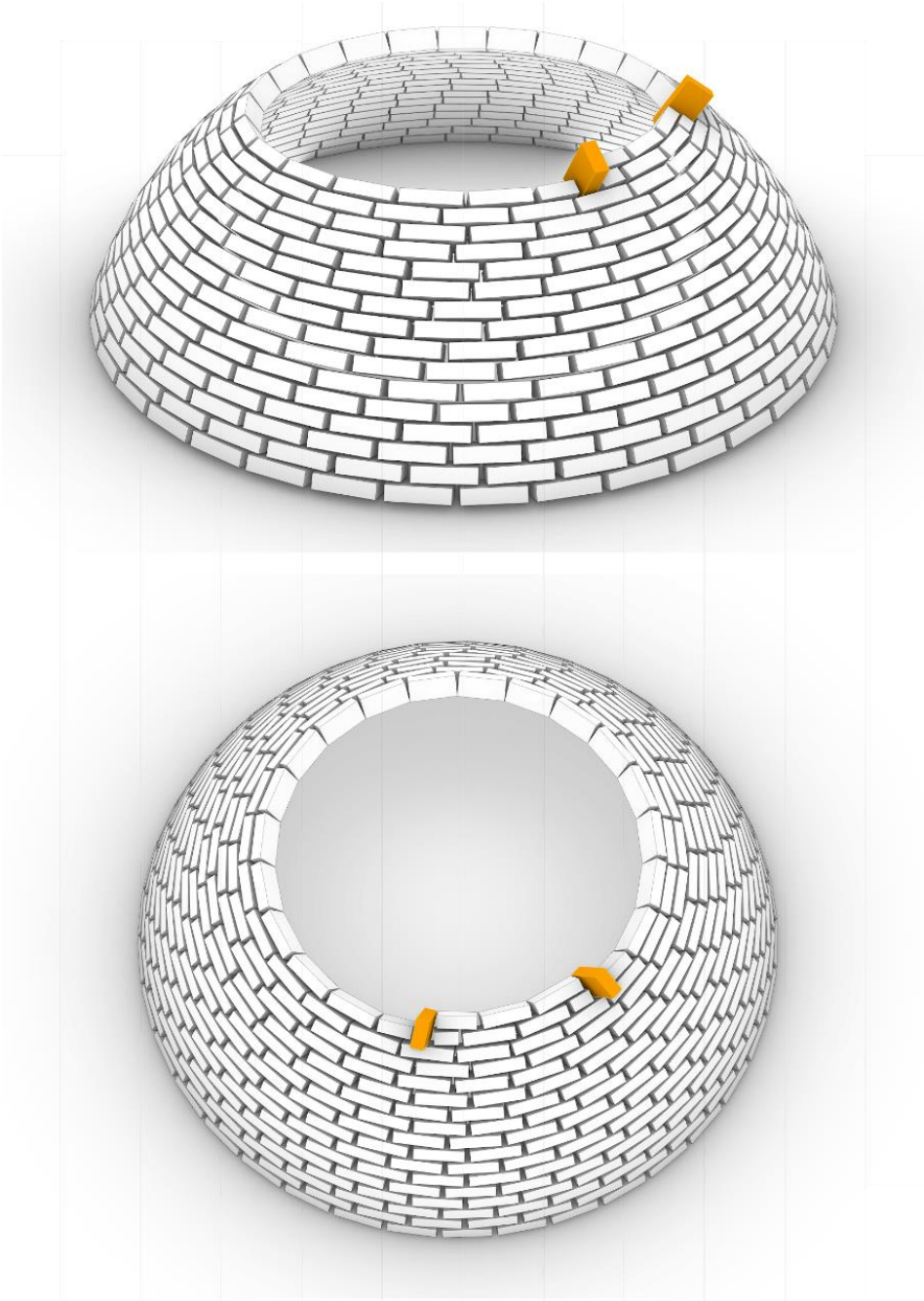

Figure 31: Hemispherical dome, the brick laid as herringbone bricks (highlighted in orange) due to their orientation, the upper bricks course is constrained.

To understand this, it is sufficient to think again about the domes of revolution. Referring to figure 31, when the course where two herringbone bricks (highlighted in orange) are laid is completed, the two mentioned bricks are fixed. Hence, they can support all bricks placed in the upper course and laid between them. Therefore, in domes built with cross-herringbone spiralling technique, whose pattern

was discussed in chapter 3.2.2, the role of herringbone bricks is to link the courses together during the construction.

The goal of cross-herringbone is the development of sub-structures, like arches, that, under construction, provide the resources necessary to guarantee a self-balance state. Thus, the stability of these resistant sub-structures determines the second condition necessary to guarantee the efficacy of the cross-herringbone spiralling technique (condition B.).

If the conditions A. and B. are respected the cross-herringbone spiralling technology permit to build domes and vaults without any formwork. Unlike herringbone technique, the presence of nodes, in the cross-herringbone one, see in figure 27, allow during the construction to adjust some errors by inserting wedges, bricks or elements to increase the compression forces within the horizontal brick courses. Indeed, from the survey, especially in Santa Maria in Ciel d'Oro dome, several node adjustments are readable.

4. Learning from the history: equilibrium under construction

Chapters 1. and 3. have presented the significant technologies that allow building masonry vaults or domes without the aid of any temporary support. The study of these techniques is relevant in the formulation of a theory for evaluating the equilibrium under construction.
Chapter 4.1 summarises and organises the principles on which the self-balanced technologies are based, while in chapter 4.2 the guidelines to the evaluation of the stability of masonry structures during their construction are illustrated.

4.1 Building factors required and self-balanced state under construction

The techniques illustrated in chapters 1. and 3. provide the information to understand the self-balanced state of masonry structures under construction. All self-supporting techniques are ruled by building factors whose principles can be either geometric, construction, mechanical, or related to material properties. These factors affect the effectiveness of the related self-supporting techniques, e.g., it is not possible to build tile vaults without the use of fast-setting mortar or by using heavy blocks.
Therefore, building factors have been derived from the study of the principles exposed in chapters 1. and 4. They are as follows:

- **Bed joints orientation.** For some technologies, such as pitched vaulting, this factor is the primary element that affects the self-balanced state. In others, like clay tubes vaulting technique, it is barely relevant. Examples are given by figure 6 c) and d) where the tubes can be oriented in two different manners for a structure with the same geometry. If this factor is primary or relevant, a preliminary design is required whose goal is to determine the correct orientation of the bed joints.
- **Bricks stereotomy**. During the construction phase, the geometry of the bricks significantly influences their stability, as witnessed by the clay tube vaulting technique or corbelled vaulting technique [37]. A wrong choice of the sizes or the shape of the bricks lead to the sliding phenomena or local failures. The study of the stereotomy of bricks still represents an active research topic [132] [133].
- **Resistant substructures**. The existence of resistant sub-structures during the construction could provide enough resources to reach the self-balanced state during the construction. This element is the primary factor for herringbone technology and cross-herringbone, but it also

influences the ability of self-balance in pitched vaults or clay tube vaults. Owing to the nature of this factor, the state of a supporting structure can be evaluated through simply mechanical analyses. The study of the equilibrium related to this factor is the primary subject discussed in chapter 5.

- **Construction sequences**. The construction sequence is a factor that influences all self-supporting technologies. This is essential for the right construction of tile vaults and all those technologies whose balance is provided by resistant sub-structures.
- **Material properties**. A right choice of building material is always significant, but for technology such as tile vaulting technique the material properties are the primary factors to reach a self-balanced state.

Each of these factors can play a key role with respect to the technology adopted. Table 1 summarises for all techniques discussed along with the occurrence of factors mentioned above and illustrates this with the aid of three grades: primary, relevant, and not required.

1) **Primary** is the indication that the factor characterises the technology analysed. An incorrect application of the building factor considered could lead to failures and collapse during construction.
2) **Relevant** indicates a factor significant for a specific technology, even though it is not the primary building factor which characterised the techniques investigated.
3) **Not required** indicates a factor that for this technology examined does not need a specific study. However, as the primary and relevant grades, if violated, could lead to failures. For example, for the right application of the herringbone vaulting technique it is assumed that the bed joints are arranged conventionally, and no study is required for the orientation of the joints. On the contrary, by adopting the pitched vaulting technique, the orientation of the bed joints is fundamental, and it differs from the common convention. However, for the herringbone technique, errors of the orientation of beds joints could preclude the self-balancing ability of the structure built.

The identification of the primary and relevant factors is fundamental to choose the method for assessing the equilibrium state during the building phase. With different factors influencing the technology, different methods of evaluation also need be adopted.

Technology	Bed joint orientation	Brick stereotomy	Resistant sub-structures	Material properties	Construction sequence
Pitched vaulting	Primary	Not required	Relevant	Relevant	Not required
Clay Tubes vaulting	Relevant	Primary	Relevant	Not required	Relevant
Tiling vaulting	Not required	Not required	Relevant	Relevant	Primary
Herringbone vaulting	Not required	Not required	Primary	Relevant	Not required
Cross-herringbone vaulting	Not required	Not required	Primary	Relevant	Not required

Table 1: Self-balanced technology and incidence factors.

4.2 Two-step approach

The evaluation of the state of a masonry building is the subject of studies by numerous researchers [134] [135] [136]. However even today, the behaviour of these structures during the construction phase is scarcely analysed [17] [37]. One of the goals of the present study is to introduce a new theory that allow evaluating equilibrium during the construction phase. The development of this theory is significant for masonry arches, vaults, or domes, but it can also be useful for other types of masonry structures.

Only from the observation of real structures and the study of historical building technologies, the reasons that guide the balanced state of domes and masonry vaults during the construction works can be understood. Referring to the building factors exposed in chapter 4.1 the equilibrium under construction is affected by a few quantities.

These building factors affect only the local behaviour of the structure. For example, referring to the tile vaulting technology, the fast-setting properties of the mortar and lightness of the tiles allow the laying without manifesting any sliding phenomena, or the presence of sub-structures provides the support needed for the stability of bricks until the brick course is complete. Likewise, these factors do not alter the state of the whole structure, whose behaviour remains unchanged. To confirm this, it is enough to revisit hemispherical domes, i.e., by applying the building process discussed in chapter 3.3, it is possible to build them without any formwork. However, independent of the construction sequence adopted, the stability of the hemispherical domes depends mainly on geometric factors [137]. Then, it is irrational to assume that the herringbone pattern governs the stability of a structure, for example, in the case of the dome of Santa Maria del Fiore. Although it may influence some aspects of its behaviour such as the position or shape of the cracks, it does not alter its collapse behaviour.

The same considerations discussed are also valid for different types of masonry structures, such as walls or structures which require support. Their overall behaviour is not modified by how they find the equilibrium during the construction phase because, if well-constructed, the overall equilibrium is determined by the geometry [2].

Therefore, to assess the balanced state of masonry structures during the construction phase, it is convenient to study their equilibrium through two different level of analysis: the first level is related to the local state and the second one is related to the global state. The two levels can be investigated separately, but they are linked, only if no local failures occur the whole structures can be built. Thus, a two-step approach is proposed, where the first step consists of the evaluation of the local equilibrium and the second one deals with the assessment of the overall stability.

The two different steps are hereby called: **Local Equilibrium Step** and **Global Equilibrium Step**.

- The study of **Local equilibrium step** (**LES**) has the goal of detecting any possible local collapses at a local level. To assess the state of structure at this scale it is necessary considers the building factors of different construction techniques especially in the case of self-supporting technologies. Thus, the criteria to assessing the stability of structures must be related to the factors that characterise the building technique adopted (primary factors). It is not possible to adopt the same criterion to technologies based on different construction factors. In this document, the calculation of local stability is carried out by referring only to the primary and relevant criteria of the cross-herringbone technology. Other criteria relating to other factors or technologies are not considered.
- The study of **Global equilibrium step** (**GES**) aims to determine the stability of the entire structure built. It can be conducted with the traditional tools developed for evaluating the state of structures.

Independent of the building technology adopted (self-supporting or not) and of the type of structure considered, if no collapse phenomena (local or global) could occur for a given construction stage, the structure is balanced at that construction stages. To guarantee the possibility to build a masonry structure without supports, it is needed to evaluate all the construction stages and if for each stage a balanced state could be found (local and global).

The flowchart shown in figure 32 describes the logic of the two-step process: before evaluating the global equilibrium (GES), it is required to determine the local balanced state (LES).This relation is justified by a simple assumption already mentioned: it is impossible to build any structure if, during the construction phase, local collapses occur. To explain the flowchart, consider a wall under construction and defined by the index i are the number of brick courses and by the index n are the construction stages. It is possible to determine the equilibrium at the n^{th} stage evaluating the local

stability, through LES, and then, through GES, the global stability at that stage. If no local or global failure phenomena are exhibited, the same logic process should be repeated for the next construction stage (n+1), and as mentioned before, the structure can be built if the equilibrium is found (local and global) for all stages.

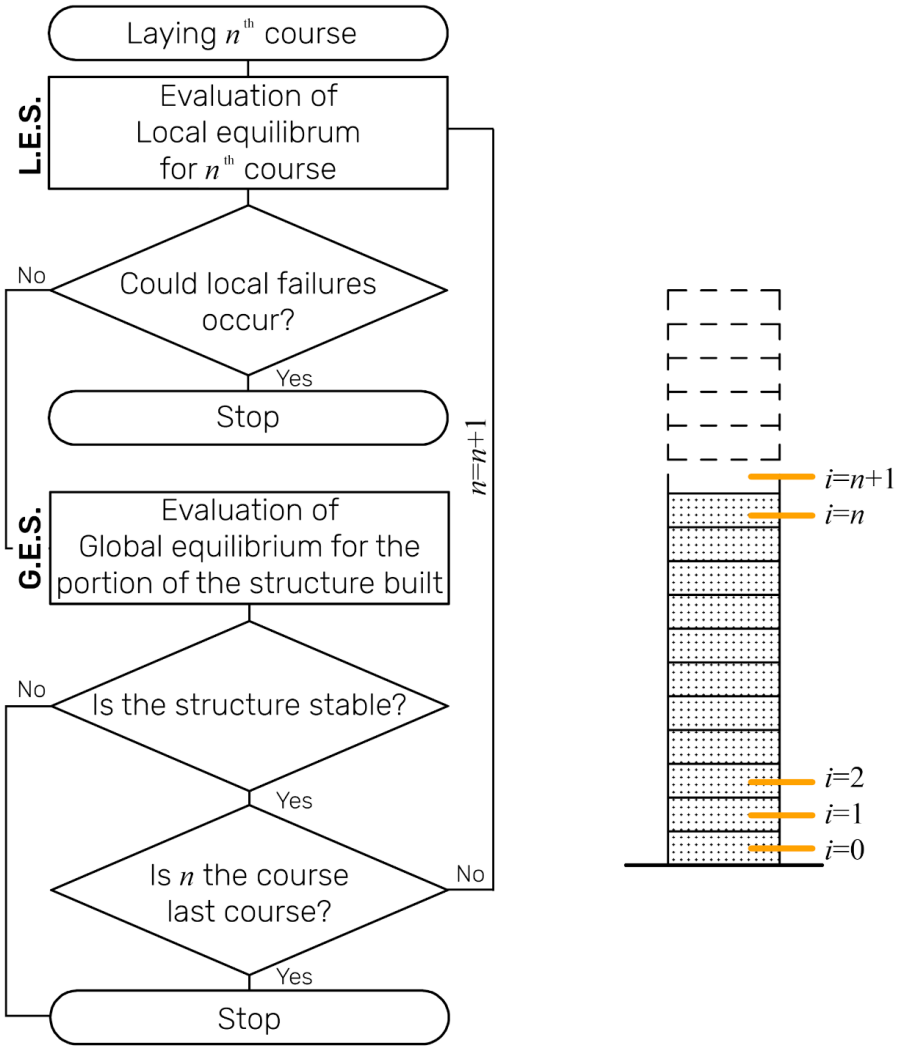

Figure 32: Flowchart to assess the equilibrium of a masonry structure during the construction (right), a model of a wall during the construction, the *i* index indicates the course, while *n* index the last stage built (left).

4.2.1 Local equilibrium step

To build a structure it is necessary to prevent any failures, even the local ones. The Local equilibrium step LES has the purpose of identifying and verifying any possible collapses of masonry blocks or portions of brickwork at the local scale. Thus, for each n^{th} construction stage, an analysis must be performed for determining the balanced state of the brick or portion of brick courses just laid (n^{th} course), and the balanced state of a portion of the structure. The choice of this portion concerns the type of structure considered and the building technology adopted, for example, for different structures like domes, arches, and tower present different critical issues during the construction could occur.

Thus, for different systems different time stages and portions of the structure should be considered for evaluation.

Despite that, some considerations which concern the construction of a generic structure can be formulated. For example, the sliding phenomenon could occur every time a brick is being laid on an inclined plane. In general, while laying the blocks in a structure, this block that is just laid is subject only to its-self weight, thus, the only failures that could occur are sliding or overturning. Further, if the **III.** Heyman's hypothesis (masonry has infinite compressive strength, chapter 2.2) is verified for the completed structure, it is also not violated for the simulation investigated. Additionally, the strains that occurs while placing the block are too small to lead to local failures. Hence, the study of the brick stability here can be considered equivalent to evaluating the equilibrium of a rigid body.

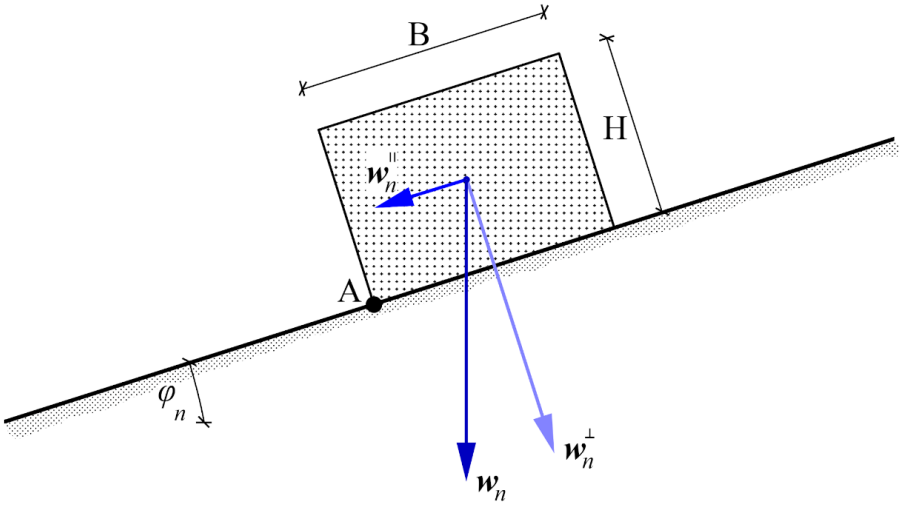

Figure 33: Block laid on the inclined plane at the n^{th} construction stage.

Referring to figure 33, for a given block, the weight is denoted by $\boldsymbol{w}$, with $\boldsymbol{w}^{\parallel}$, $\boldsymbol{w}^{\perp}$ respectively its components parallel and orthogonal to the inclined plane and μ the Coulomb's friction. The equilibrium of the block at the n^{th} construction stage is described by (1) and (2) [138].

$$\mu \cdot w_n^{\perp} \geq w_n^{\parallel} \tag{1}$$

$$\frac{B}{H} \cdot w_n^{\perp} \geq w_n^{\parallel} \tag{2}$$

Where H and B are the height and width of the block considered. The inequality (1) expresses the equilibrium condition at the translation of the block on an inclined plane, while (2) expresses the overturning equilibrium condition with respect to the point A. If both conditions (1) and (2) are verified, the system is balanced, while if one or both are violated, the block is in motion. Denoting the slope angle of the laying plane as φ, it is possible to express (1) and (2) in terms of φ:

$$\mu \cdot \cot\left(\varphi_n\right) \geq 1$$

$$\frac{B}{H} \cdot \cot\left(\varphi_n\right) \geq 1$$

Therefore, the study of the block equilibrium is related to the three geometric parameters B, H and φ, to the friction factor μ and the stage n. The limit condition for the equilibrium of the block is described by the equations (3) and (4).

$$\mu \cdot \cot\left(\varphi_n\right) = 1 \tag{3}$$

$$\frac{B}{H} \cdot \cot\left(\varphi_n\right) = 1 \tag{4}$$

For this analysis, the angle φ could assume values between 0 and $\pi/2$. In such a domain, the cotangent function is defined, and the nature of this function is continuous, strictly monotonically decreasing. Thus, independently of the values of B, H and μ, there exists a limit value of the angle φ for which the block is not stable. This value is called the limit angle of equilibrium and can be determined from (5).

$$\varphi_{n_L} = \left\{ \min\left(\varphi_n\right) \middle| \frac{B}{H} \cdot \cot\left(\varphi_n\right) = 1 \vee \mu \cdot \cot\left(\varphi_n\right) = 1 \; ; \; 0 < \varphi_n \leq \frac{\pi}{2} \right\} \tag{5}$$

For angles greater than the limit angle of equilibrium, (1) and (2) are violated, and failure occurs. The nature of the motion that causes this failure depends on B, H and μ and their relation to the angle of inclination φ. To be more precise, when corresponding to the limit angle of equilibrium, it is enough to study the relation as shown in (6) to understand the nature of this motion. If the (6) is verified, sliding occurs. Otherwise, the block fails due to overturning.

$$\frac{B}{H} > \mu \; ; \; \varphi_n = \varphi_{n_L} \tag{6}$$

Ultimately, the block's equilibrium condition is dictated by the condition described in (7), this condition is represented by the intersection of the areas illustrated in figure 34.

$$\frac{B}{H} \cdot \cot\left(\varphi_n\right) \geq 1 \wedge \mu \cdot \cot\left(\varphi_n\right) \geq 1 \; ; \quad 0 < \varphi_n \leq \frac{\pi}{2} \tag{7}$$

During the construction of simple arches, vaults or domes, the inclination of the plane increases through its construction stages, and the limit angle of equilibrium can exceed; thus condition (7) is eventually violated. In this case, the system represented in figure 33 is not able to supply all the

resources needed to avoid slippage or overturn. Therefore, when using traditional building techniques to construct these structures, formwork and shoring is required. Self-supporting technologies on the other hand aim to provide all resources needed to achieve the self-balanced state. Hence, when φ is greater than the limit angle of equilibrium, (7) cannot be valid and to express the block equilibrium a new relation should be found. The nature of this new relation depends on factors that rule the self-supporting technology adopted during the construction.

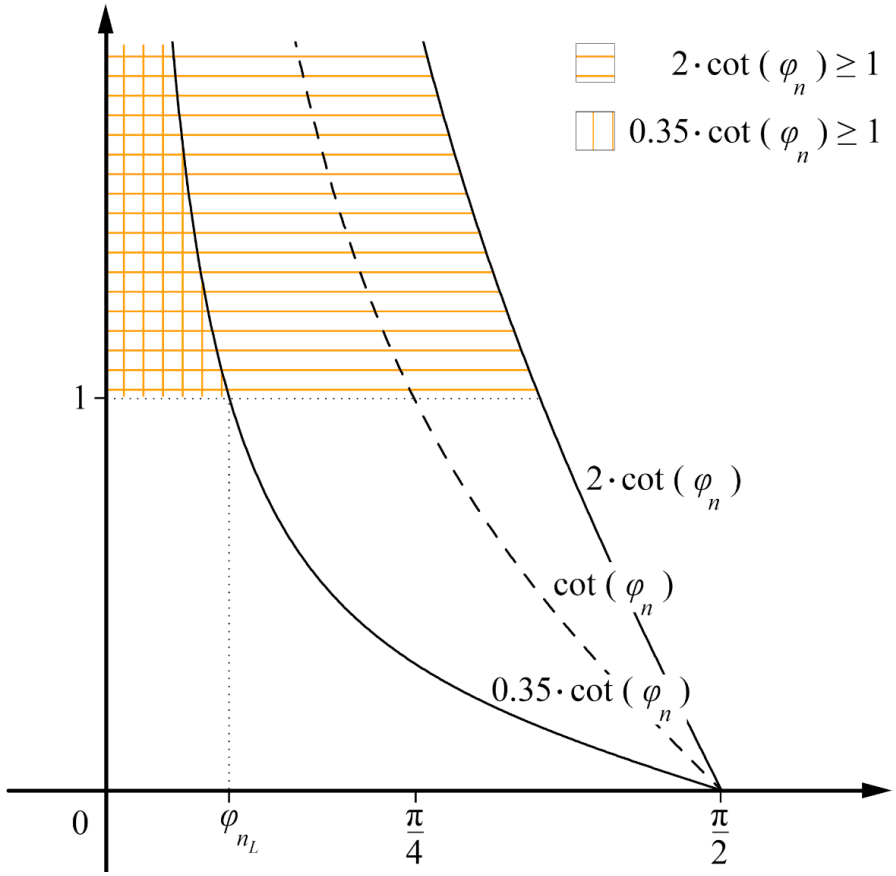

Figure 34: Representation of condition (7) and the limit angle of equilibrium determined by (6) (μ = 0.35 and Ratio B/H = 2).

It has to be noted that, relations (5), (6) and (7) do not consider the presence of any mortar, and they describe the situations where the joint are dry-joints, with an approximation that they can depict the situations in traditional construction processes where hydraulic mortar are used [139]. To represent structures built using fast-setting mortar, such as gypsum or epoxy, the relations (5) (6) and (7) should be adjusted by considering the cohesive capacity of mortar.

4.2.2 Global equilibrium step

The Global equilibrium step GES, as mentioned in chapter 4.2, aims to evaluate the stability of the entire built structure. Unlike “traditional” analyses, the evaluation of the state of the structure under construction must be performed several times, once for each construction stage. For example,

referring to figure 35 a), at the n^{th} construction stage, the equilibrium is determined by analysing the state of the elements that constitute all i courses already built, i.e., all courses between $i = 0$ up to $i = n$. Then, the GES must be repeated for all the construction stages, and only if a balanced state is determined for all the stages, it is possible to affirm that no failures occur. Further, to state this, the forces estimated in the LES must be compatible to the ones in the GES. Due to the scale of the analysis, the GES can be performed using traditional methods, such as graphic statics or numerical analysis.

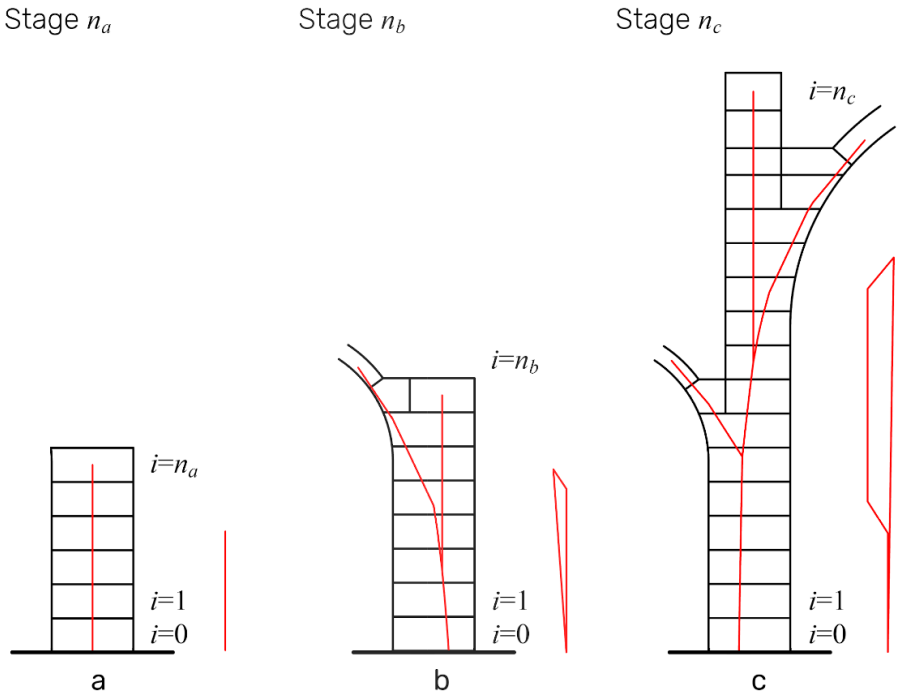

Figure 35: a), b) and c) G. E. S. for three different construction stages n_a, n_b, n_c The geometry of the structure changes during construction, the number I of course increases. For each stage considered, a balanced state is found.

5. Two-step approach: the cross-herringbone spiralling technology

The two-step approach, introduced in chapter 4.2, shows the logic for assessing the balance of masonry structures during their construction. It does not provide the exact tools suitable for performing analyses, but it broadly describes the steps (LES and GES) necessary for the evaluation of the behaviour of the structures.

In chapter 5.3, adopting this two-step approach, a detailed formulation for determination of the self-balanced state of domes built through the cross-herringbone spiralling technique is presented. Consistent with the previously determined factors in chapter 4.1, the developed formulation is an example on how this two-step approach can be applied in a specific building technology for the evaluation of the balance state, considering its governing factors.

Further, the existence of resistant sub-structures, such as arches and plate-bandes, is also proven by the numerical model illustrated in chapter 5.4. Numerical simulations developed with DEM are intended to describe the behaviour of cross-herringbone domes during construction, both in terms of displacements and brick configuretions, but beyond this to also verify the presence of these sub-structures.

The models on which the analyses, simulations and the formulation were carried out was derived from the study of the two domes Santa Maria in Ciel d'Oro and Simon Mago, as discussed in chapter 3.2. The digital models on which the numerical analyses are executed are presented in chapter 5.1. The models respect the geometric characteristics described in that previous chapter, as well as the analyses conducted taking into account the building factors as describe in chapter 4.1.

5.1 Geometry of the dome

The formulation developed in the following chapters has been applied to an octagonal dome, whose geometry consisting of eight identical sails, and it has been elaborated from the considerations discussed in chapters 3.2.2, 4.2.3 and 3.2.4. on the dome of Santa Maria in Ciel d'Oro. Despite this, under some conditions illustrated in chapter 5.3.2, adopting the same approach, different dome shapes could also be analysed. Appendix B is another example that reports these analyses performed on the hemispherical dome.

As describe in the previous chapter 3. And as shown in figure 20 and 36, the herringbone bricks are arranged in a radial manner and laid in regular intervals at the same plane to the horizontal bricks.

This geometric property is the key to understand the structural behaviour of the dome under construction.

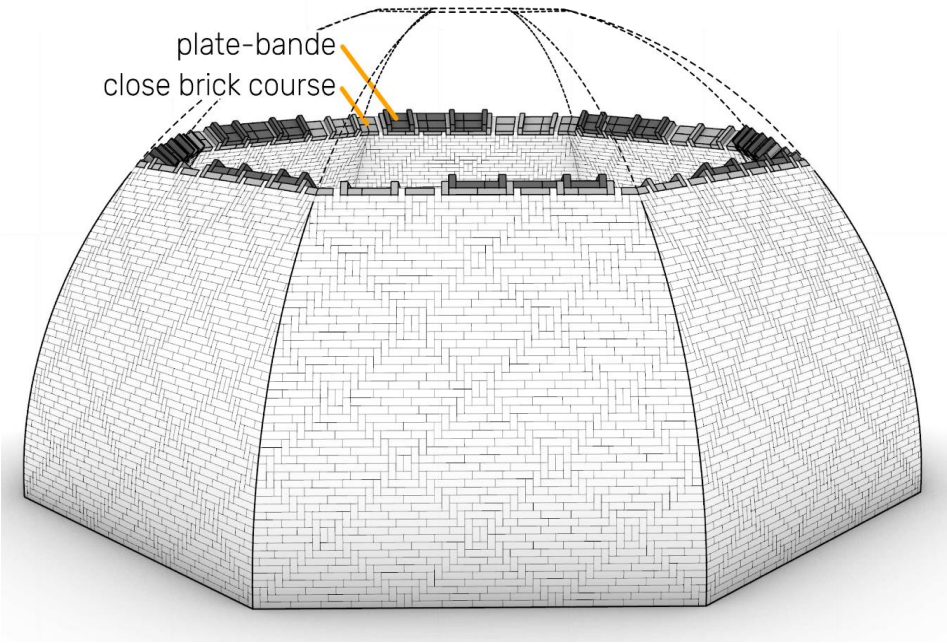

Figure 36: Octagonal dome during the n^{th} construction stage. The geometry of each block modelled are constituted by the mortar thickness and the brick geometry. The last complete brick course laid ($i = n-1$) is coloured light grey, while the one under construction, ($i = n$) is dark grey. From now on, this style it is adopted along the document.

5.2 The self-balance state of cross-herringbone domes

As already described, to understand how the cross-herringbone spiralling pattern allows the construction of a self-balancing dome, the analysis needs to be conducted at different construction stages. According to what is described in chapter 4.1, to achieve this objective, the primary building factors are considered in the analysis performed. Further, as described in chapter 1.4.2, it is assumed that the octagonal dome is built through complete courses, i.e., and only when the previous course is completed, the mason begins to lay a new course of bricks (Condition A).

Under construction, the local equilibrium state of a dome built through the cross-herringbone technique is characterised by two resistant sub-structures: the closed course structure (local 1) and the plate-bande structure (local 2). The first structure (local 1) manifests itself when the brick course is completed. The second structure (local 2), the plate-bande, occurs when the bricks are laid in a course which is not yet closed. Both structural systems are illustrated in figure 36 and numerically simulated for different construction stages. Meanwhile, the assessment for overall stability of the dome has also been performed; thus, it is possible ensuring a full evaluation at both the local and global equilibrium states.

At first, it is possible to divide the octagonal dome by vertical planes (meridian one) and evaluate only one of them during the construction works. Referring to figure 37, the sail analysed can be

represented by an incomplete voussoir arch shape, where each of the voussoir describes a brick. It is further assumed that friction about their interfaces is present, and the blocks can slip as a rigid body on an inclined plane, leading to overturning of the incomplete voussoir arch.

Using Coulomb's law of friction, the equilibrium can be expressed as relations given by (1) and (2) from chapter 4.2.1 and ultimately the balance condition provided by (7).

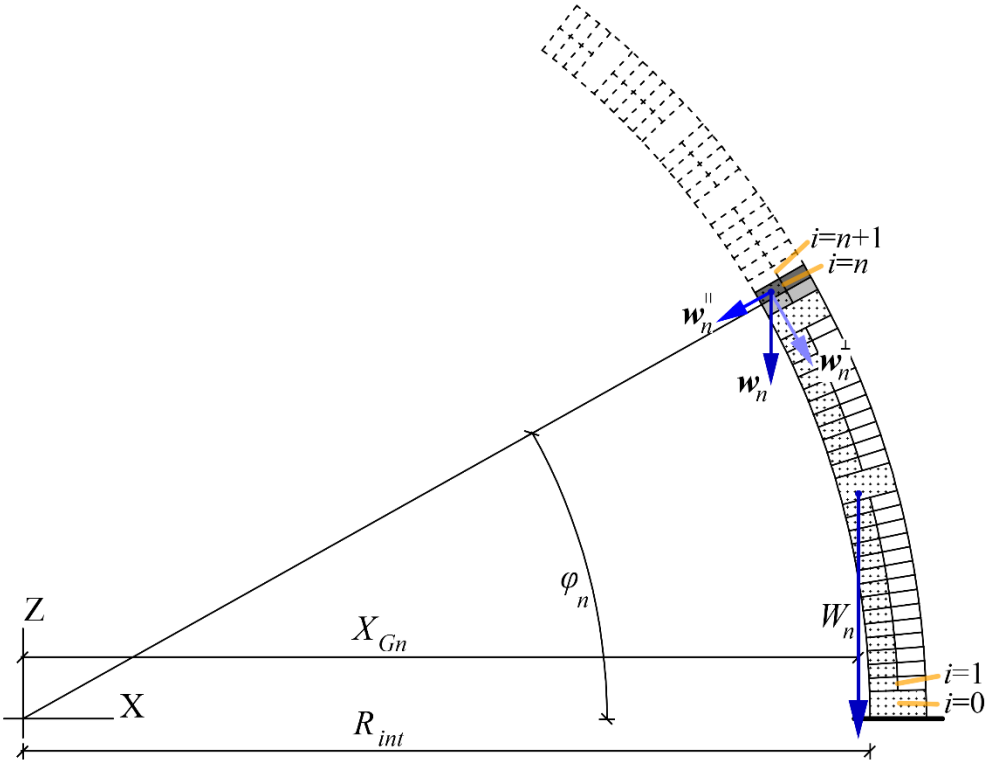

Figure 37: Meridian section of a dome: the incomplete arch and rigid bodies (n^{th} construction stage).

The second equation of equilibrium, which relates to the overturning moment of the incomplete voussoir arch about its springing, is formulated as:

$$X_{Gn} \geq R_{int} \tag{8}$$

where X_{Gn} is the distance from the origin to the centroid of incomplete voussoir arch, and R_{int} is the distance from the origin to the center of rotation of the voussoir arch (or springing), both defined by the X, Z coordinates system. The structure could be said to be in equilibrium, only if both inequalities given by (7) and (8), are verified. This is expressed by case 1 (S1):

$$\frac{B}{H} \cdot \cot\left(\varphi_n\right) \geq 1 \quad \wedge \quad \mu \cdot \cot\left(\varphi_n\right) \geq 1 \quad \wedge \quad X_{Gn} \geq R_{int} \; ; \quad 0 < \varphi_n \leq \frac{\pi}{2} \tag{S1}$$

Alternatively, if at least one of the two inequalities is not satisfied, the system of rigid bodies is not able to guarantee a self-balanced state. This can be expressed as case 2 (S2):

$$\frac{B}{H}\cdot\cot\left(\varphi_n\right)<1 \;\vee\; \mu\cdot\cot\left(\varphi_n\right)<1 \;\vee\; X_{Gn}<R_{int}\;;\;\; 0<\varphi_n\leq\frac{\pi}{2} \tag{S2}$$

In the case (S2), to achieve a balanced state, a system of auxiliary forces must be considered. The role of the cross-herringbone spiralling pattern is to provide such auxiliary forces system through the plate-bandes (local 2).

Therefore, during all construction stages, sliding and overturning of the bricks are avoided through, both, the construction of complete bricks courses, and the presence of plate-bandes. Referring to figure 34 and recalling the relationship between the dimensions of the bricks 1-α·1-2·α (α>1), it is possible to understand that the sliding is the first collapse phenomenon that could occur in such type of domes. Therefore, the limit angle of equilibrium is defined by (4). We define the limit course of equilibrium ($i = L$) as the first brick course in which the angle is greater than the limit angle of equilibrium. In the case analysed, the friction forces between the bricks are not sufficient to avoid slippage (S2) and at this limit course the bricks should slide towards the centroid of the dome. However, the presence of the herringbone bricks in the spiralling pattern prevents them from slipping, indeed when these bricks at the limit course try to slip, they collide against the previously laid herringbone bricks, which are fixed trough the lower course ($i = L$-1). This lower brick course is closed; hence it is stable. Further, even if the bricks of the lower course ($i = L$-1) try to slide, the same mechanism will be countered by the course laid before it, i.e., the previous course ($i = L$-2).

Within each of the brick courses, plate-bande sub-structures may be identified. Each of these are bounded by two herringbone bricks secured into the lower course. The plate-bandes act to prevent the failures by exerting a thrust against the herringbone bricks which further transmit it to the lower completed brick courses. Therefore, even in the case (S2) where the friction forces are not sufficient to ensure a state of equilibrium, the cross-herringbone spiralling pattern provides internal support so that the dome can be in equilibrium (local 2). These conclusions are further supported by the interpretation of the results of the DEM analysis reported in chapter 5.4. Thus, even during the construction, the equilibrium of the masonry dome can be achieved through different systems. Firstly, in the initial stages of construction, the equilibrium is provided by the system of friction forces (S1). In the later stages, when these frictional forces are insufficient (S2), the cross-herringbone spiralling pattern starts to operate, the structures of the closed brick courses (local 1) and the plate-bandes (local 2) provide the auxiliary forces required to maintain the static equilibrium of the dome under construction.

5.3 Limit analysis for the building phase

Two methods are adopted to analyse the equilibrium states of the spiralling cross-herringbone dome. Both are based on the limit analysis: the thrust line method (TLM) and the modified thrust line method (MTLM) [87] [140]. The three hypotheses given by Heyman introduced in chapter 3.2 are assumed at the base of these analyses [2]. In traditional constructions, the completed masonry domes experience stresses of one order of magnitude lower than the masonry's crushing strength. However, it will be shown in Appendix B, that during construction their value might be larger than the ones that occur post construction. Despite this, the stresses remain significantly lower than that of masonry's crushing strength. Hence, for this study, the assumption of infinite compressive strength (**III.**) is valid as the internal compressive stresses are very low. During construction, when the bricks are being laid, sliding may occur. This sliding, however, relates to the settlement needed to reach an equilibrated state, rather than to enable motion or to lead to a collapse. Therefore, the limit state analysis can be applied, and no significant motion is seen manifested. In the analyses executed a finite value of friction angle is also considered [104].

According to the Safe Theorem [2], the equilibrium of the dome is guaranteed if a thrust line exists that lies entirely within the cross-section of the dome. Therefore, a two-step approach consisting of LES and GES for evaluating the state during the construction works, is adopted. The analyses have been performed for different construction stages, for each stage the TLM and MTLM are executed. The TLM aims to verify the equilibrium of the completed courses (local 1) and the plate-bandes, i.e., during the laying operation (local 2), that is LES. While the overall equilibrium of the dome under construction is assessed using the MTLM (global 1) which corresponds with GES. For this study, both the graphic static methods (TLM and MTLM) have been fed into the graphical editor algorithm Grasshopper for Rhinoceros software.

5.3.1 LES and GES for cross-herringbone dome

As introduced in chapter 4.2, to uniquely identify the brick courses the subscript *i* has been assumed, but within each course, several plate-bande structures exist. Therefore, as shown in figure 38, to identify every plate-bande structure, the *j* subscript has been adopted. Considering one of any courses and referring to figure 38, the subscript *j* is equal to zero at the southern edge of the east sail of the dome, and the value of *j* increases in the anti-clock direction.

The two-step approach, which has been developed to perform the equilibrium state analysis of the cross-herringbone dome (both local and global) under all construction stages, is summarized in the flowchart in figure 39. First, for each n^{th} construction stage the bricks are verified for their self-balanced state (S1). If this is not verified, the analyses are performed to assess the state of the sub-

structure: the plate-bande and the closed brick courses (LES), and subsequently the whole constructed portion of the dome is evaluated (GES). Following this, all *j* plate-bandes at the laying course are evaluated. Once the thrust of all plate-bandes in that laying course is computed, the stability of the compressive rings of the underlying closed brick course is verified. Finally, the overall equilibrium of the dome is verified using MTLM approach, illustrated in figure 39. This process is repeated for all construction stages until the last course is laid.

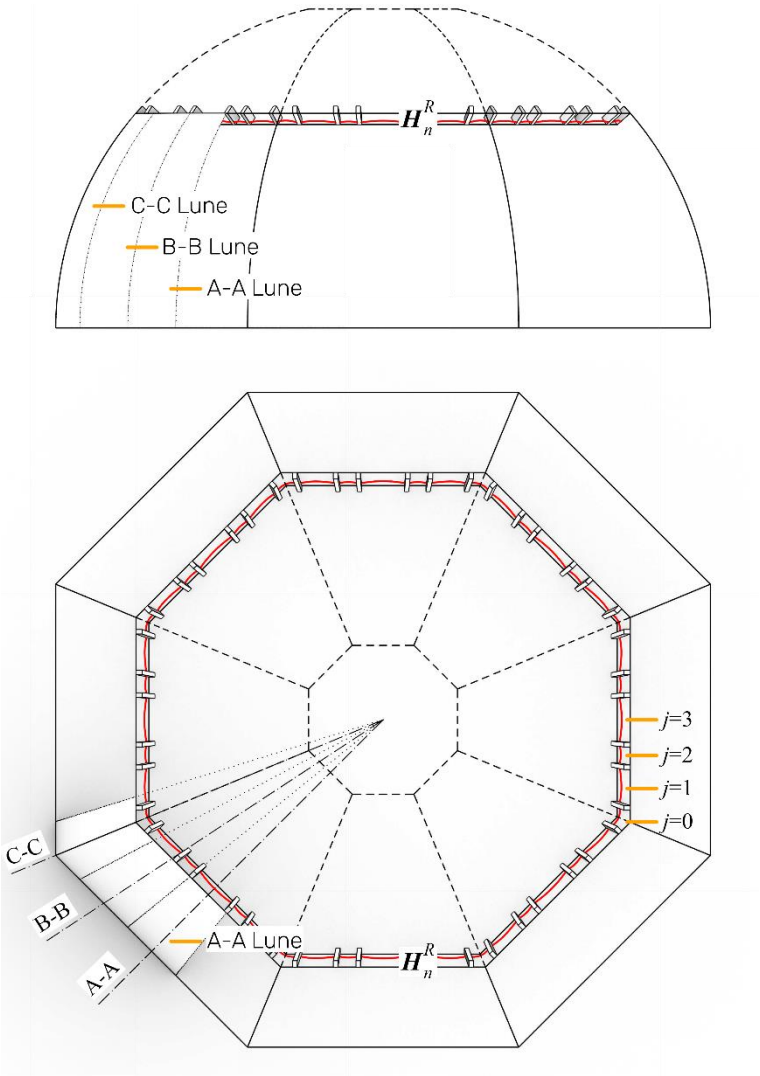

Figure 38: Elevation (top) and plan view (bottom) of octagonal dome under construction. In the plan view: enumeration of plate-bandes within a course, and closed brick course resulting in the n^{th} compression ring (highlighted red). Lunes: A-A, B-B, C-C (plan view and elevation) and their middle section (plan view

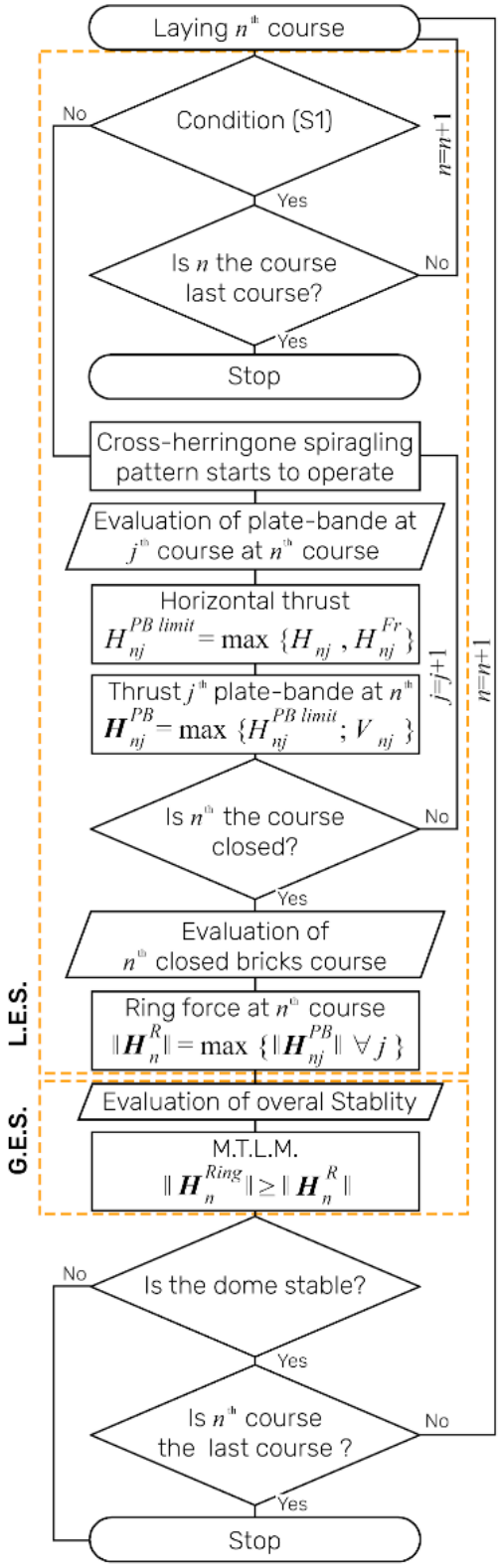

Figure 39: Flow chart of two-stepped approach for cross-herringbone spiralling technique applied to build a dome.

5.3.2 Plate-bande (LES)

The plate-bande is a straight arch and, because of its geometry, it is impossible to find a collapse mechanism, hence, the maximum thrust of the plate-bande structure is related to the crushing strength of the bricks. The thrust of plate-bande can be defined through considerations of equilibrium. Two formulations have been adopted and both evaluate without considering friction on the laying plane (i.e., the bricks are laid onto a smooth surface). This, however, is a conservative assumption and actually, the bricks and mortar bed would facilitate both frictional resistance and cohesive capacity. The first formulation respects all Heyman's assumptions, (**I.**), (**II.**) and (**III.**) discussed in chapter 2.2. The limit thrust is related to the loads applied, the length, and thickness of the plate-bande [141]. The length of plate-bande is a function of its location in the dome (i.e., the higher up in the dome, the smaller its length) and it also depends on its position within the course. We define the brick dimensions as multiples of b: b the height (1), 2b the width ($\alpha \cdot 1$) and 4b the length ($2 \cdot \alpha$) (in the model b=6 cm) and the ρ density of bricks. The horizontal thrust H and the vertical thrust V are evaluated through the equilibrium equations (9) and (10) by considering only the parallel component of the self-weight to the φ (the laying plane).

$$w_{nj}^{\parallel} = 2 \cdot \left(l_{nj1} + l_{nj2} \right) \cdot b^2 \cdot \rho \cdot sin\left(\varphi_n \right)$$

$$H_{nj} = \frac{w_{nj}^{\parallel} \cdot l_{nj1}}{32 \cdot b}$$

$$H_{nj} = \frac{\left(l_{nj1} + l_{nj2} \right) \cdot l_{nj1} \cdot b \cdot \rho \cdot sin\left(\varphi_n \right)}{16} \tag{9}$$

$$V_{nj} = \left(l_{nj1} + l_{nj2} \right) \cdot b^2 \cdot \rho \cdot sin\left(\varphi_n \right) \tag{10}$$

Referring to the n posing in time, the loads carried by the plate-bande are derived from the component of self-weight parallel to the laying plane as illustrated in figure 40. The other approach adopts a finite friction angle and no sliding assumption. Using equation (13), it is possible to evaluate the horizontal thrust H^{Fr}. To differentiate it with respect to the horizontal thrust calculated by equation (9), which relies on the Heyman's assumption of infinite friction, the Fr in the superscript (13) that denotes the horizontal thrust defined by considering the friction between the faces of herringbone bricks. As shown in figure 40, the herringbone bricks have a radial arrangement, with their long side not running parallel to the normal of the imaginary surface of a cylindrical sail. Hence, referring to figure 41, β angles are defined. These angles are bound by the normal of the imaginary surface of the cylindrical sail and the long side of herringbone bricks, Φ is the friction angle and the γ angle which describes

the inclination of the thrust with respect to the intrados of the sail (11). To avoid sliding of the bricks, the γ angle must be defined as described in (12).

$$tan(\gamma_{nj}) = \frac{V_{nj}}{H_{nj}^{Fr}} \tag{11}$$

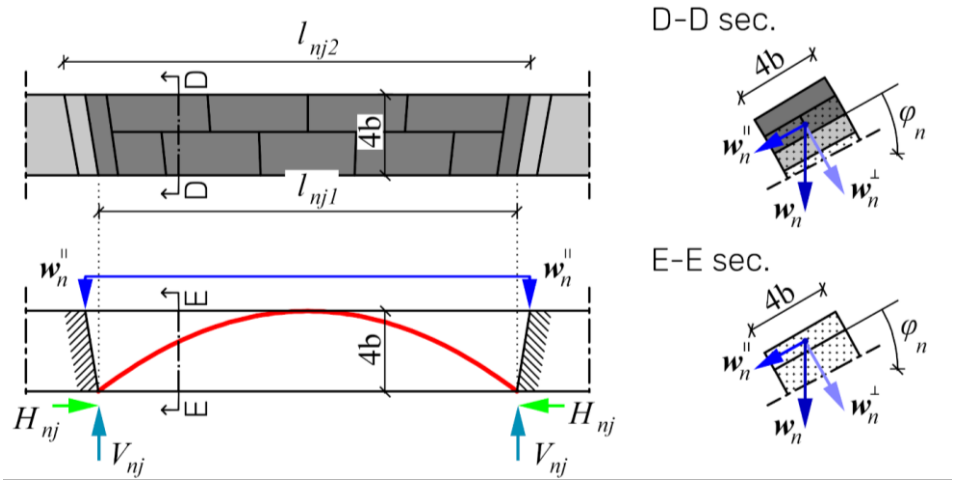

Figure 40: Plate-bande at the n^{th} course. Plan view (left) and section (right), the graphical representation (top) and free body diagram (bottom).

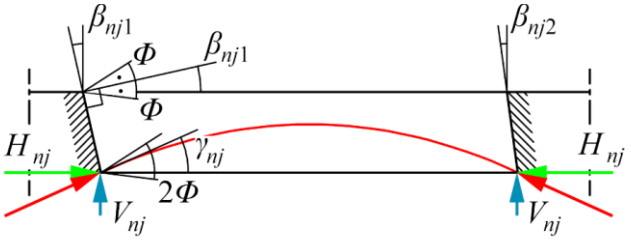

Figure 41: Plate-bande. Angles: β, γ and Φ and a thrust line in red.

The limits horizontal thrust which prevents slipping can be determined considering by equations (13).

$$\beta_{njk} - \phi \le \gamma_{njk} \le \beta_{njk} + \phi \qquad k = (0, 1) \tag{12}$$

$$H_{njk}^{Fr} = \frac{(l_{nj1} + l_{nj2}) \cdot b^2 \cdot \rho \cdot sin(\varphi_n)}{tan(\beta_{njk} \pm \phi)} \qquad k = (0, 1) \tag{13}$$

Equation (13) provides an estimate of the minimum horizontal thrust and the maximum horizontal thrust, but in the present formulation, the maximum horizontal thrust is neglected. Even if we assume a low angle of friction (e.g., Φ=20°) the octagonal geometry of the dome does not allow the consideration of maximum horizontal thrust defined by (13). In fact, the values of the β decrease from the base to top dome and by corresponding of the limit course (i=L), defined in chapter 5.2, even assuming γ = 0° the condition (12) is verified. Hence the (13) assumed is given as:

$$H_{njk}^{Fr} = \frac{\left(l_{nj1} + l_{nj2}\right) \cdot b^2 \cdot \rho \cdot sin\left(\varphi_n\right)}{tan\left(\beta_{njk} + \phi\right)} \qquad k = (0, 1)$$

The limit horizontal thrust in the plate-bande at the time of laying the bricks can be defined as the maximum horizontal thrust (14) required by the two approaches expressed in equations (9) and (13), thus:

$$H_{nj}^{PB\ limit} = max\{H_{nj}\ ,\ H_{njk}^{Fr}\ \ \forall\ k\} \tag{14}$$

At the sail edges, where the two laying planes intersect each other and result in a geometric discontinuity (or fold line), a component of the thrust of the plate-bande pushes the dome outwards. However, the symmetry of the dome about this fold line, the reinforcements (that exist in the real structures) and the loads acting, the outward component of the thrust does not lead to failures. The $\boldsymbol{H}^{PB}$ thrust which acts on herringbone bricks laying on the previous layer is defined as:

$$\boldsymbol{H}_{nj}^{PB} = \left(H_{nj}^{PB\ Limit}\ ; V_{nj}\right) \tag{15}$$

The formulation presented (10) (13) (14) (15) is also validated for hemispherical domes. In fact, figure 42 shows the possibility of tracing a straight line which lies entirely within the thickness of the dome which is bounded by two consecutive herringbone bricks.

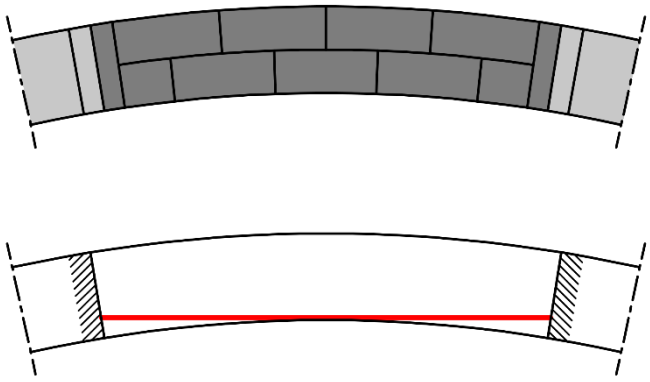

Figure 42: Portion of a hemispherical dome (radius 3.5 m), the straight line (highlighted red) of thrust lies entirely in the geometry, thus no cinematic mechanism can be individuated.

This geometrical peculiarity indicates that, although the geometry of the dome is hemispherical, the sub-structures can be described by plate-bandes. This statement is also complying to (13), i.e., considering a finite friction value (Φ=20°), even in the case of a modest dome, the (12) is verified. Considering that S^{Fr} denotes the limit span which allows describing the structural behaviour of arches as plate-bande, or hemispherical dome with inner radius 3.5 meters, this S^{Fr} corresponds of a value greater than 2 meters. On the other hand, as presented in chapter 3.2.2, the maximum distance between two consecutive loxodromes is lesser than 2 meters, thus a plate-bande behaviour is within the

acceptable limits. Figure 43 shows the limit condition to define the S^{Fr}, when $\beta = \Phi$ if $\beta > \Phi$ the maximum horizontal thrust must be considered.

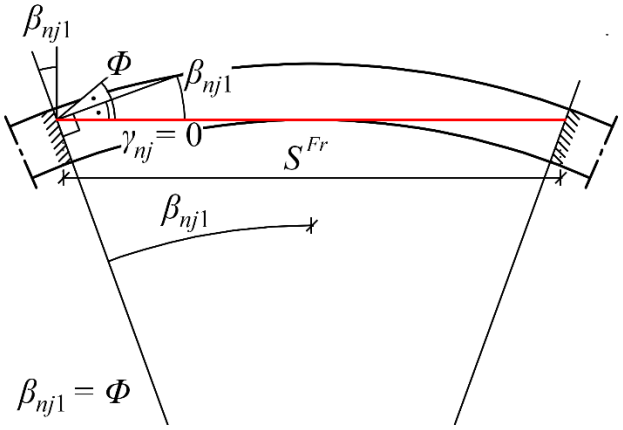

Figure 43: Plate-bande mechanism and a portion of a hemispherical dome (radius 3.5 meters, γ=0° and $\beta_{nj1} = \beta_{nj2} = \Phi$ = 20°). If S the span of arch, defined by two herringbone bricks, is greater than S^{Fr}, the limit span, than the maximum horizontal thrust is derived by condition (13).

5.3.3 Closed brick course (LES)

At the n^{th} construction stage, once the entire n^{th} bricks course is completed, a spatial compression ring is formed as shown in figure 38 (highlighted red). The magnitude of the ring force is estimated as the maximum thrust present in all the plate-bandes at the n^{th} course or:

$$\| \boldsymbol{H}_n^R \| = max\{ \| \boldsymbol{H}_{nj}^{PB} \| , \forall j \} \tag{16}$$

When the next course is positioned (n+1), the value of compression force in the n^{th} completed ring and in the underlying completed rings changes. To determine these ring compression forces, other approaches need be adopted. For example, the contribution of the normal component of the self-weight of the bricks can be considered, in such manner the friction forces increase, and the compression forces required to prevent sliding decrease. Another possible evaluation involves the variation of the plate-bande horizontal thrust caused by the slight incline at which the herringbone bricks are laid and their effect on the underlying closed brick courses. However, due to the hyperstatic nature of the closed brick courses, all approaches proposed under this hypothesis do not allow for the quantitative definition of the equilibrium state of the rings, but only give a qualitative definition. Therefore, equation (16) allows us to compute the compression force value in the ring at the nth course at the nth construction stage.

5.3.4 Overall stability (GES)

The compressive forces in the closed brick courses act as hoop forces in domes of revolution. Thus, to evaluate the overall stability of the dome it is possible to assume the existence of a membrane

behaviour and to determine a balanced surface [135]. Such surface depends on the compressive forces on the closed brick courses and due to the brick's self-weight. To estimate the balance surface, we adopt MTLM. The MTLM combines Heyman's theory and membrane theory [142]. To perform the analyses with this method the loads must be uniform and axisymmetric. As shown in figure 38 (lunes representative A-A, B-B, C-C,) the octagonal dome is sliced by meridian planes into 32 lunes. For example, this slicing is done considering that the A-A section of A-A lune lies in the plane of symmetry of the sail. The balance surface is identified through the thrust traced in all different sections (for example sections A-A, B-B, C-C in figure 38) one for each different lune, thus the thrust in all different sections needs to be assessed.

As denoted in chapter 5.3.3, the compression ring forces of each closed brick course are constant, exactly as the hoop forces in domes of revolution. Therefore, to trace the thrusts, one for each section, the same distribution of compressive ring forces must be considered. In domes of revolution that are under axisymmetric loads, the geometry of the hoop forces are described by circles, thus the hoop force can be described through their x-component Δh^{xHoop} and the angle ϑ (17), which is the half angle defining a lune measured on a horizontal plane as shown in figure 44.

$$\| \boldsymbol{H}_i^{Hoop} \| = \frac{\Delta h_i^{x\ Hoop}}{2 \cdot sin(\vartheta)} \tag{17}$$

However, in the octagonal dome under study, the actual geometry of rings compressive forces is not known they are affected by dome's geometry and by bricks pattern. Even from observing the spans of plate-bande structures, whose lengths vary from course to course, it is clear, that the shape of ring forces is affected by their shape. Thus, we assume that the ring forces H^{Ring} act normal to the lunes side faces, namely, the *x* component of ring forces can be described by the relation (18).

$$\Delta h_i^{x\ Ring} = 2 \cdot \| \boldsymbol{H}_i^{Ring} \| \cdot sin(\vartheta) \tag{18}$$

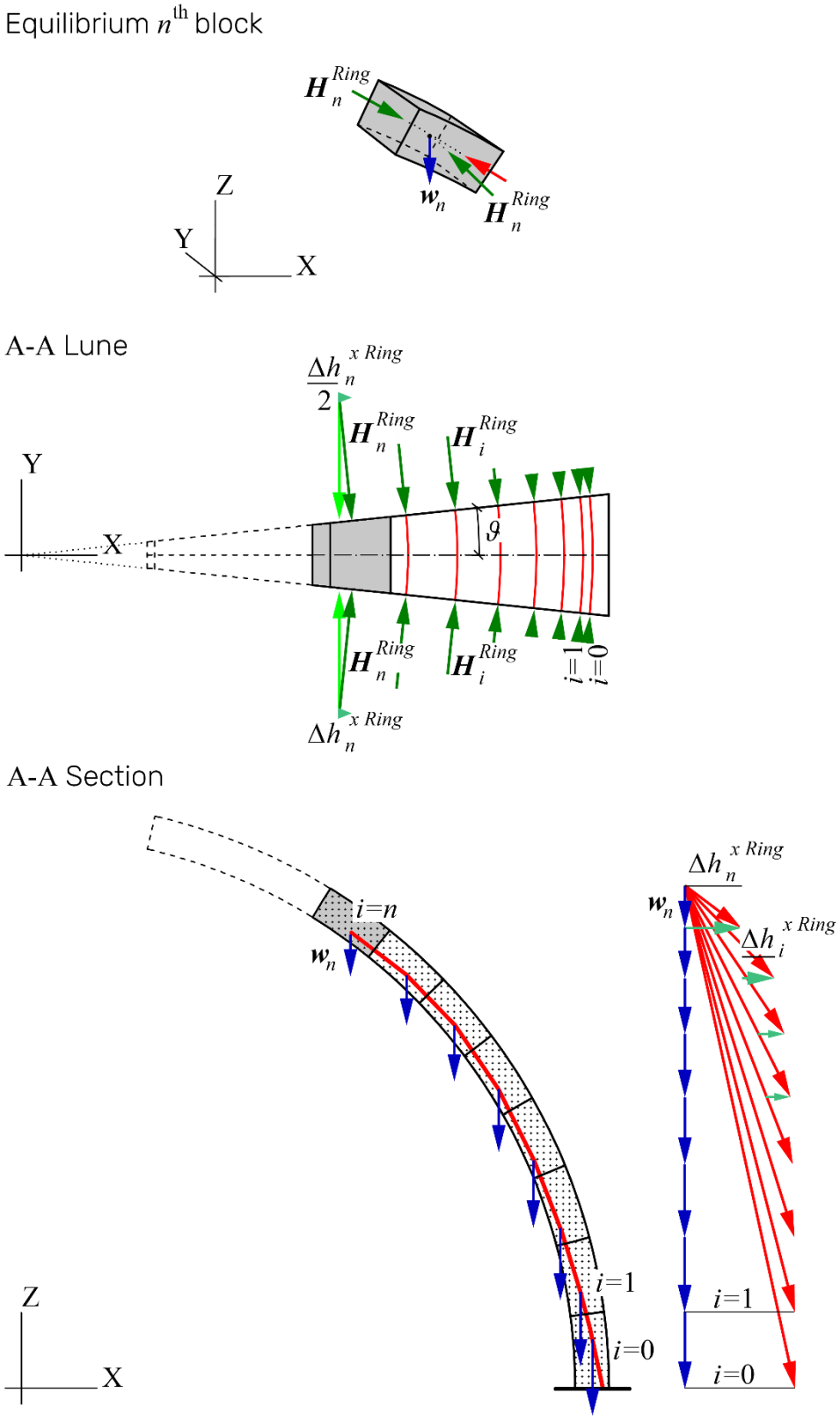

Figure 44: MTLM for A-A lune at the n^{th} stage: equilibrium of the n^{th} wedge-shaped element (top), plan view of A-A lune and ring forces (center), A-A section and thrust line (bottom).

This adopted relation does not rely on the description of the actual geometry of ring forces, but it is based on the principle of equilibrium. According to the Safe Theorem [2], the real shape of the

compressive rings is not significant, as long as the thrust line of the ring lies entirely within the thickness of the brick courses.

To prove the stability of the dome under construction, we compute the thrust at different construction stages. For each construction stage, the thrust line has been evaluated, at first the section A-A, shown in figure 44, subsequently, for sections B-B and C-C at the same construction stage (sections A-A, B-B, C-C are referred to figure 38). To calculate the thrust for sections B-B and C-C, the same distribution of ring forces found in section A-A is assumed. At the n^{th} construction stage, to guarantee that the ring forces are sufficient to provide the forces required to achieve a stable equilibrium state of the n^{th} closed bricks course, the inequality (19) must be satisfied:

$$\| \boldsymbol{H}_n^{Ring} \| \geq \| \boldsymbol{H}_n^{R} \| \tag{19}$$

Therefore, if all thrusts are compatible with the Safe Theorem and the inequation (19) is verified, we can affirm that the dome is in a balanced state.

5.4 The numerical model

The state of the dome under construction have also been verified through DEM numerical analysis. The dome analysed has been modelled in the commercially available software 3.D.E.C. (Itasca, Minneapolis, MN, U.S.A.) based on a Discrete Element Modelling (DEM) approach [99].

As introduced in chapter 2.3, discrete element method is a numerical method where discontinuities can be represented; consequently, the masonry can be modelled in each of its parts: the bricks and the joints. In this numerical analysis the structure is described through a system of discrete rigid bodies (the bricks), and their interfaces (the joints). Adopting a central finite-difference procedure, the behaviour of the system of rigid bodies is calculated by the explicit integration of the motion laws (20) (21), where (20) equation describes the translational motion law, while (21) equation corresponds to the rotational motion law, and k subscript denotes the k^{th} centroid of rigid body of the system modelled. The sliding, the overturning, the collision, and detachment of the rigid bodies can be simulated.

$$\ddot{x}_k + \alpha \dot{x}_k = \frac{F_k}{m} + g_k \tag{20}$$

$$\dot{\omega}_k + \alpha \omega_k = \frac{M_k}{I} \tag{21}$$

In the model, each rigid body is constituted by the composition of an actual brick, see chapter 3.2.3, and a portion of mortar which surrounds it. Therefore, the laws which define the connection of the joints should consider average deformations of mortar and bricks together. In the analyses performed, a Mohr-Coulomb constitutive model has been implemented to represent the mechanical behaviour of

the joints, with no cohesive strength, finite compressive strength, and no tensile strength. Three penalty coefficients govern the behaviour of the interfaces are given by *jKn* - the joint normal stiffness, *jKs* - the joint shear stiffness and *Φ* [109]. The *jKn* coefficient describes the resistance while pressing two blocks against each other: it rules the intensity of the distributed compressive force that occurs at a unit depth of penetration between the two bodies [111]. The shear stiffness of the contact is also ruled by this coefficient. It also ensures that when a slight increment in relative displacement occurs between two blocks in the tangential direction, a countering a tangential force occurs, whose value is equal to the product of displacement and tangential stiffness. This prevents the contact from any unrestricted sliding [111]. The last parameter *Φ* is the angle for calculating the Coulomb friction coefficient.

All simulations performed have the purpose of evaluating the state of structures during the construction, following the two-step approach, the first simulation performed is focussed to assess the stability of the plate-bande, whose results are reported in chapter 5.4.1. The second step illustrated in chapter 5.4.2 and in Appendix C, the simulations conducted aims to establish the overall dome behaviour under construction.

5.4.1 Plate-bande numerical analyses

The numerical tests conducted for the plate-bandes (PB test) (**LES**) have the purpose of verifying the balanced state of the plate-bande during the construction. Thus, to simulate different construction stages various inclinations of φ (the inclination of the laying plane) have been taken into consideration, as reported in figure 45.

The volumetric mass assumed in all analyses is equal to 2000 kg/m^3 and the gravitational acceleration considered is g=9.81 m/sec^2. Due to the specific goal of the analyses performed, except for the self-weight no other loads have been considered. The values assumed for the penalty coefficients *jKn* and *jKs* are not constant and as the research conducted in last decades suggests, several theories addressing these were developed [108] [143]. To be rigorous and for respecting the composite characteristics of the rigid bodies modelled, these values should be defined through a weighted average of mechanical and geometrical properties of joint mortar and bricks. Nevertheless, abiding by the aim of the PB tests (verify the stability of plate bande structure) and due to their low influence in the stability with respect to the role of the Coulomb coefficient, it was found that these values can be assumed from literature on similar assessments [108] [111] [144]. The implemented values are E=36 GPa and G =21 GPa, thus the values of penalty coefficients adopted are *jKn*=135 GPa/m, *jKs*=11 GPa/m.

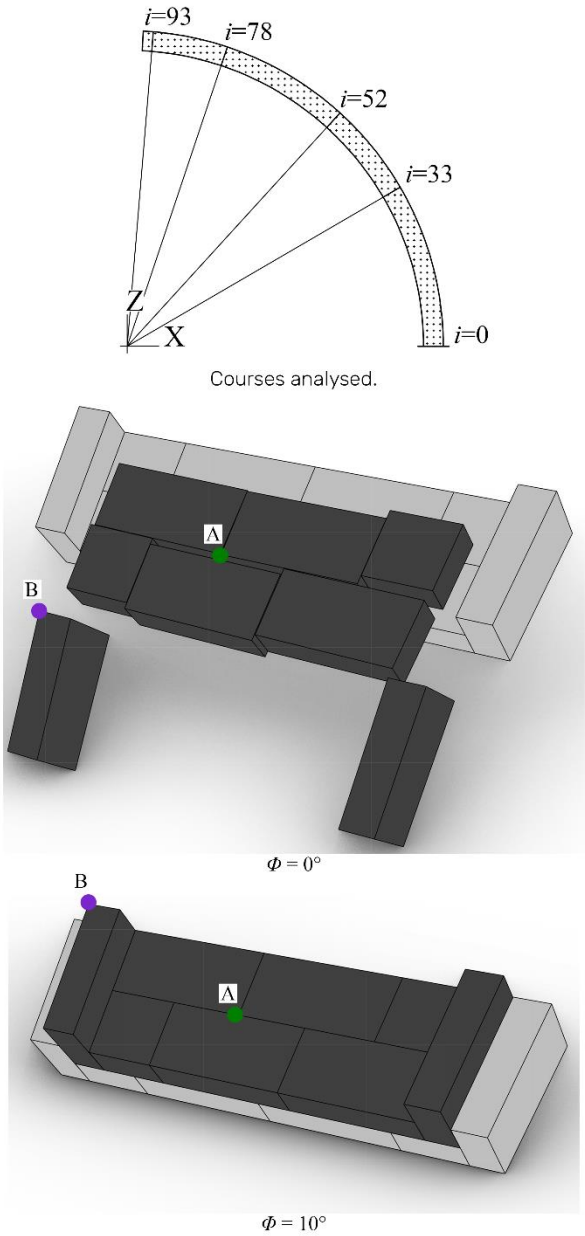

Figure 45: (from top to bottom) Courses analysed for PB tests; plate-bande during collapses (*i*=52, *φ*=47°, *Φ*=0°); plate-bande equilibrates (*i*=52, *φ*=47°, *Φ*=10°).

The influence of *Φ* (the friction angle) has been detected evaluating a variety of values: 0°, 10°, 15°, 20°, 40°, 60°, 80°, 90° for each plane laid; the results of the PB tests shows that the stability of plate-bandes is related to the *Φ* and to the angle of inclination of laying plane. As reported in figure 45 (bottom), if the *Φ* is equal or larger than 10°, the plate-bande structures are stable. The results also show that with low angles of *φ* (the inclination of the laying plane), corresponding up until the course *i*=33, the equilibrium of plate-bandes structures is not related to the *Φ*. These results are presented in Table 2.

The main outputs recorded through the numerical simulations are these three: the displacement, the z component of velocity (z-velocity) and the unbalanced force. The first two elements are directly

related to the motion of the discrete system, they provide information about the motion of specific points of the structure observed.

		Φ	
	φ	0°	⩾10°
i= 33	30°	stable	stable
i= 52	47°	unstable	stable
i= 78	71°	unstable	stable
i= 93	86°	unstable	stable

Table 2: Stability of plate bande.

Referring to figure 45 for each simulation, displacement and z-velocity are registered for two points (A and B), (B) the first is adopted to illustrate the motion of herringbone bricks and the other (A) for recording the behaviour of the horizontal bricks.

The unbalanced force represents the summation of all nodal forces for each time-step of simulations, for static analyses, this unbalanced force furnishes global information regarding the state of the system. Theoretically, when the equilibrium state reaches the net nodal force, the resultant at the centroid of all rigid bodies is zero, thus the unbalanced force is zero. Nevertheless, for numerical analyses, such quantity tends to zero, but practically this will never reach zero. The discrete system of rigid bodies can be assumed to be at equilibrium when the magnitude of the maximum unbalanced force is small enough when compared to the representative forces of the previous problem [99].

figure 46 reports the variation of three quantities (unbalanced force, displacement, and z-velocity) calculated for the plate-bande illustrated in figure 45, during the simulations. For all graphs the x-axis reports the time-step of analyses, a parameter which describes the progression of the simulation. The y-axis illustrates the quantity recorded.

The first graph reports the evolution of the unbalanced force, the red line describes the behaviour of plate-bande analysed with Φ that is 10°. In this case, after few time-steps a peak occurs then the unbalanced force moves to zero.

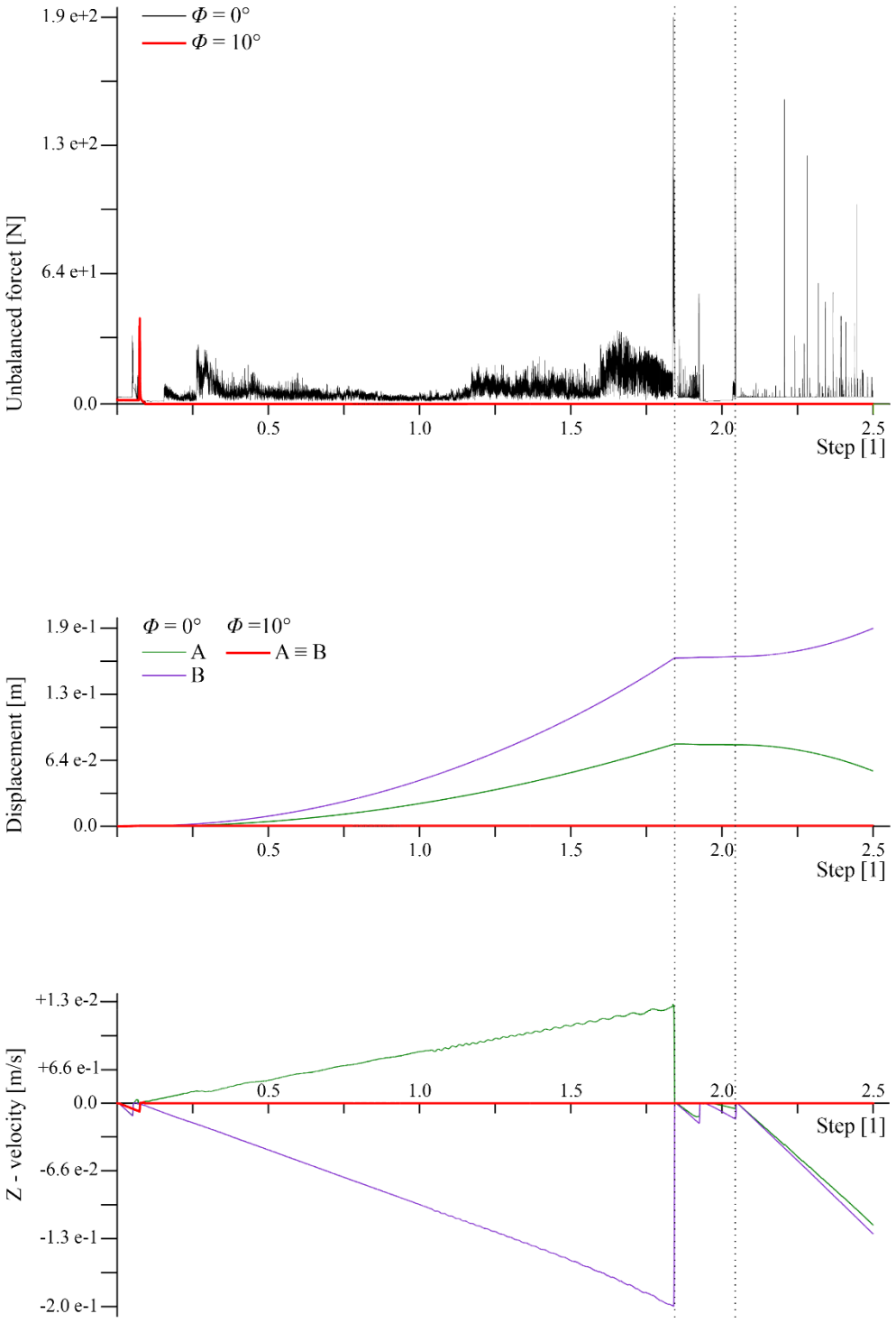

Figure 46: Graphs for evaluating the state of a plate-bande represented in figure 45. From top to bottom: unbalanced force, displacement, and z-velocity.

Consequently, the structure is balanced, after an adjustment phase, where the rigid bodies act against one another. This behaviour is also shown in the z-velocity graph where, with respect to the unbalanced peak force, the z-velocity is not zero, but, after that, this quantity becomes zero and no motion occurs. Instead, the displacement graph is practically zero all through the simulation. In the simulation conducted with Φ=0°, the unbalanced force never attains the zero and z-velocities of the

A and B points fluctuates. At the beginning of the numerical analysis, the two z-velocities have opposite signs, but then the sign of z-velocity at point B changes and both quantities are negative. This indicates that the vertical blocks, which represent the herringbone bricks, push the horizontal elements towards the plate-bande, while they slide on the inclined plane in the opposite direction. After a few steps even the horizontal blocks slide down.

The displacement graph is coherent to the behaviour described. On the graph three different phases are readable: the first in which displacements at A and B increase, the second corresponds to the inversion of motion and the last one where the displacement at A decreases because the horizontal blocks slide on the laying plane. Due to the small number of rigid bodies modelled in the PB Test, all of which are involved in an eventual collapse, it can be assumed that the system is balanced when the z-velocity of even just one point is zero and constant for a finite time interval.

5.4.2 Numerical analysis of dome under construction

Following the two-step approach presented in chapter 4.2, once stability of plate-bande through the PB Tests is verified, two other structures are evaluated for different construction stages (n): the closed bricks course (CBC Test) (LES) and the dome under construction (DUC Test) (GES).

Two geometrical models have been evaluated: the octagonal dome of Santa Maria in Ciel d'Oro, and a hemispherical dome with similarities to Simon Mago. Both systems of rigid bodies are constituted by blocks with dimensions corresponding to their brick's dimensions, as described in chapter 5.4.1. The masonry patterns adopted coincide with the pattern formed by cross-herringbone spiralling technique.

Both types of numerical analyses (CBC Test and DUC Test) have been conducted simulating the construction process, i.e., adding one bricks course upon another. Once the equilibrium state has been reached for a given completed course, the next one is added, and the overall analysis is performed again to assess the stability of the new overall structure built. This process evaluates the stability relative of the new construction stage.

The graph presenting the unbalanced forces recorded in these analyses, shows numerous peaks, at least one for each brick course. The first graph shown in figure 47 illustrates the evolution of this quantity recorded for the octagonal dome analysed, while the other two graphs represent the unbalanced force of the same structure recorded under different conditions. The central graph refers to a complete dome analysed applying g = 9.81 m^2/s, while the graph at the bottom describes the case of the gravity value is applied in different time intervals, i.e., first g = 0.981 m^2/s, then g = 1.96 m^2/s up to g = 9.81 m^2/s, reflecting the formwork removal operations. The temporal evolution of the unbalanced force in the three graphs reflects of the nature of simulations, with the alternation of peaks

and flat sections readable in the first diagram correctly describing the evolution of the state of equilibrium during the construction stage of the dome built without the aid formwork.

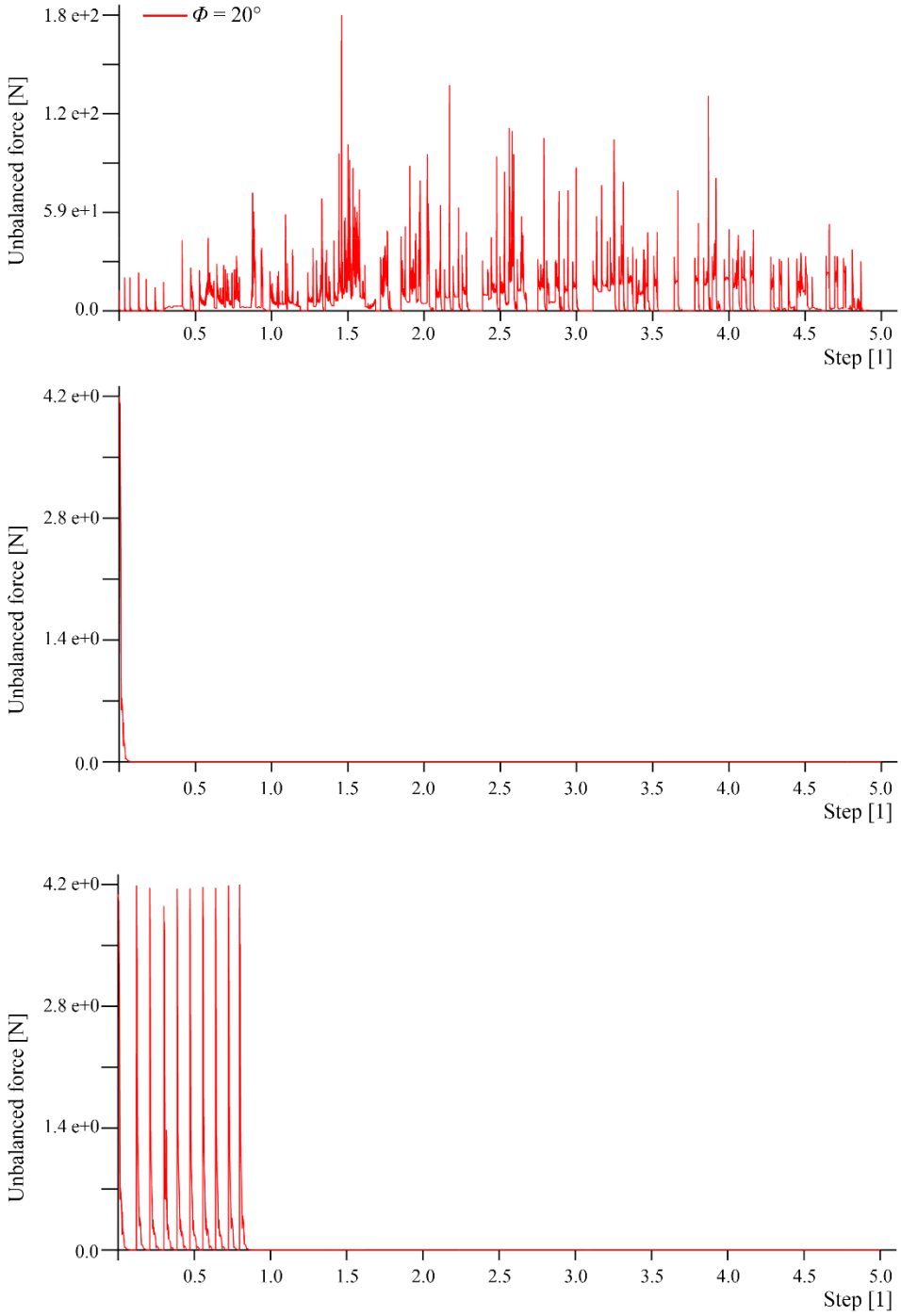

Figure 47: Unbalanced force graphs. (from top to bottom) dome under construction, complete dome (g=9.81 m^2/s), complete dome considering the formwork removal operations (g=9.81, 1.962, ..., 9.81 m^2/s).

As shown in Appendix A, the hoop forces and the meridian forces change during the construction. This variation is intuitable even by the distribution of the unbalanced force, which for each brick course shows a peak, and after this, a flat section manifests, that testifies the new state of equilibrium.

Figures 48 and 49 highlight this concept, where a portion of the dome is analysed. More precisely, the graphs of figure 49 are referred to the dome portion modelled in f The subject of the graph is the evaluation of the balance of the courses between the 28th and 33rd ones (i=28-33) of the octagonal dome. The simulation has been carried out assuming jKn=100 GPa/m, jKs=10 GPa/m and Φ=89° [111], and adding the courses one at a time (as described above), with the exception of the 33rd brick course, which, as shown in figure 48 (in the centre and bottom), is simulated in two different time intervals: the first, only three plate-bandes (j=1, 2, 3; i=33), and then the remaining part of the course. This process is clear in the plot of the unbalanced forces where seven peaks are recorded, one for each brick course, plus another, the low intensity one, for the addition of the three plate-bandes. In figure 49each peak is located in a specific and distinct time interval; thus, it is possible to correspond the different construction stages with the time-steps of analysis.

The other two graphs of figure 49 show the evolution of displacement and z-velocity components relating to point A and B belonging to 28th bricks of course (see figure 48). On these two graphs no variation is recorded relative to the addition of blocks of plate bande (j=1, 2, 3; i=33). Such behaviour indicates that the balanced state due to the three plate-bandes is just local, confirming the hypotheses proposed previously in chapter 4.2.

With respect to the displacement graph reported in figure 46, the similarity with quantities illustrated in figure 49 highlights the presence of settlements the previously laid courses when a new brick course is added.

To demonstrate the stability of the complete courses, a series of CBC Test is performed, precisely at n=28, 52, 65, 78 construction stages for the octagonal dome and at n=27, 43, 66, 70 for hemispherical one. For each of these stages the same physical properties as for the PB test have been considered. The CBC test evaluates the displacement, z-velocity, and unbalanced force relative of the last bricks course laid (i=n) at the n^{th} construction stage. Further, the structural behaviour of the whole structure under construction is assessed with the DUC Test, where displacement and z-velocity have been recorded at several courses. For all numerical analyses (CBC Test and DUC Test) only the first laying plane has been constrained and none of the other bricks. The joint penalty coefficients assumed here are jKn=100 GPa/m, jKs=10 GPa/m, while a variety of friction angle is investigated.

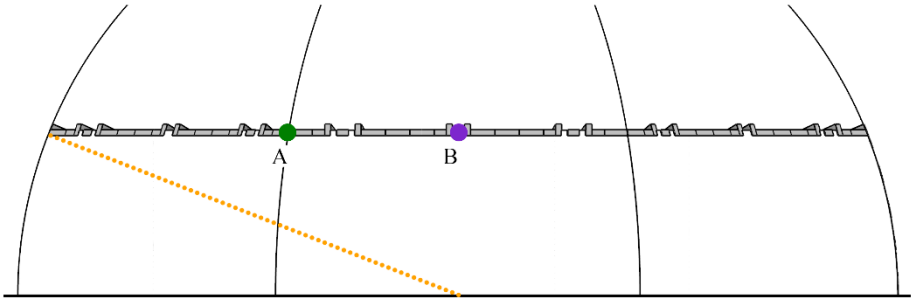

Course analysed: $i = 28$
Construction stage: $n = 28$

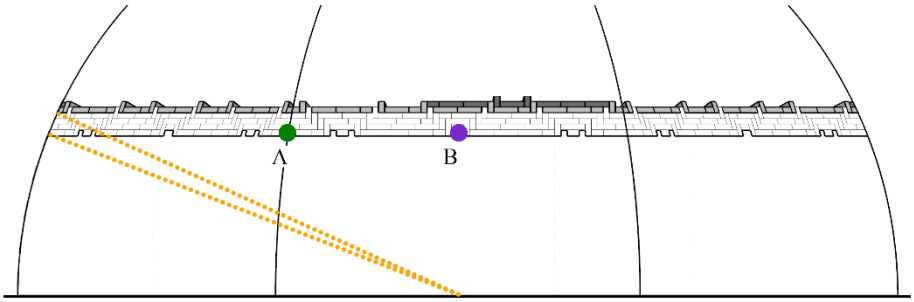

Course analysed: $i = 28$
Construction stage: $n = 33$ $j = 1, 2, 3.$

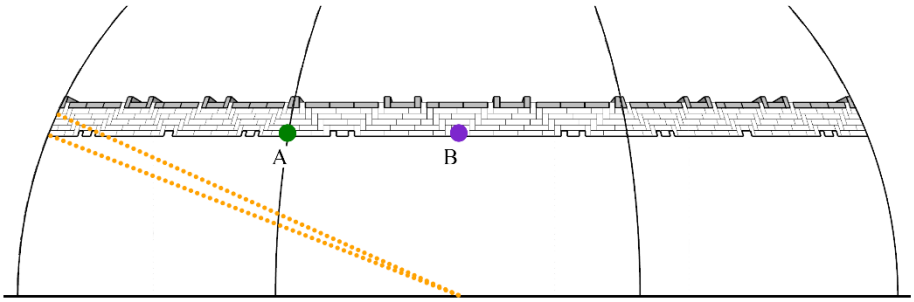

Course analysed: $i = 28$
Construction stage: $n = 33$

Figure 48: Dome under construction. From top to bottom brick course *i*= 28, brick courses from *i*= 28 to i=32 and plate bande *j*= 1, 2, 3, brick courses from *i*= 28 to *i*=32.

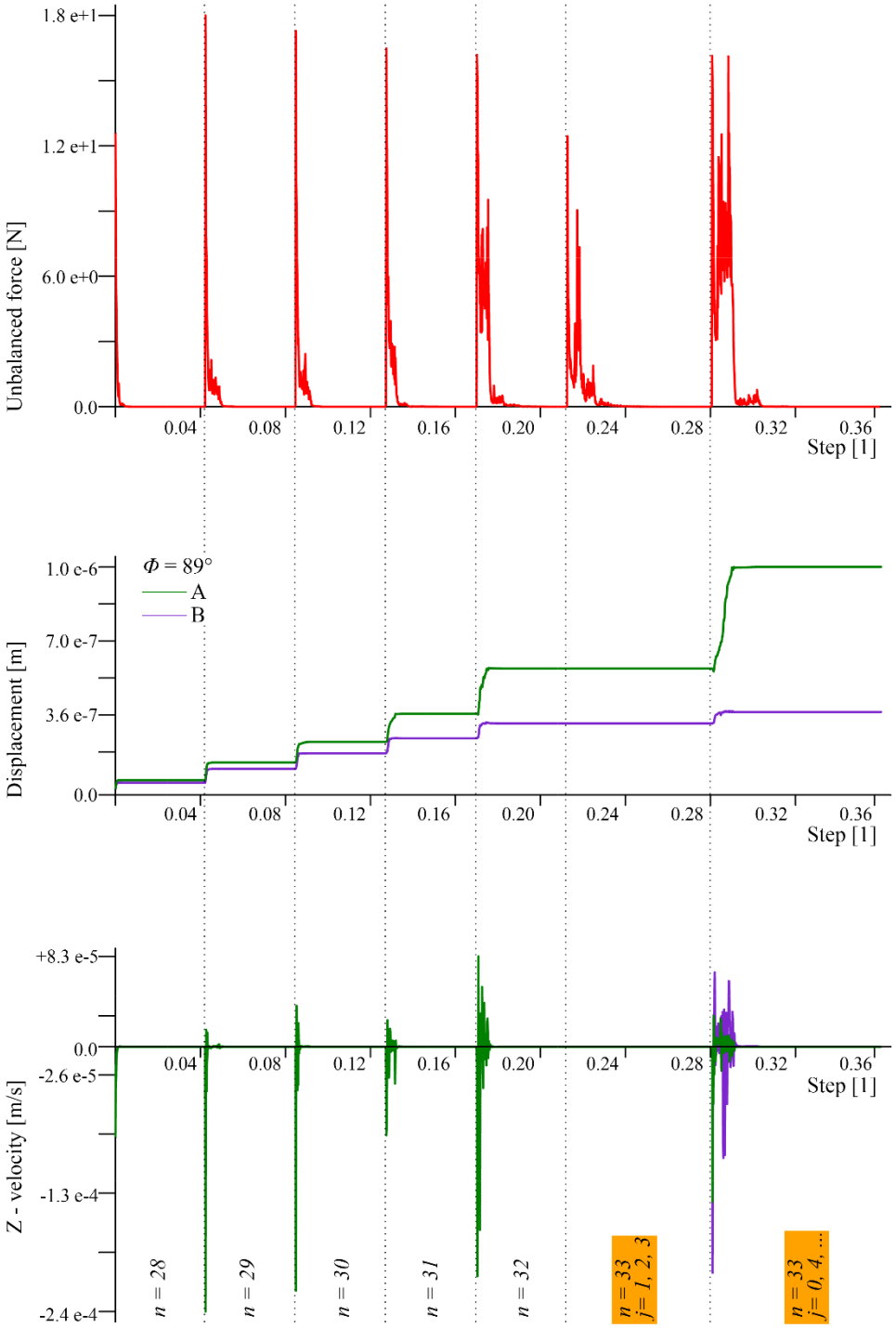

Figure 49: Graphs of dome under construction shown in figure 49. (from top to bottom) unbalanced force, displacement, and z-velocity.

The results of CBC and DUC Tests show that the maximum z-velocity that the blocks present, coincides with that of the construction stage in which they are laid. Random yet rare occurrence of high magnitude z-velocities is seen, especially in the hemispherical model. These random occurrences could be a result if the presence of the geometric imperfections considered in the modelling process

[98]. Appendix C reports the z-velocity graph, where their evolution to different points of octagonal and hemispherical domes are plotted.

		Φ	
	φ	0°	⩾10°
i= 28	26°	Unstable	stable
i= 52	47°	Unstable	stable
i= 65	59°	Unstable	stable
i= 78	71°	Unstable	stable
i= 93	86°	Unstable	stable

Table 3: Stability of DUC tests.

Table 3 summarizes results of DUC tests that were executed on the octagonal dome modelled considering the interval of brick courses between i=28 up to i=93. The same variation in friction as the PB tests have been adopted here. As Appendix C shows, the results in terms of stability are coherent with table 3, even for the hemispherical structure analysed.

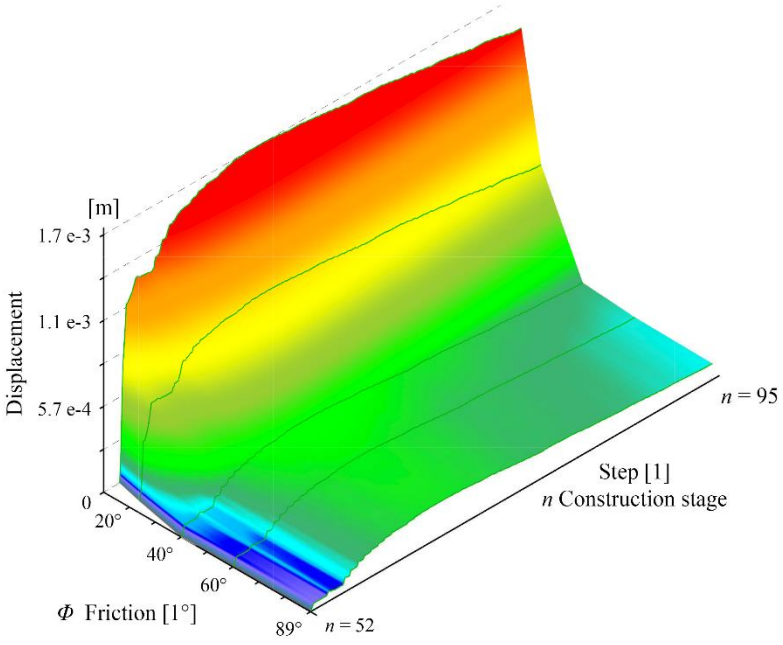

Figure 50: Graphs of displacement surface relative to A point for an octagonal dome placed in the middle of sail at 52nd brick course.

Based on the results of the analysis for a wide range of friction angles and construction stages, displacement surfaces relative to a specific point of the dome under construction can be derived. Figure 50 shows the displacements surface recorded for a point in the middle of the sail at the 52nd course of the octagonal dome. Thus, the surface is related to the construction stages ranging for n=52-

93 and the friction angles between Φ=10° and 89°. It is to be noted that the friction angles less than 10° have not been considered because even the plate-bandes structures are not stable at such low friction angles. Referring to figure 50 the maximum dome displacement recorded is less than 2 mm, a value low even for structures built with the aid of formworks. Despite this displacement, the surface provides valuable information relative to the inter dependence of displacement, friction, and construction stages.

Part III: Conclusions and Apparatuses

6. Conclusion

The research presented in this dissertation cannot be considered concluded, this document is only a first stone placed for building a new frame theory. However, interesting various considerations can be traced, like the actual relevance of the herringbone spiralling technology through the history or the high potential related to application of the self-balanced technologies.

6.1 The cross-herringbone technique: a self-balanced technology

Brunelleschi's herringbone technique was certainly known by the Sangallo architects in the 16th century, who developed the cross-herringbone spiralling technology, a self-supporting construction method for building masonry domes and vaults based on the Brunellsechi's technique, see chapter 3.1.

The herringbone and cross-herringbone were applied for over a century in the central region of Italy, the reason for their limited period of application and restricted spread have not been investigated, but a justification could be derived based on the historical-cultural context it was set in. Various factors including the disappearance of the Sangallo school of architects, or the evolution of the building techniques could have led to the abandonment of these techniques.

A detailed list of domes built adopting the herringbone pattern is reported in Appendix A. Among these, due to their peculiar characteristics, two structures have been studied: Santa Maria in Ciel d'Oro and Simon Mago, see chapter 3.2.2, both designed by Antonio da Sangallo the Younger, and both display a cross-herringbone tessellation. In fact, these two structures are not plastered, exposing the texture of the masonry, providing valuable information on the peculiarities of the cross-herringbone techniques.

Further, the historical documents conserved in the Uffizi Museum (figure 18, drawing 1330 (n. 594469) GDSU), provides evidence of the existence of cross-herringbone spiralling technique. This technique is different from the herringbone one and, unlike Brunelleschi's one, it requires a detailed execution scheme and a precise tracing system, without which a self-supporting system cannot be implemented. For this reason (the need of a preliminary project), the cross-herringbone technique should be considered one among the first modern building methods.

6.2 Considerations concerning: the two-step approach

From the observation of self-supporting technologies, considering Heyman's theory and the behaviour of masonry while laying, the two-step approach to assess the state of masonry structure during the construction is proposed. The core of two-step approach, see chapter 4.2, is based on two analyses: the first one the **Local Equilibrium Step**, and the second one the **Global Equilibrium Step**. The approach is formulated primarily to verify the state of shells under construction, nevertheless, it also provides a logical approach to evaluate the stability of other masonry structures. Further, due to the introduction of the temporal variable related to the construction works, and referring to the n^{th} construction stage of a masonry shells, different considerations are proposed:

- **1st independent property**: the equilibrium at $i=n^{th}$ brick course, i.e., at the local scale, is related to the building technology adopted, while the overall equilibrium, i.e., referring to the whole structure already built, is ruled by geometry.
- **2nd independent property**: the methods to assess the local state and the overall state can be not related, Further, for evaluating the stability of the n^{th} brick course, the nature of the primary and relevant factors, chapter 4.1, must be consider.
- **1st dependency property**: to achieve a balanced state during the construction, the overall state of shells must satisfy the conditions required to balance the local scale of structures analysed.
- **2nd dependency property**: Even during the construction stage, the Heyman's hypotheses are not violated, thus the overall equilibrium of masonry shells, built using self-supporting technologies, is governed by their geometry.

It is important to note that the implementation of the two-step approach must consider the technology used to build this structure.

This research is developed by considering the cross-herringbone spiralling technology and the two-step approach has been implemented following the limit analysis, adopting static graphic tools (see chapters 5.3.2, 5.3.3 and 5.3.4). Even the numerical simulations have been performed following the logic of two-step approach (DEM simulations, chapters 5.4.1 and 5.4.2).

6.3 Dome behaviour during construction – the case study

During the construction of masonry domes built without shoring or formwork, the overturning of a partially constructed sail and/or the sliding of local bricks or brick courses can lead to an unstable equilibrium state and ultimately the failure. Traditional masonry construction technologies do not intentionally address such construction failure mode and resort to costly auxiliary support systems.

The case studies of an octagonal and a hemispherical dome with a spiralling cross-herringbone texture, proves that this brick layout enables domes to find a self-balanced state during all phases of their construction. Through the plate-bande structures, found within the incomplete brick course (a course under construction), a resistance mechanism is occurred that enables an equilibrate state. This resistance involves the herringbone bricks at incomplete brick course as well as the contribution of the previous brick courses (already completed). Once the brick course is closed, the plate-bandes structures are no longer necessary. This structural behaviour is demonstrated through the DEM analysis performed; as highlighted in chapters 5.4.1 and 5.4.2, even for low values of friction between the brick surfaces, the dome is able to find a balanced equilibrium state. For real friction angle values, DEM analysis shows a maximum displacement of 1.8 centimetres (hemispherical dome displacement recorded at i=64 brick course and n=73 construction stage, Appendix C).

As detailed described in chapter 2.2 no violation to Heyman's of the **I.** hypothesis is seen under construction and further, the verification of both **II.** and **III.** hypotheses (2^{nd} dependency property) confirm the validity of Heyman assumptions.

The limit analyses performed during the construction of the two case studies (see Appendix B) highlights the variation in forces required to reach the self-balanced state. This is independent of the i^{th} brick course observed, and the maximum compressive ring forces are always recorded in correspondence to the $i = n^{th}$ construction stage. In other words, the most critical construction stage is precisely when the bricks of i course is still being laid.

6.4 Future vision

Although the equations of equilibrium defined in chapter 5.3.2, 5.3.3 and 5.3.4 are used to verify the equilibrium state of the dome, they can be easily adapted to design and assess other self-balanced domes. Currently, three-dimensional rigid structural surfaces (such as shells and domes) need formwork and shoring material during construction, which goes to waste once the structure is completed, adding to the economic and environmental cost of the project. Through the implementation of the two-step approach proposed in this research, these productivity and economic issues encountered during construction, can be correlated to the stability problem. With evaluating of the state of structures all through the construction, the exact need for supports or vulnerable stages can be identified, and other unnecessary costs can be eliminated.

This document presents a historic masonry dome construction technique, based on the spiralling cross-herringbone pattern, that enable statically stable geometries throughout the construction process, without the need for any external support system. These self-balancing structures have no theoretical limit to their size. The potential of the cross-herringbone tessellation could be unearthed

in today's construction industry, where, it can be applied in the context of other emerging innovations such as novel structural form-finding approaches and robotic construction technologies [145] [146] [147]. It is envisaged that the form of masonry rigid surfaces could be tailored through form-finding approaches [19] [148] [149] and designed with the herringbone pattern to be effectively built using robots and without any falsework, and yet be stable during all the construction stages and through their service life.

Appendices

Appendix A

The following list provides an overview of buildings designed by the Sangallo architects, especially by Antonio the Younger, in which the herringbone or cross-herringbone spiralling technology was probably applied. These buildings have been chosen because the presence of domes is testified and for other similar structure the herringbone or cross-herringbone technique was applied.
The list was written by consulting various sources but cannot be considered complete. The purpose of this document is to prove that the use of the herringbone technique and of the cross-herringbone is not sporadic but rather systematic. The date reported against the sites marks the year of construction of the structures. The ** notion against the site shows the testified presence of the herringbone or cross-herringbone spiral technique.

List of sites:
Basilica of Santa Casa**
Place: Loreto (Ancona).
Date: 1468.
Architect: Giuliano Sangallo.
Source: [124].

Porta Nova
Place: Colle di Val d'Elsa (Siena).
Date: 1479.
Architect: Giuliano Sangallo.
Source: [124].

Medici Villa
Place:Poggio a Caiano (Prato).
Date: 1480.
Architect: Giuliano Sangallo.
Source: [124].

Santa Maria delle Carceri
Place: Prato.
Date: 1484.
Architect: Giuliano Sangallo.
Source: [124].

Poggio Imperiale**
Place: Poggibonsi (Siena).
Date: 1488.
Architect: Giuliano Sangallo, Antonio Sangallo the Elder.

Source: [62] [124].

Palazzo Della Rovere
Place: Savona.
Date: 1489.
Architect: Giuliano Sangallo.
Source: [58] [122].

Fort Sangallo
Place: Civita Castellana (Viterbo).
Date: 1495.
Architect: Antonio Sangallo the Younger, Antonio Sangallo the Elder.
Source: [58] [122].

Medici Fortress di Sansepolcro**
Place: Sansepolcro, (Arezzo).
Date: 1500.
Architect: Giuliano Sangallo.
Source: [123] [124].

Medici Fortress**
Place: Arezzo.
Date: 1502.
Architect: Giuliano Sangallo, Antonio the Younger and Antonio Sangallo the Elder.
Source: [62] [123].

Church of Santissima Annunziata
Place: Arezzo.
Date: 1503.
Architect: Antonio Sangallo the Elder.
Source: [123]. [150].

Fortress of Nettuno
Place: Nettuno (Rome).
Date: 1503.
Architect: Giuliano Sangallo Antonio Sangallo the Elder.
Source: [123].

Fortress of Castrocaro**
Place: Castrocaro Terme and Terre del Sole (Forlì).
Date: 1504.
Architect: Antonio Sangallo the Younger, Antonio Sangallo the Elder.
Source: [62] [123].

Temple of San Giovanni in Oleo

Place: Rome.
Date: 1509.
Architect: Antonio Sangallo the Younger.
Source: [122].

Church of Sant'Egidio
Place: Cellere (Viterbo).
Date: 1513.
Architect: Antonio Sangallo the Younger,
Source: [122] [123].

Rocca Farnese
Place: Capodimonte (Viterbo).
Date: 1513.
Architect: Antonio Sangallo the Younger,
Source: [122] [123].

Oratorio di Santa Caterina
Place: Bisentina di Capodimonte island, Bolsena lake, (Viterbo)
Date: 1516.
Architect: Antonio Sangallo the Younger.
Source: [123].

Church of San Biagio
Place: Montepulciano (Siena).
Date: 1518.
Architect: Antonio Sangallo the Elder.
Source: [151].

Fortress Vecchia**
Place: Livorno.
Date: 1519.
Architect: Antonio Sangallo the Elder.
Source: [62] [124].

Church of Santa Maria in Ciel d'Oro**
Place: Montefiascone (Viterbo).
Date: 1523.
Architect: Antonio Sangallo the Younger.
Source: [69] [126].

Cappella Cesi in Santa Maria della Pace**
Place: Rome.
Date: 1530.
Architect: Antonio Sangallo the Younger.

Source: [123] [152].

Palazzo Farnese
Place: Caprarola (Viterbo).
Date: 1530.
Source: [122].

Fortezza da Basso**
Place: Florence.
Date: 1534.
Architect: Antonio Sangallo the Younger.
Source: [122]. [123].

Bastion Sangallo
Place: Rome.
Date: 1537.
Architect: Antonio Sangallo the Younger.
Source: [124].

Rocca di Nepi
Place: Nepi (Viterbo).
Date: 1537
Architect: Antonio Sangallo the Younger, Antonio Sangallo the Elder.
Source: [122] [152].

Rocca Paolina
Place: Perugia.
Date: 1540.
Architect: Antonio Sangallo the Younger.
Source: [58] [122].
Simon Mago dome and domes of Octagons in San Pietro**
Place: Roma.
Date: 15--.
Architect: Antonio Sangallo the Younger.
Source: [59] [126].

Appendix B

The limit analysis has been performed for two different domes, one octagonal and the other hemispherical, the two structures have dimensions comparable to the Santa Maria in Ciel d'Oro dome. The internal diameter of the octagonal dome is 9.4 m, and the thickness is 0.24 m, and on the other hand the hemispherical one has a radius of 4.0 m and a thickness of 0.24 m. The two structures present the cross-herringbone pattern with the maximum distance between two loxodromes is given as 1.4 m, measured at the base of the hemispherical one. The analyses have been conducted for different construction stages, following the formulation introduced in chapter 5.3 and considering ρ=20 kN/m^3 and Φ=20°. The results are summarised in tables 4 and 5 and technical sheets that follow.

The hemispherical dome has been divided by an angle of ϑ =11.25°, while the three lunes exposed in chapter 5.3.4 has been studied. According to the literature [90] [153] the octagonal dome is not stable, the thrust at the complete dome of C-C section does not lie entirely in the section of the dome, hence fill or abutment should be considered. Nevertheless, the purpose of the analyses is to highlight the variation of the hoop forces during the construction. As expected, the thrust or ring forces, listed in in tables 4 and 5, change as a function of the construction stage. For all construction stages the ring forces are larger near the last course laid than, those located at the level laid first. From these tables, it can be seen that, the magnitude of ring forces required to achieve stability decreases drastically during construction. At the early construction stages, the magnitude of the ring forces is comparable to the thrust forces required to balance the plate-bandes (octagonal dome) or arches (hemispherical dome). When we approach the crown, their magnitude increases independently of the plate-bandes thrusts. This observed difference is due to the geometry and dimension of both the plate-bande sub-structure and that of the entire dome. The spans of plate-bandes decrease from the base to the dome's crown by around 70-80%. On the contrary, when the construction is complete the ring forces required to achieve a balanced state for the whole dome, increase from the base of the dome to the crown by more than 100%.

Plate-bande			
	Stage $n = i$		
	33	52	93
j	1	3	1
$\|\|H_{nj}^{PB}\|\|$ [N]	104.4	243.6	113.5
Closed brick course			
	Stage n		
	33	52	93
$\|\|H_{n}^{R}\|\|$ [N]	104.4	243.6	113.5
Dome under construction			
	Stage n		
	33	52	93
$\Delta h_{33}^{x\ Ring}$ [N]	210.0	35.6	3.0
$\Delta h_{52}^{x\ Ring}$ [N]		276.0	3.5
$\Delta h_{93}^{x\ Ring}$ [N]			794.0
$\|\|H_{n}^{Ring}\|\|$ [N]	538.2	707.4	2034.9

Table 4: Results of limit state analysis for the octagonal dome analysed.

Arch				
	Stage $n = i$			
	27	59	68	77
$\|\|H_{nj}^{PB}\|\|$ [N]	117.6	152.3	68.0	56.2
Closed brick course				
	Stage n			
	27	59	68	77
$\|\|H_{n}^{R}\|\|$ [N]	104.4	243.6	113.5	
Dome under construction				
	Stage n			
	27	59	68	77
$\Delta h_{27}^{x\ Ring}$ [N]	386.0	15.4	1.9	1
$\Delta h_{59}^{x\ Ring}$ [N]		640.0	34.0	24.0
$\Delta h_{68}^{x\ Ring}$ [N]			720.0	35.4
$\Delta h_{77}^{x\ Ring}$ [N]				918.0
$\|\|H_{n}^{Ring}\|\|$ [N]	989.3	1640.3	1845.3	2352.8

Table 5: Results of limit state analysis for the hemispherical dome analysed.

Octagonal dome

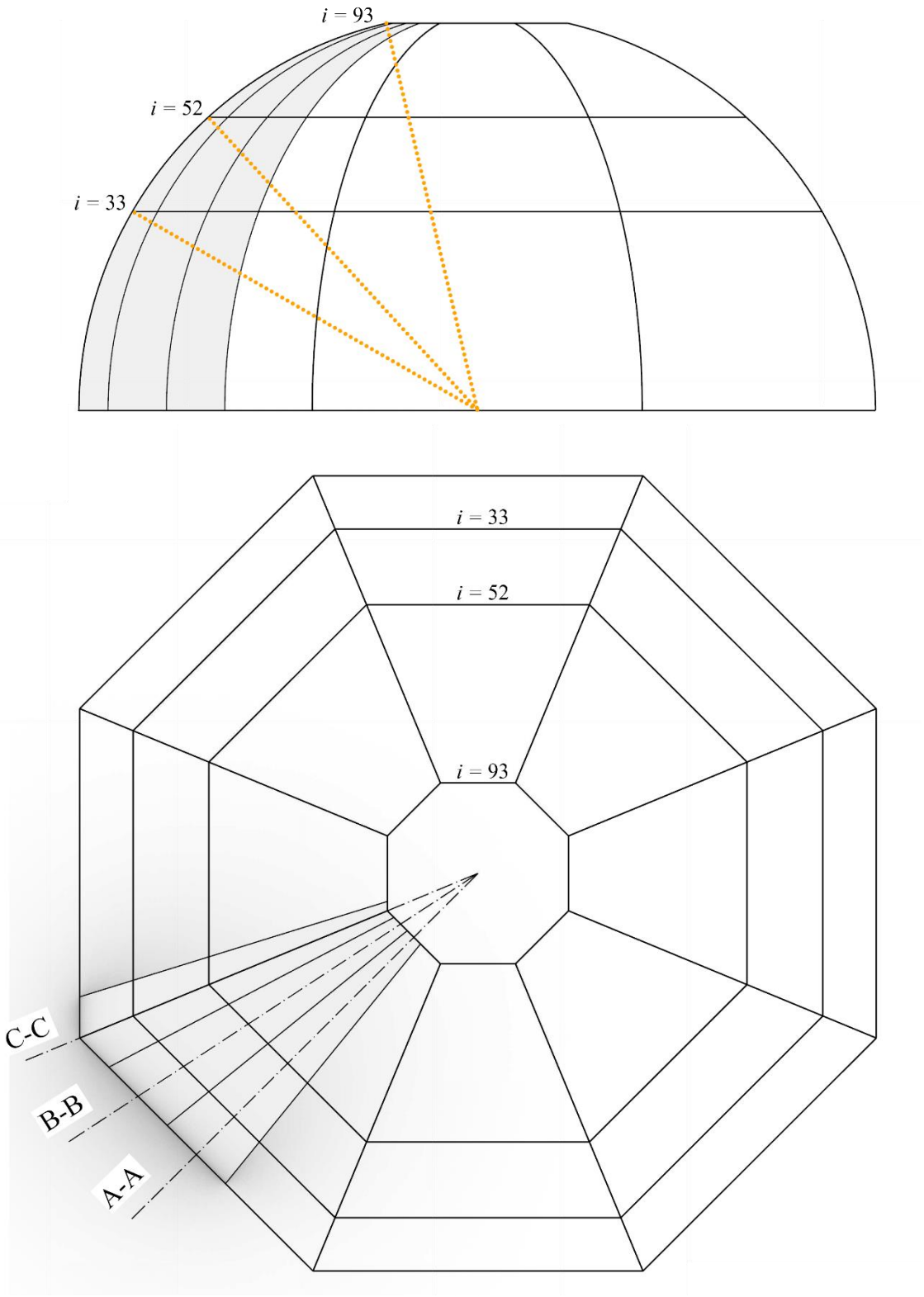

Key-section for analyses:
Constrcution stage analysed: i =33, 52, 93

Construction stage n=33

A-A section

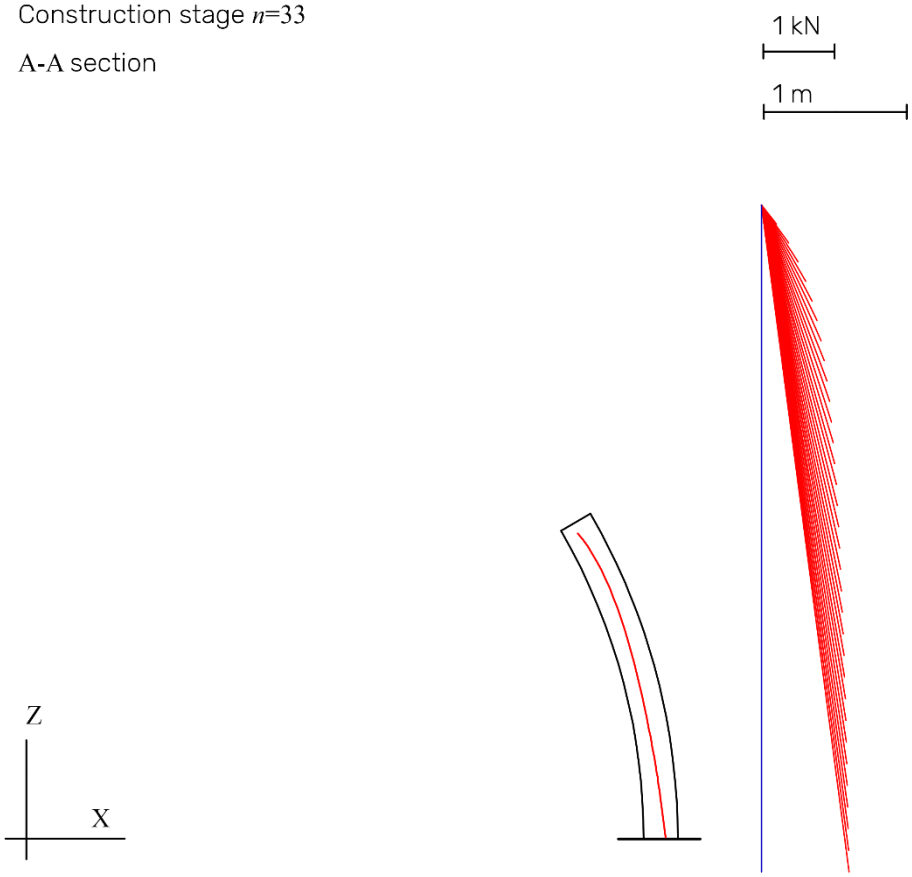

Construction stage n=33

B-B section

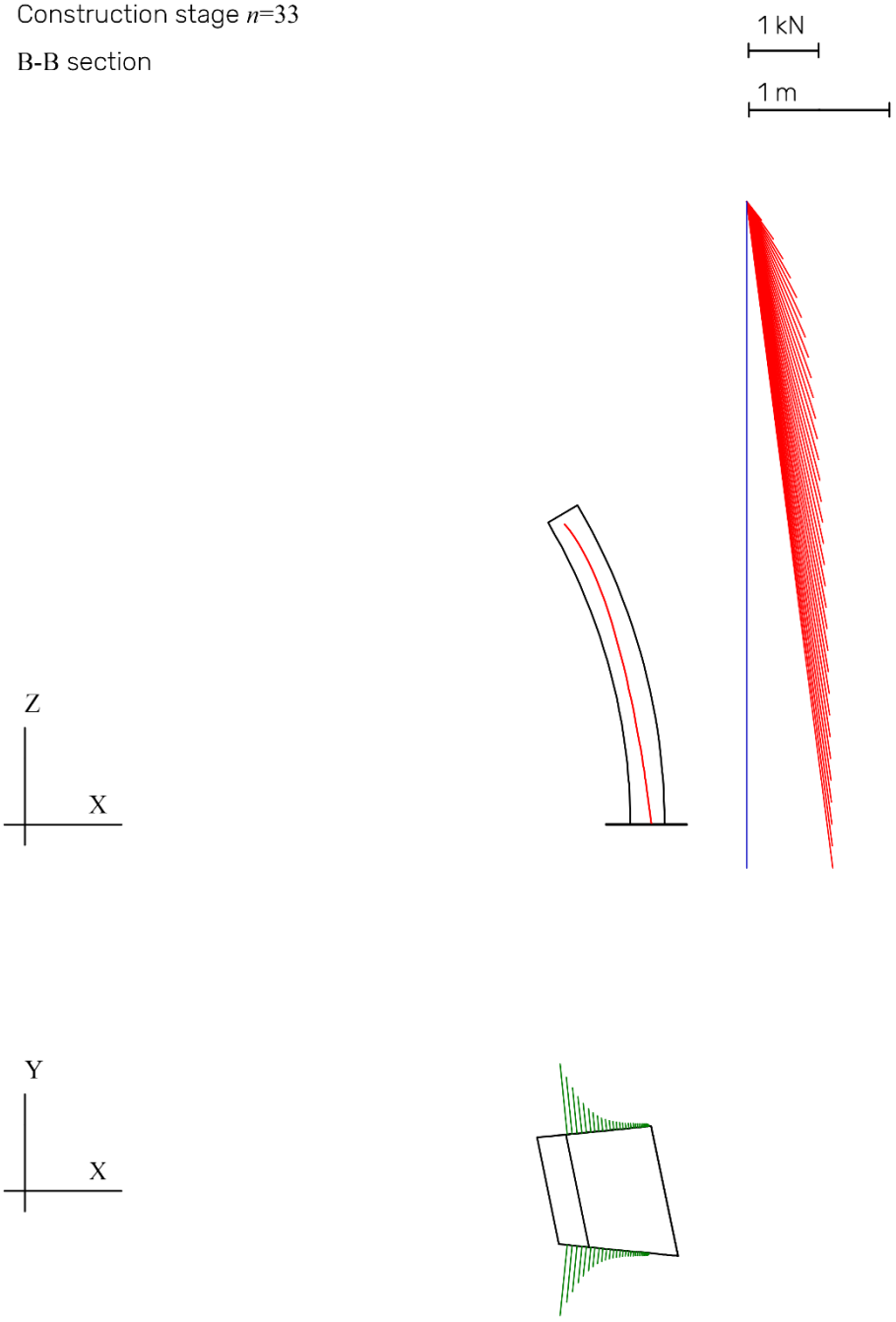

Construction stage n=33

C-C section

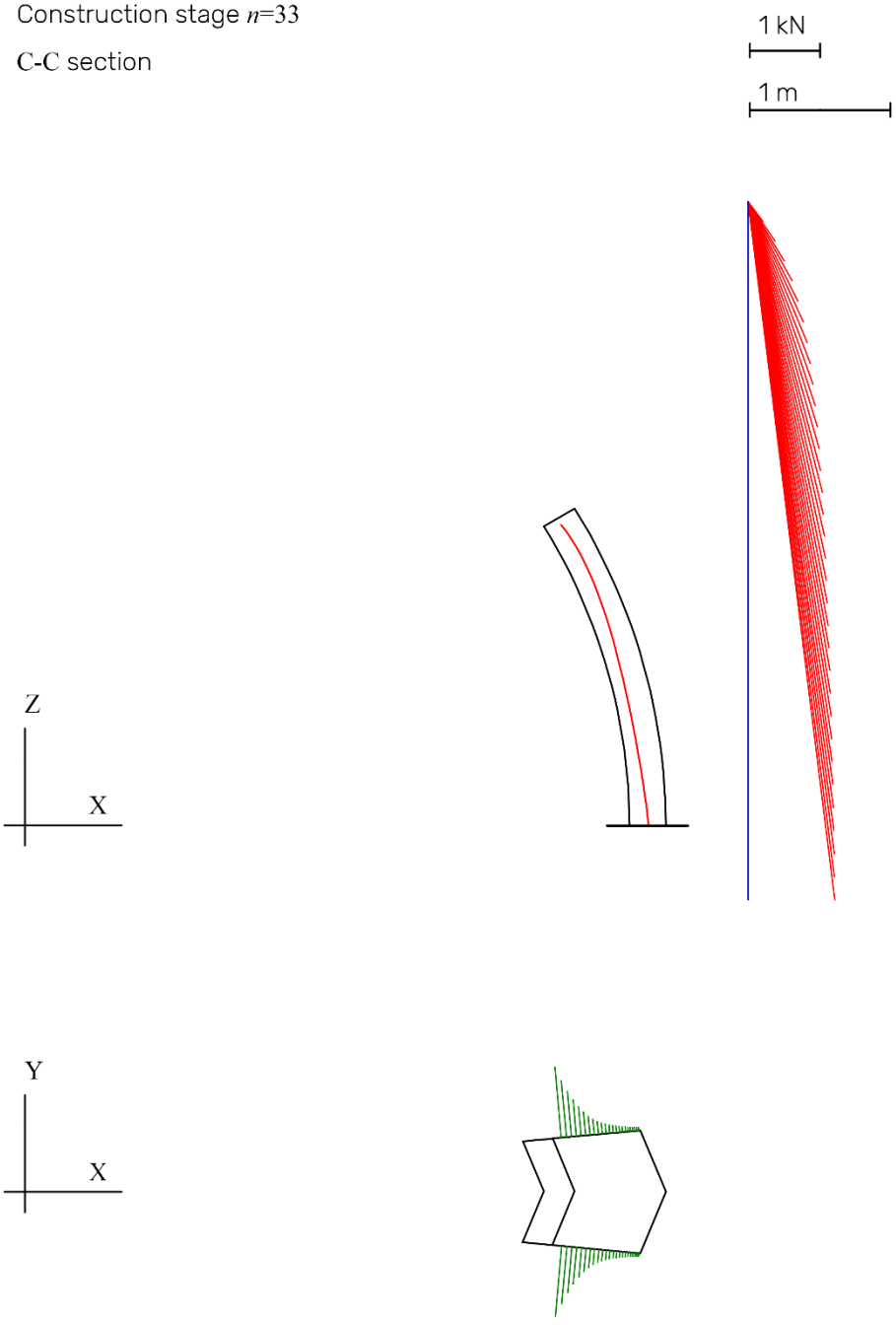

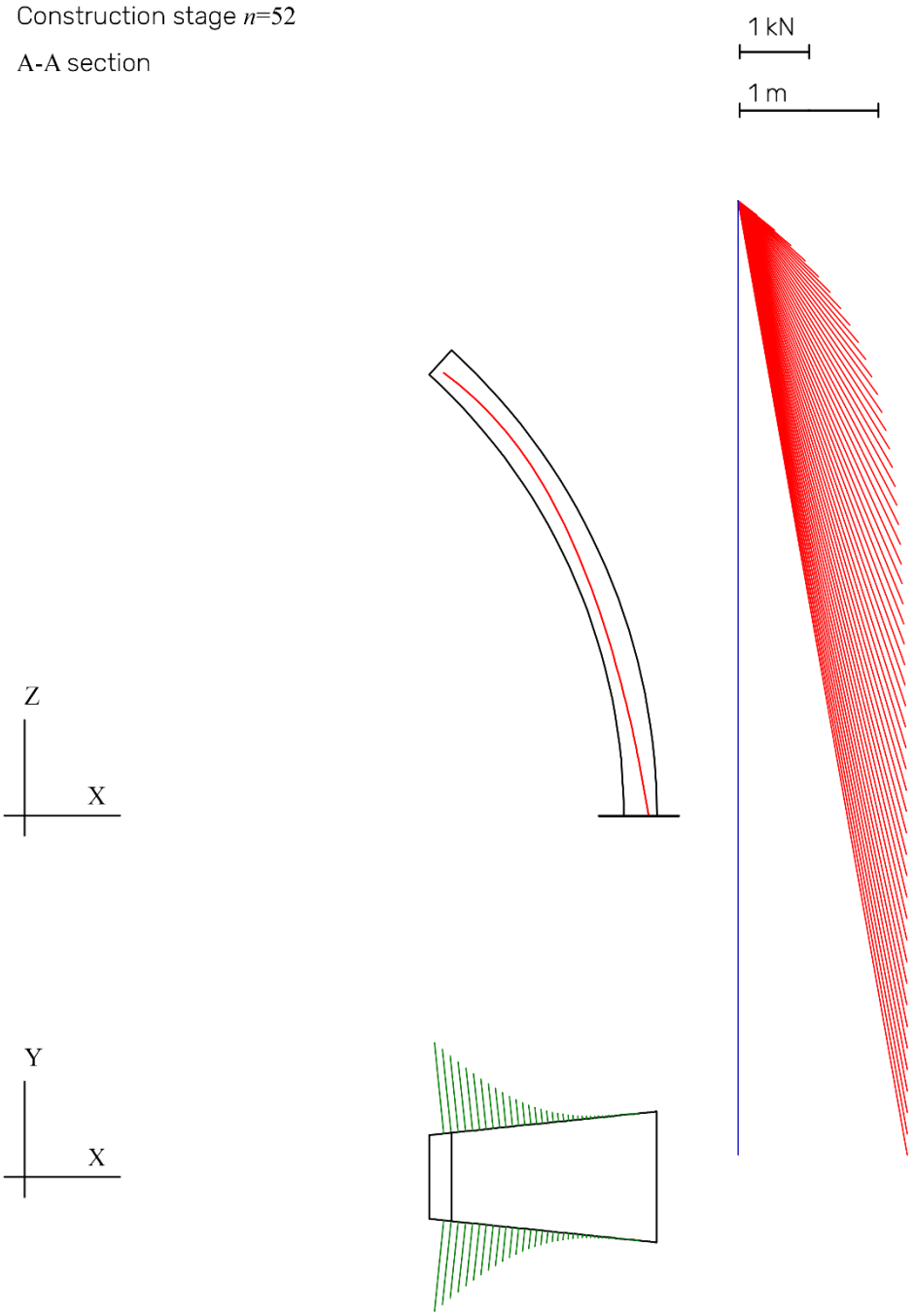
Construction stage n=52
A-A section
1 kN
1 m
Z
X
Y
X

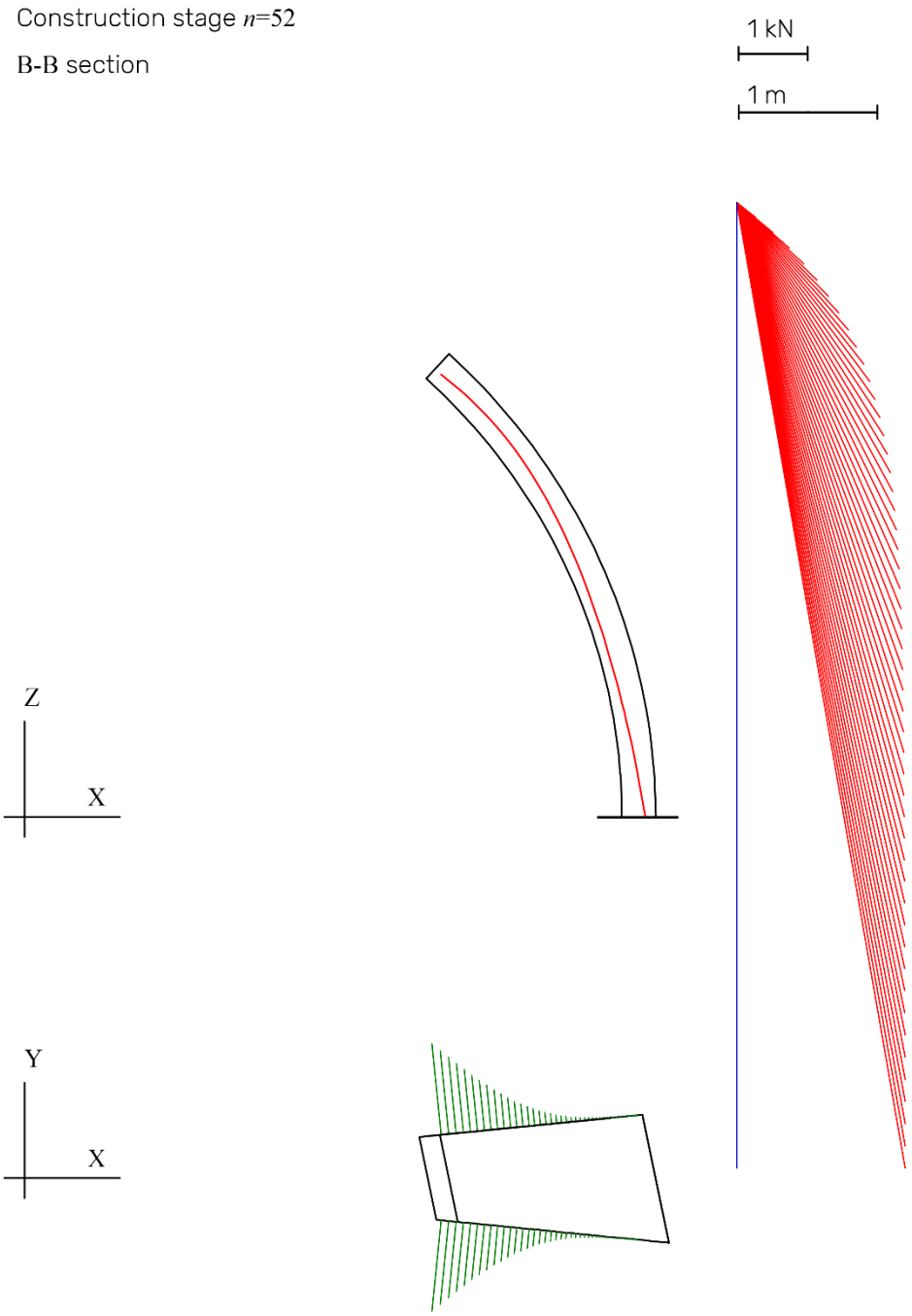
Construction stage n=52
B-B section
1 kN
1 m
Z
X
Y
X

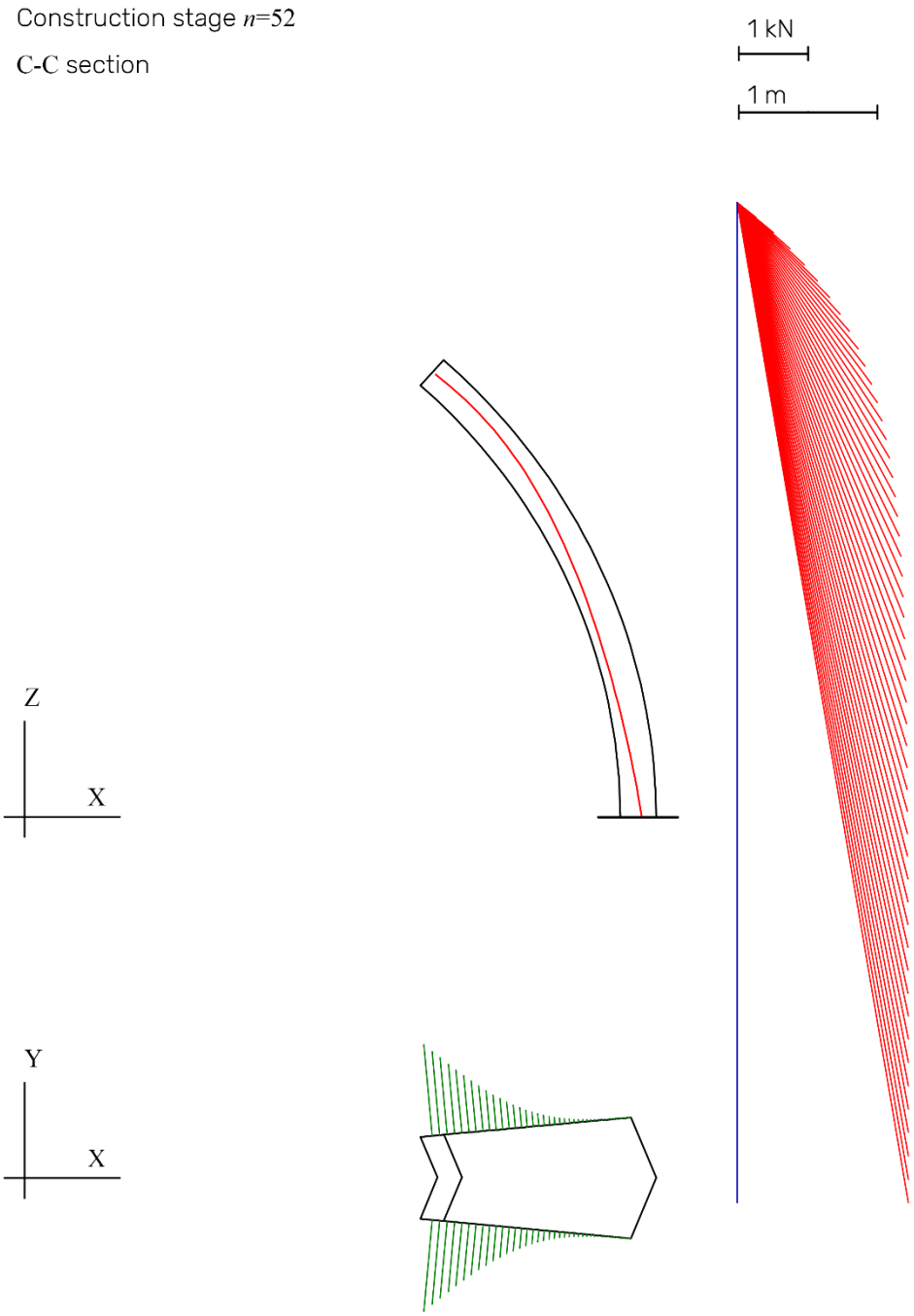
Construction stage n=52
C-C section
1 kN
1 m
Z
X
Y
X

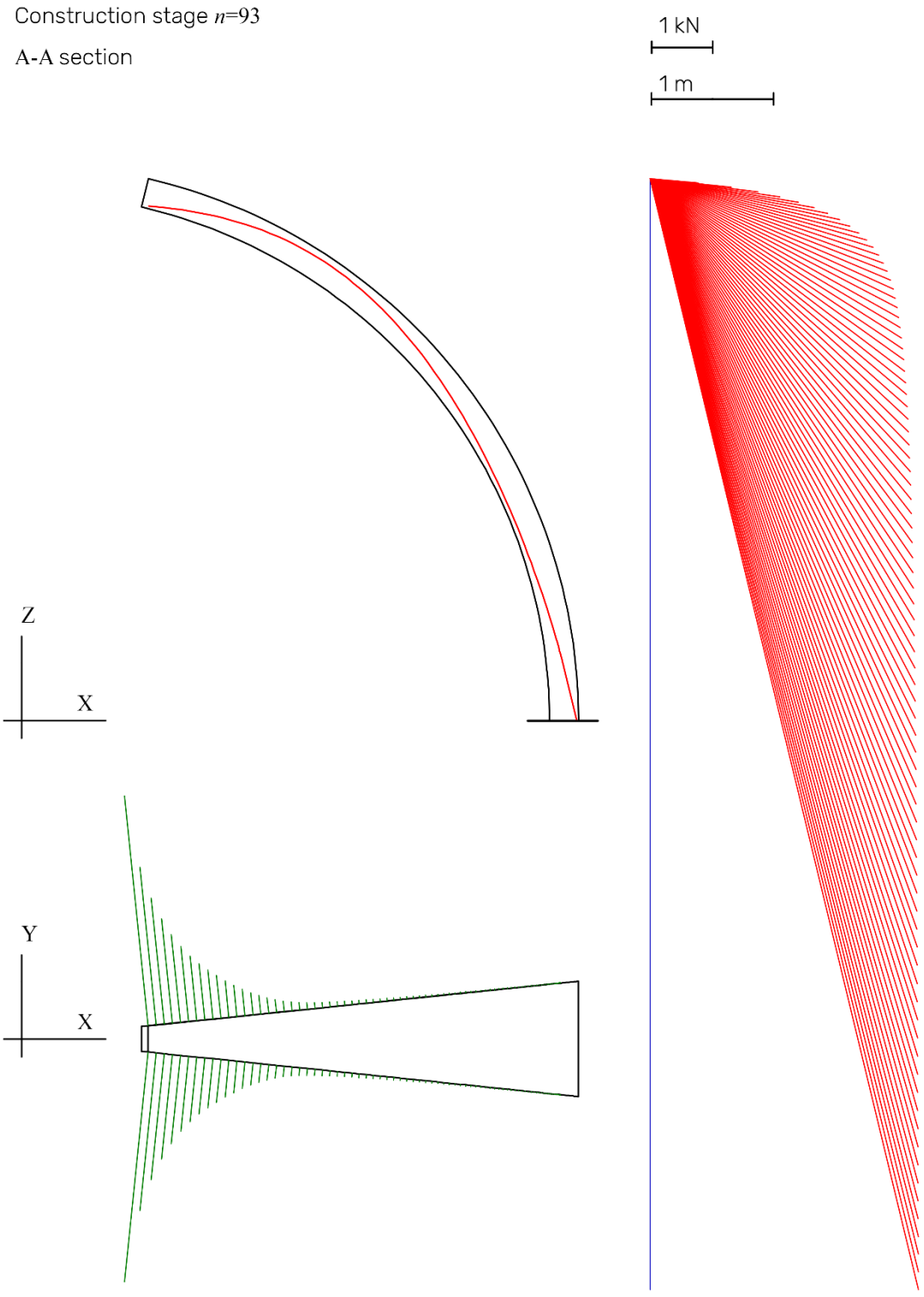
Construction stage n=93
A-A section
1 kN
1 m
Z
X
Y
X

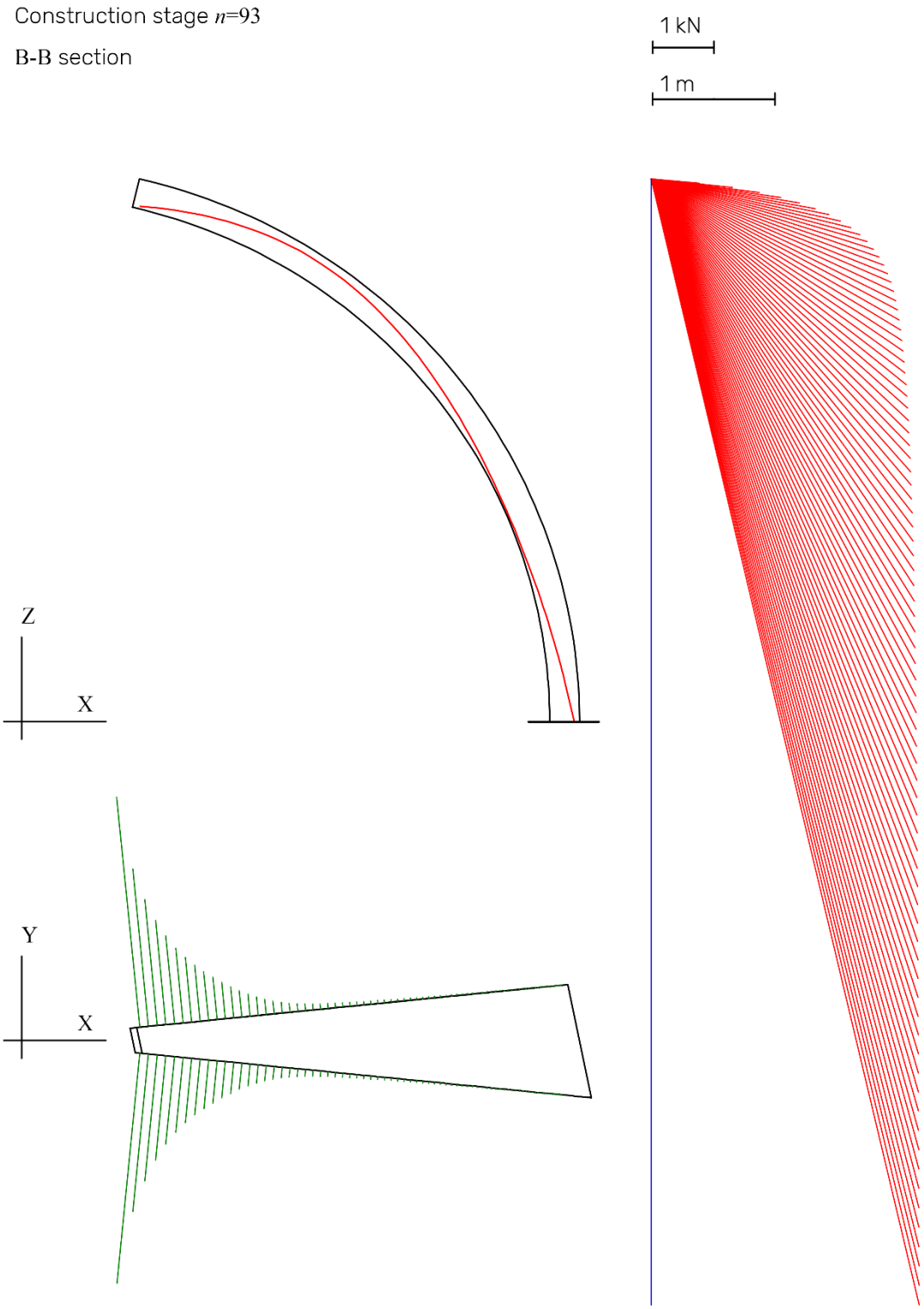
Construction stage n=93
B-B section
1 kN
1 m
Z
X
Y
X

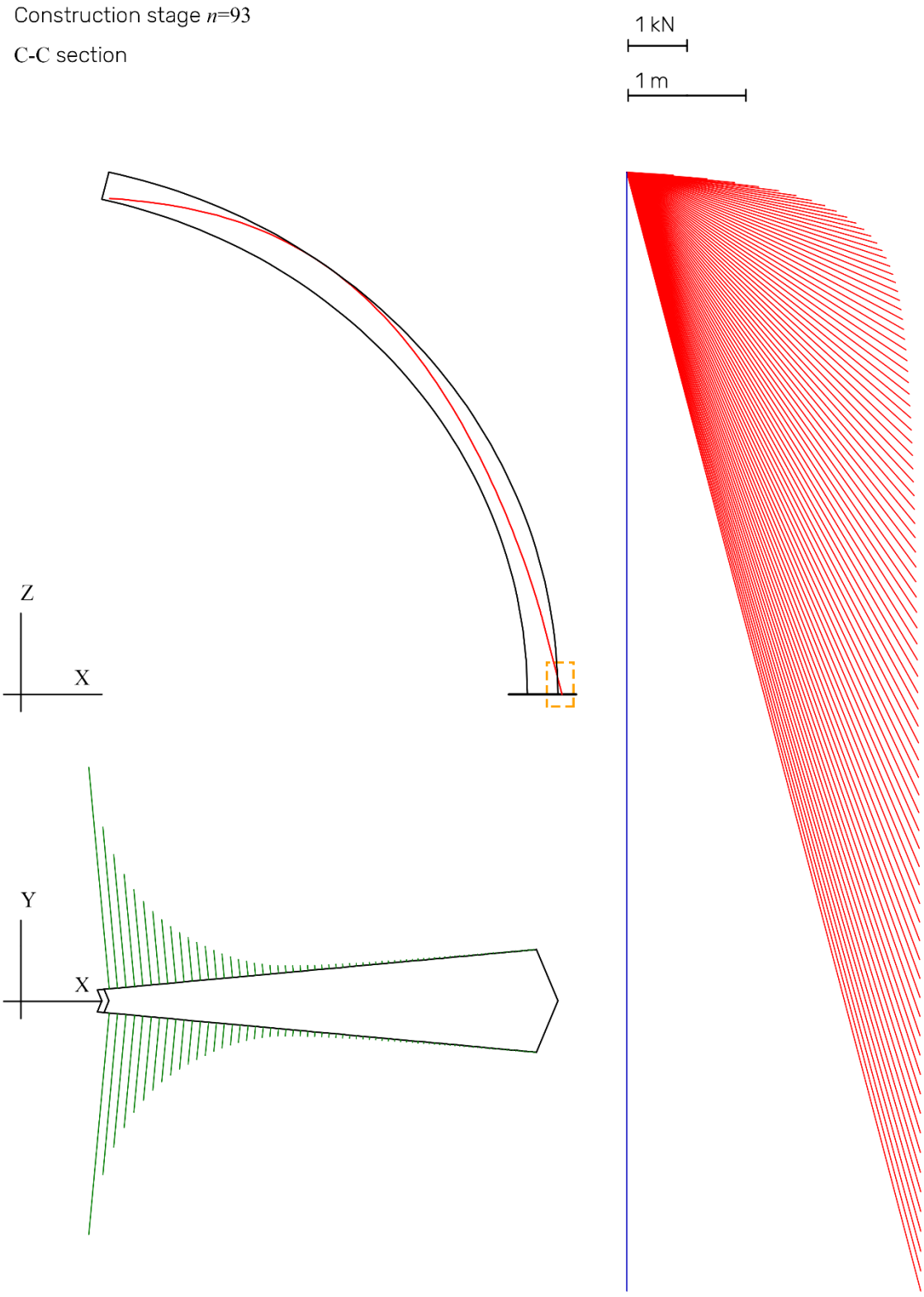
Construction stage n=93
C-C section
1 kN
1 m
Z
X
Y
X

Hemispherical dome

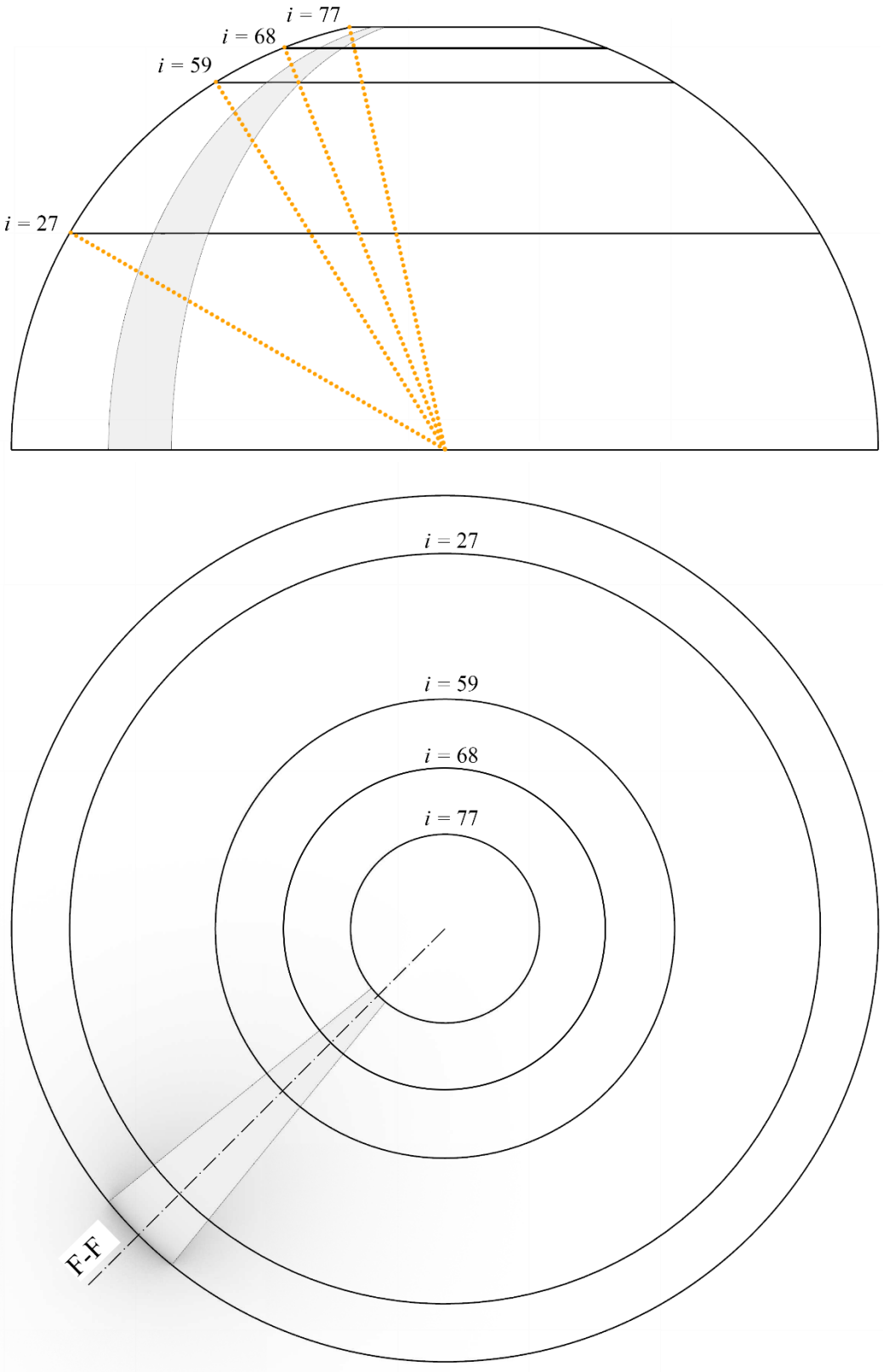

Key-section for analyses:
Constrcution stage analysed: i =27, 59, 68, 77

Construction stage n=27

F-F section

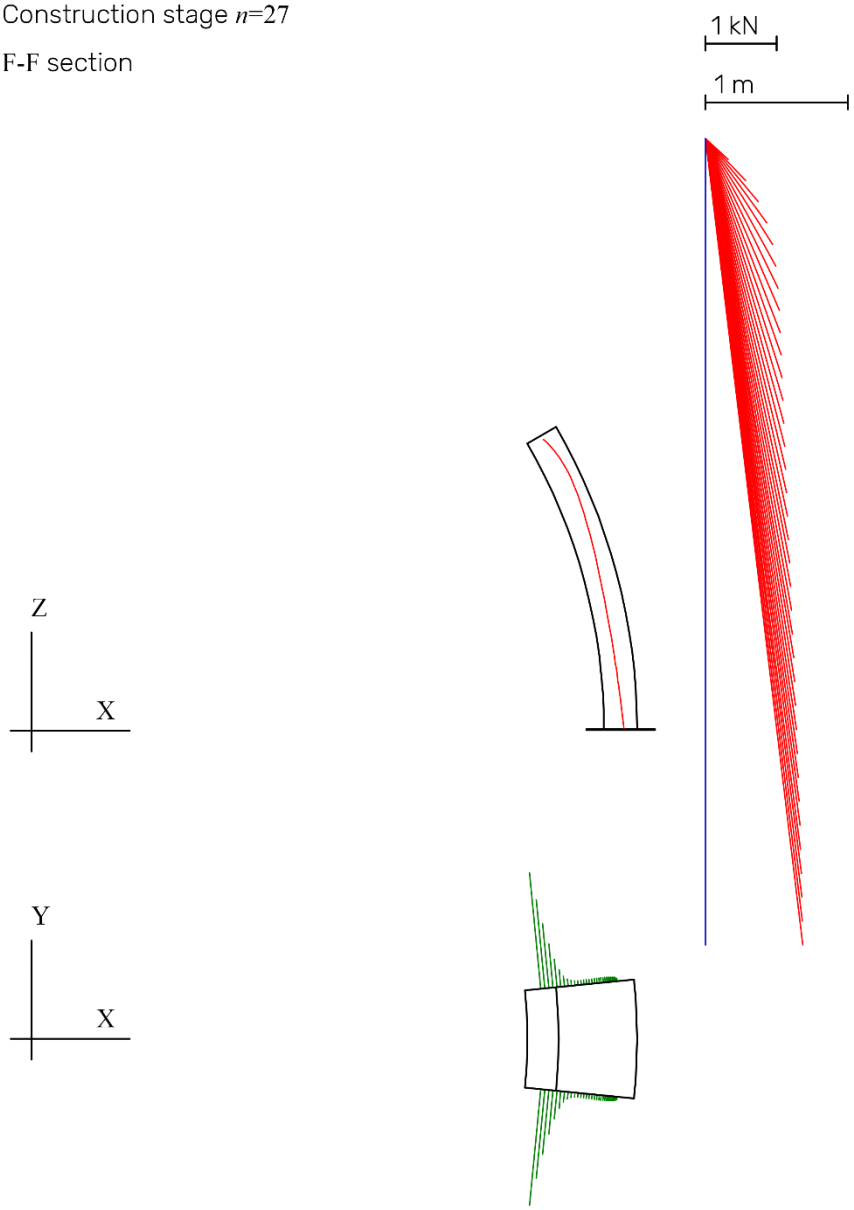

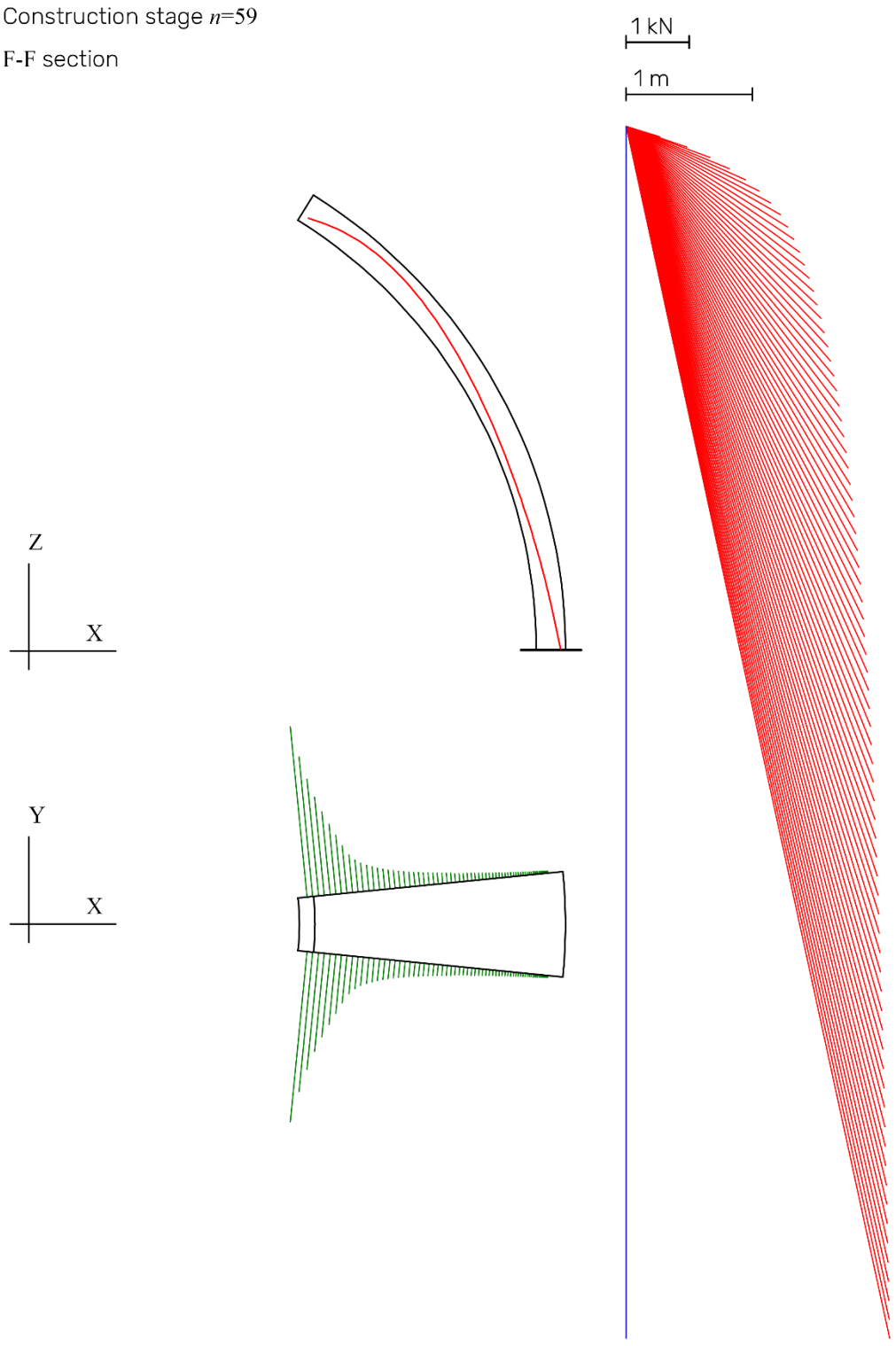
Construction stage n=59
F-F section
1 kN
1 m
Z
X
Y
X

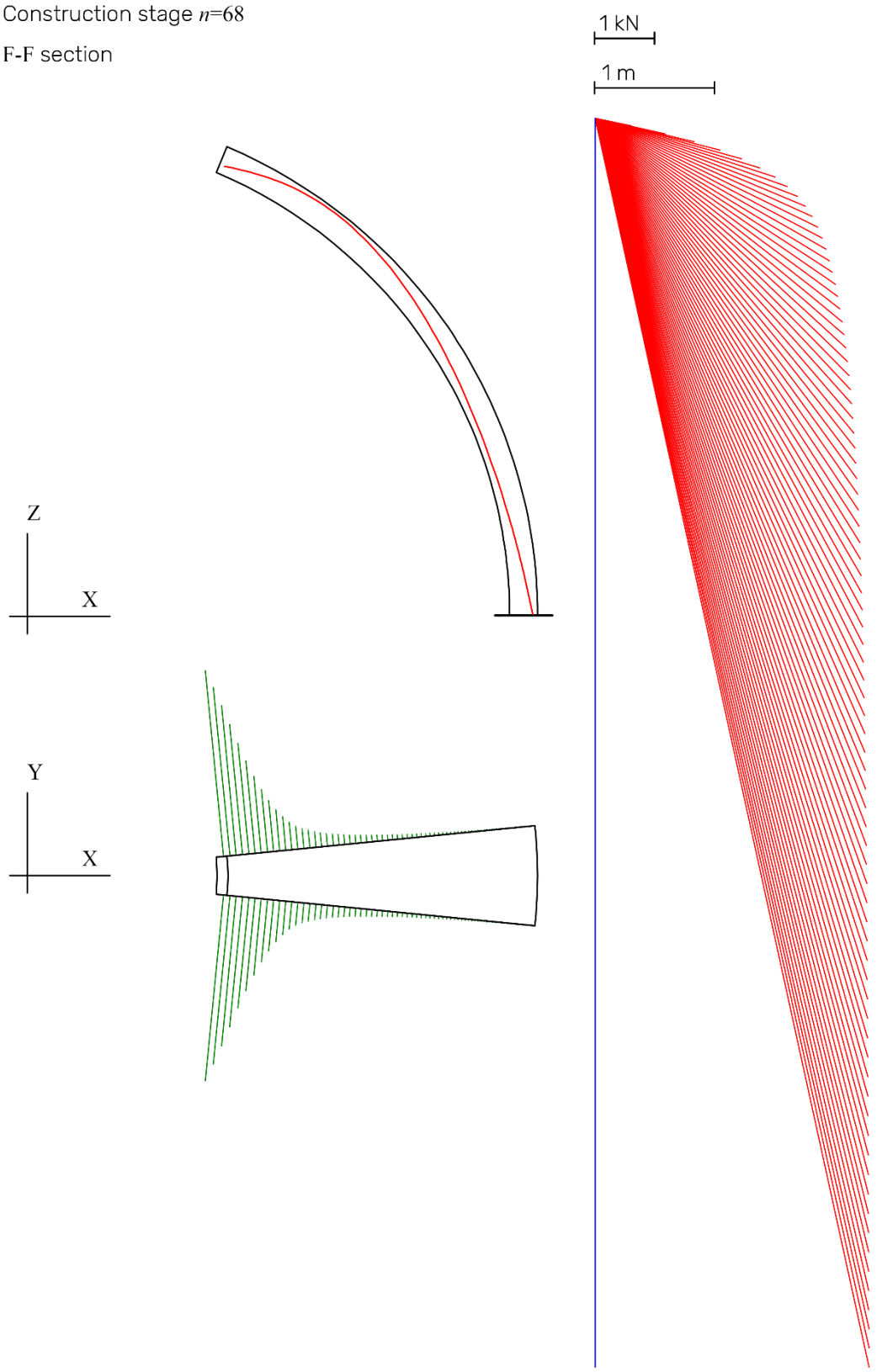
Construction stage n=68
F-F section
1 kN
1 m
Z
X
Y
X

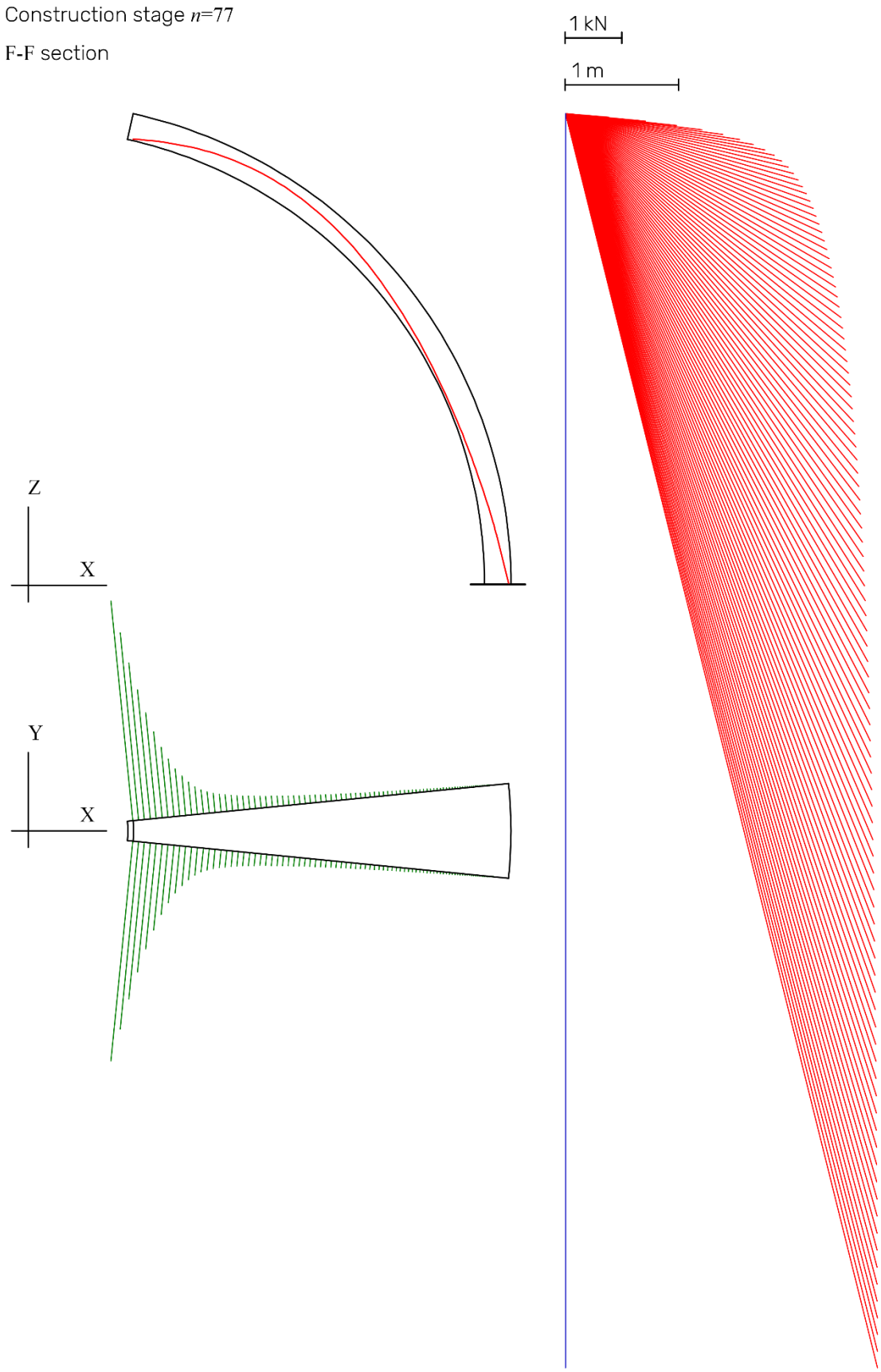
Construction stage n=77
F-F section
1 kN
1 m
Z
X
Y
X

Appendix C

The structures investigated are the same two domes analysed in Appendix B, an octagonal and a hemispherical structure. However, in the DEM analyses the domes are modelled starting from the 28th brick course (i=28) for the polygonal one, and 27th brick course (i=27) for the hemispherical one. The dimensions of the rigid bodies assumed to perform the analyses correspond to the sizes of bricks along with the portion of mortar which surrounds the brick itself, as described in chapter 5.4. The results reported show the time evolution of the unbalanced force calculated for a friction angle ranging from Φ=0° up to Φ=89° and z-velocity from Φ=10° up to Φ=89°. Along with the displacement surfaces, the z-velocity graphs have also been traced. The graphs illustrate the results obtained relative to the bricks course: i=28, 52, 65, 78 for the octagonal model and i=27, 43, 66, 70 hemispherical structure. All analyses were performed with values of jKn=100 GPa/m, jKs=10 GPa/m.

As mentioned in chapter 5.4.2, the geometries provide interesting information on the time evolution of displacements at different courses, different construction stages and with friction values. The irregular region of displacement surfaces highlights the settlements that occur during construction. These movements have low magnitudes, with even the order of maximum displacement recorded at least two orders smaller than over all maximum displacement. Referring to the octagonal dome, the "breath" phenomenon is more evident in the courses between i=28-75 and in the middle of the sails of octagonal dome. This is due to the inclination of the laying plane. However, this phenomenon is practically insignificant with relation to point B (near the edges of sails), and generally speaking, the displacement surfaces relative to B is of an order lower than that of the point A, recorded with the same conditions (Φ, n).

With the introduction of geometric imperfections in the blocks of the hemispherical dome, the "breath" phenomenon does not occur. The displacement surfaces recorded here, relative to the upper portion of this structure (i=56-77) show a remarkable vertical section even in the early construction stages. This denotes that these geometrical errors lead to an increase in the settlements but without compromising the balanced state of the dome.

Octagonal dome

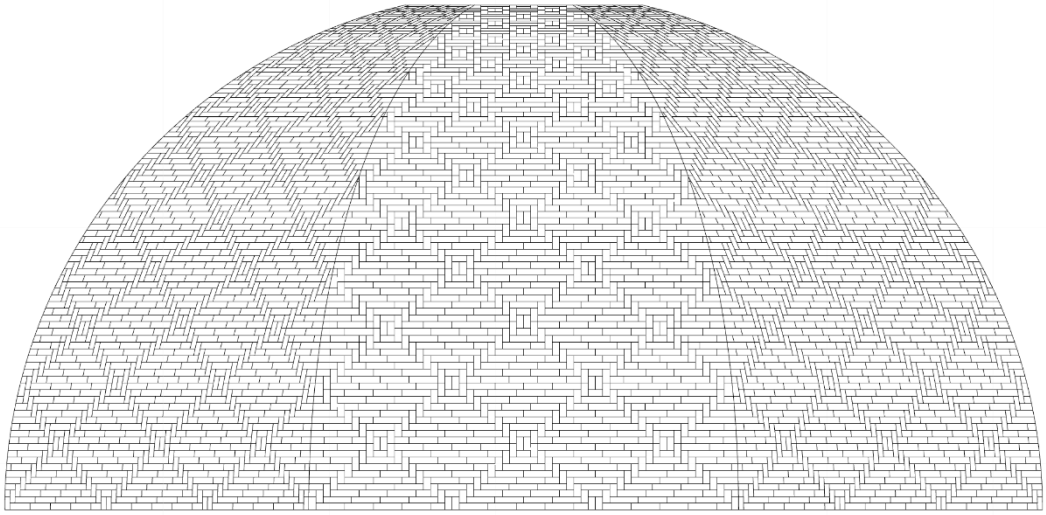

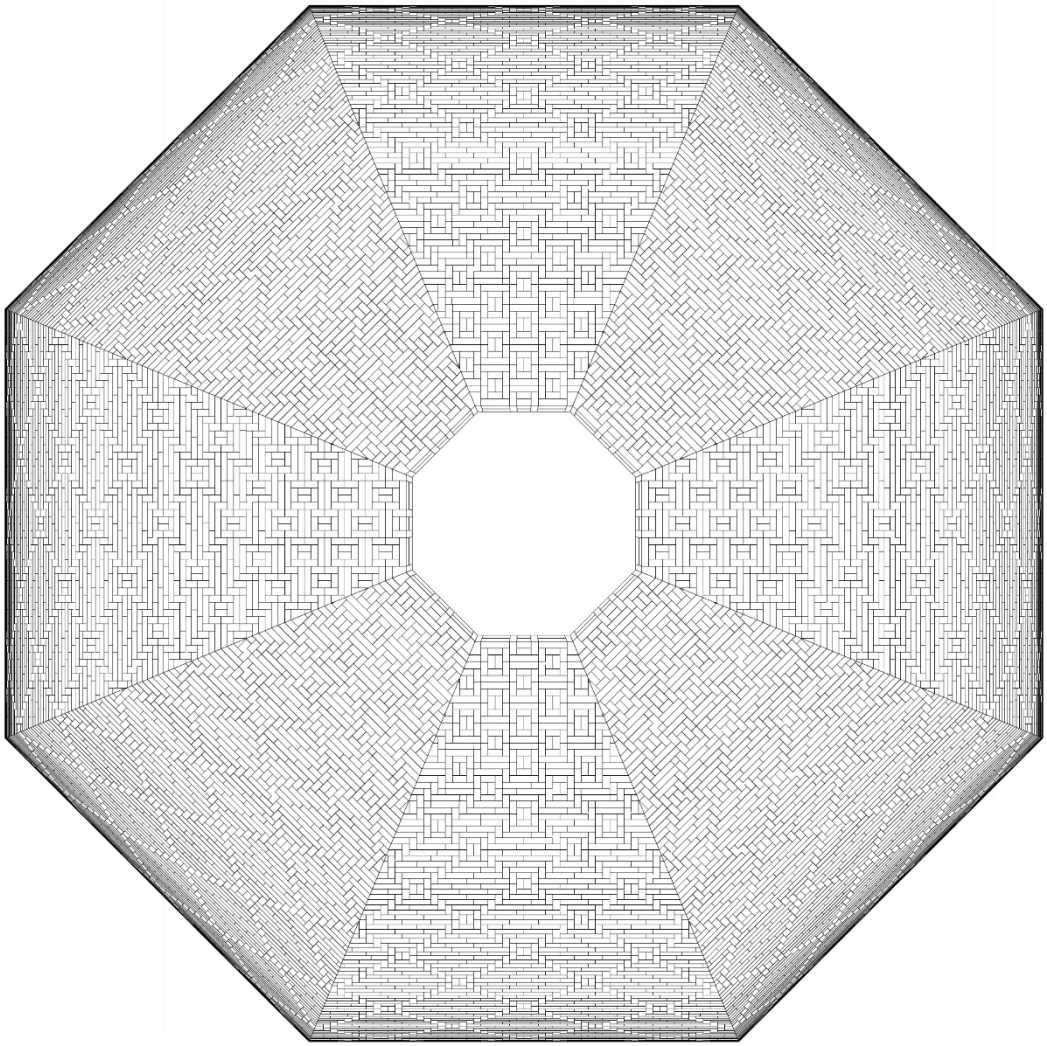

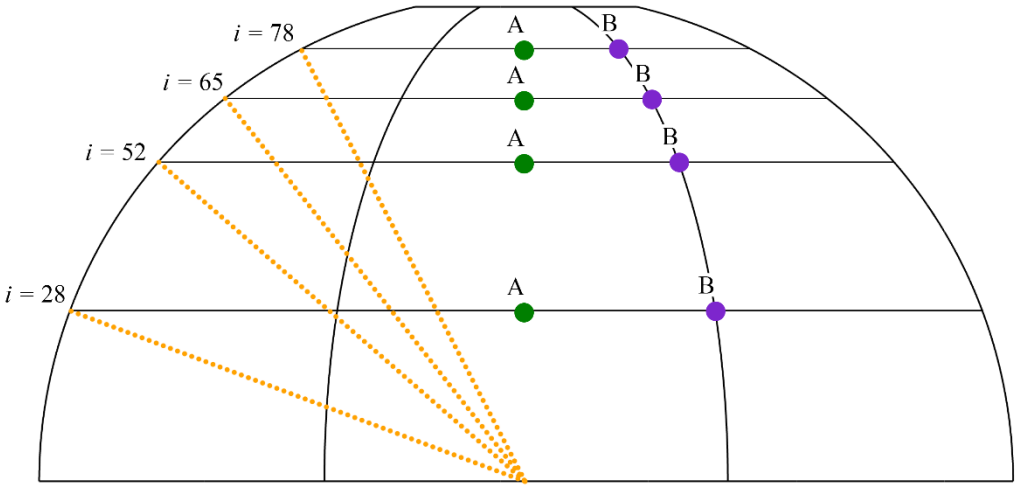

Key-section for analyses:
Courses analysed: i =28, 52, 65, 78

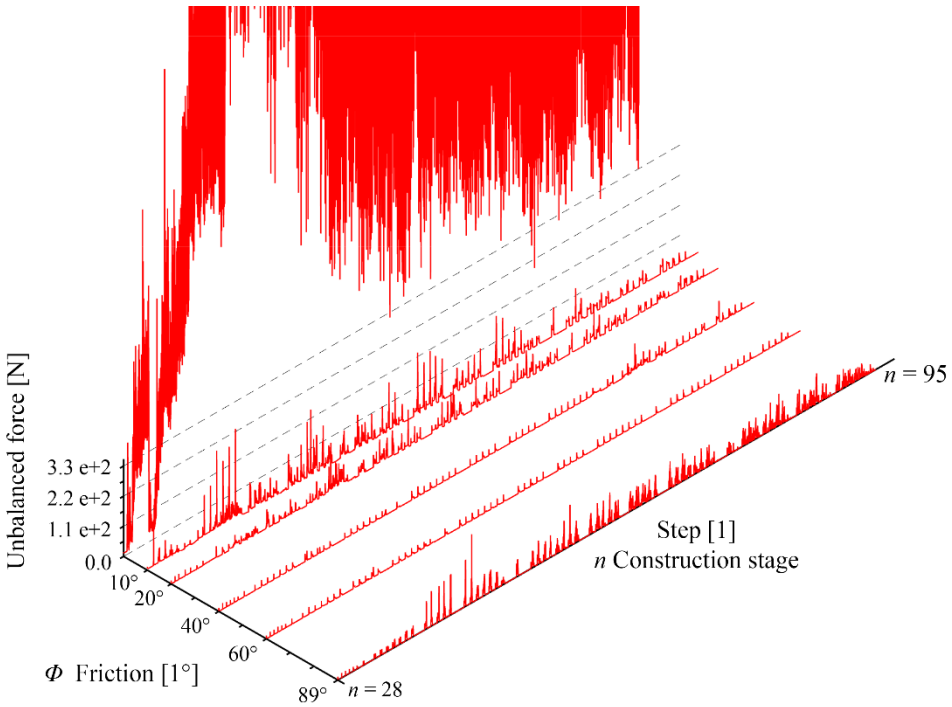

Unbalanced force $\Phi = 0°, 10°, 20°, 40°, 60°, 89°$
Construction stages: $n = 95$

Course $i = 28$, Point A
Construction stages: $n = 95$
$10° < \Phi < 90°$

Z-Velocity

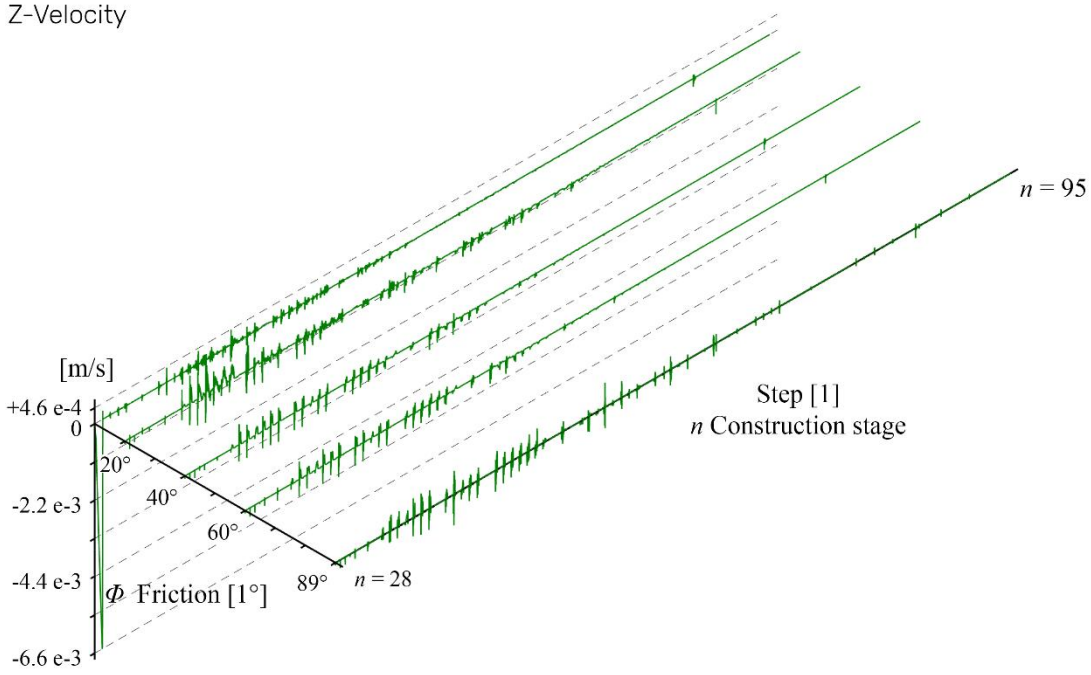

Displacement

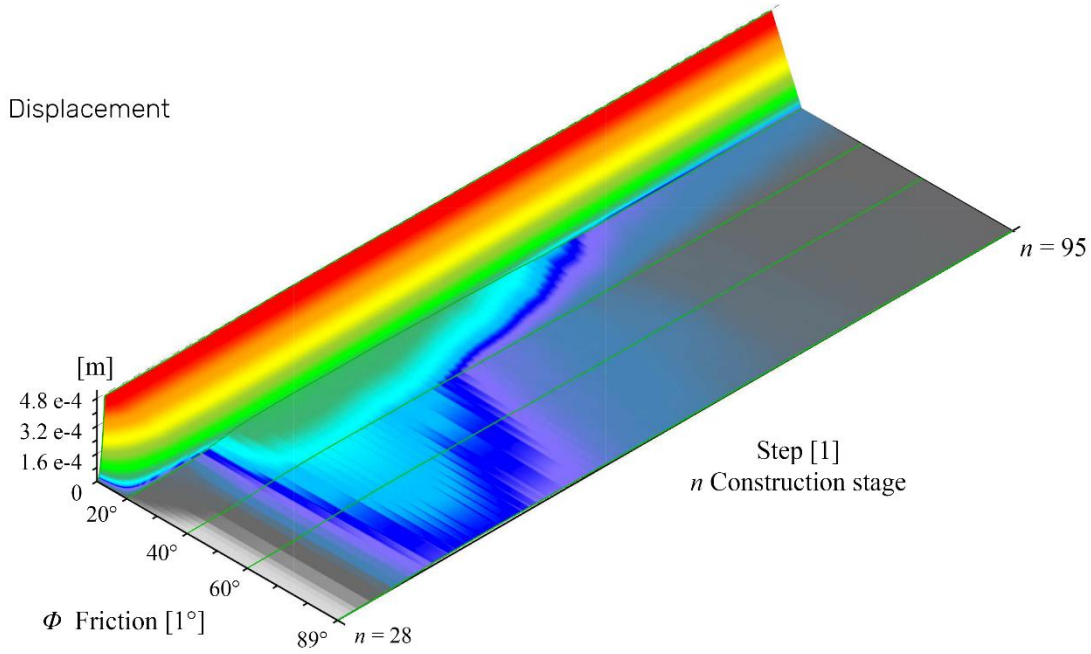

Course $i = 28$, Point B
Construction stages: $n = 95$
$10° < \Phi < 90°$

Z-Velocity

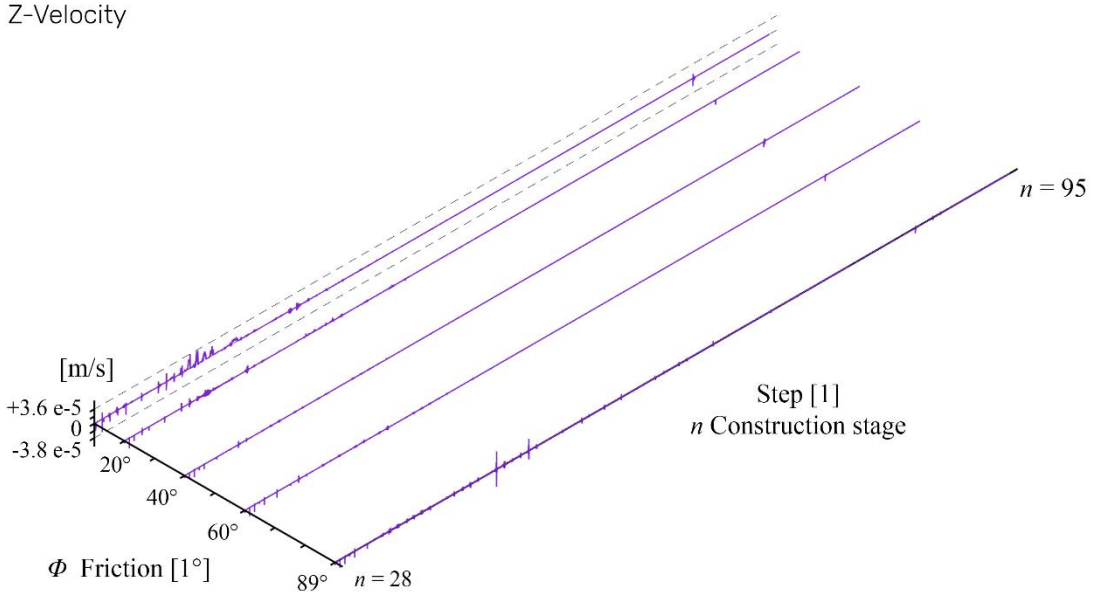

Displacement

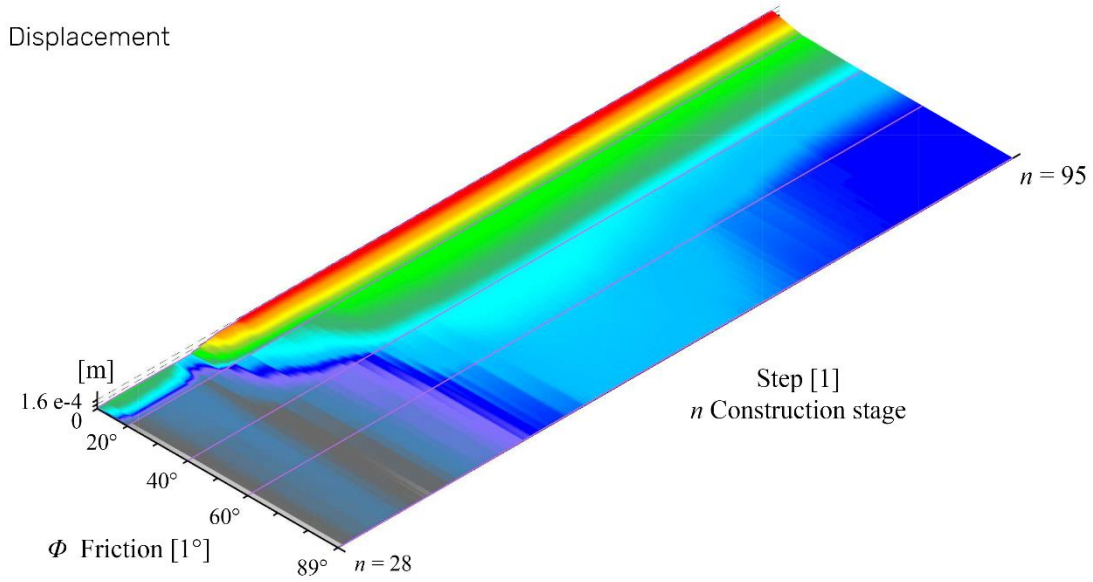

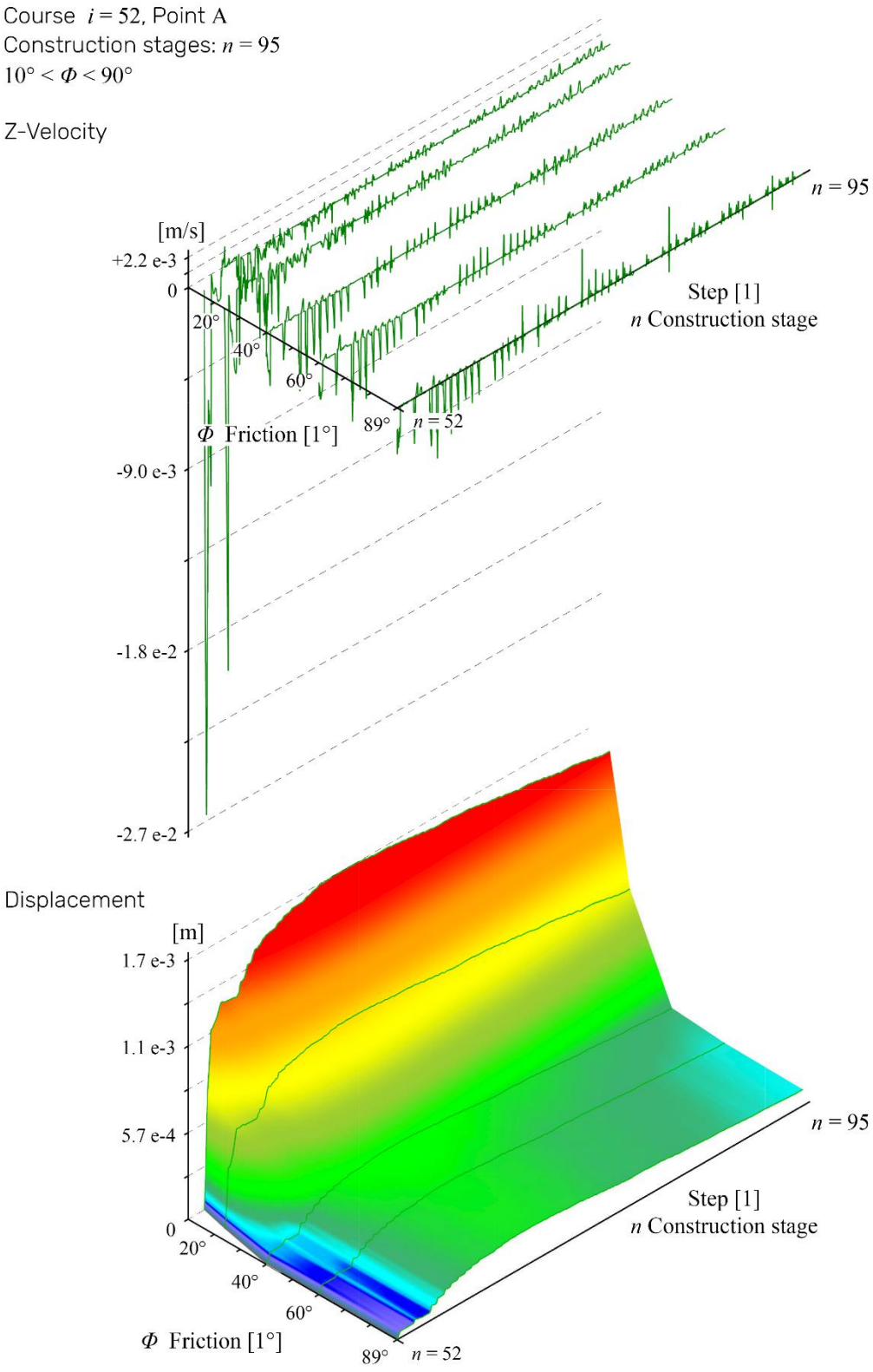
Course $i = 52$, Point A
Construction stages: $n = 95$
$10° < \Phi < 90°$
Z-Velocity
[m/s]
+2.2 e-3
0
-9.0 e-3
-1.8 e-2
-2.7 e-2
20°
40°
60°
89°
Φ Friction [1°]
$n = 52$
$n = 95$
Step [1]
n Construction stage
Displacement
[m]
1.7 e-3
1.1 e-3
5.7 e-4
0
20°
40°
60°
89°
Φ Friction [1°]
$n = 52$
$n = 95$
Step [1]
n Construction stage

Course $i = 52$, Point B
Construction stages: $n = 95$
$10° < \Phi < 90°$

Z-Velocity

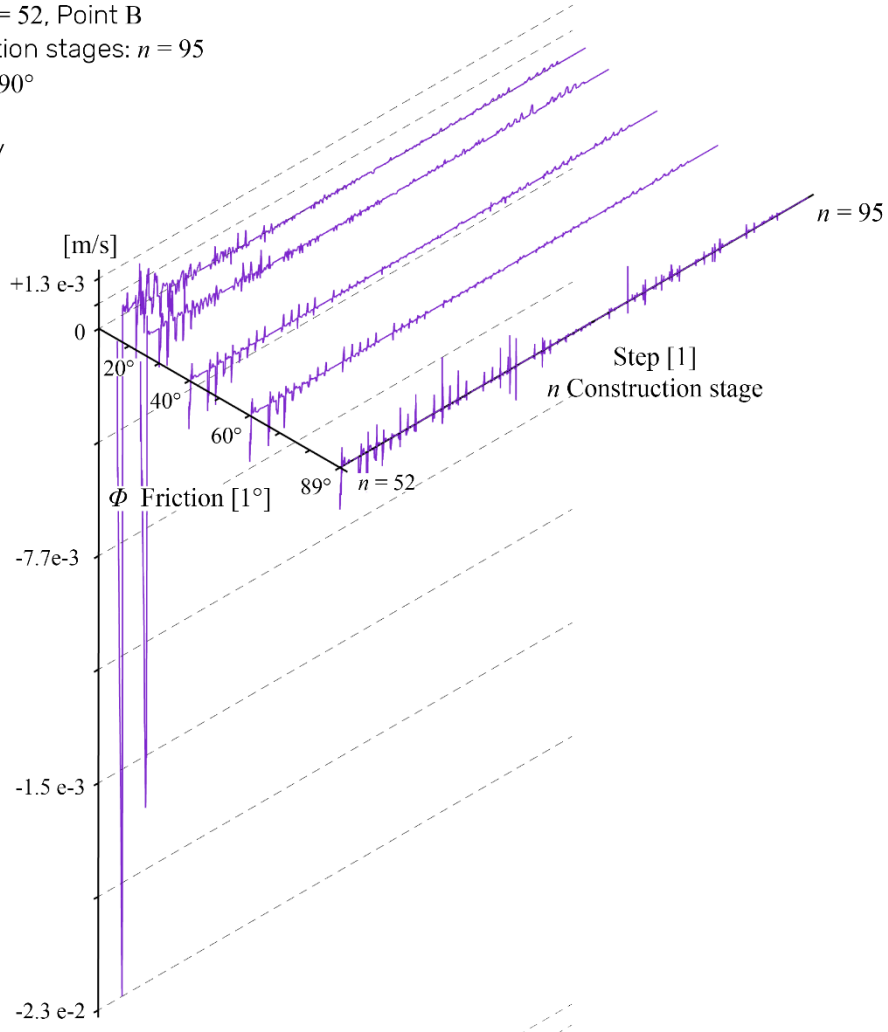

Displacement

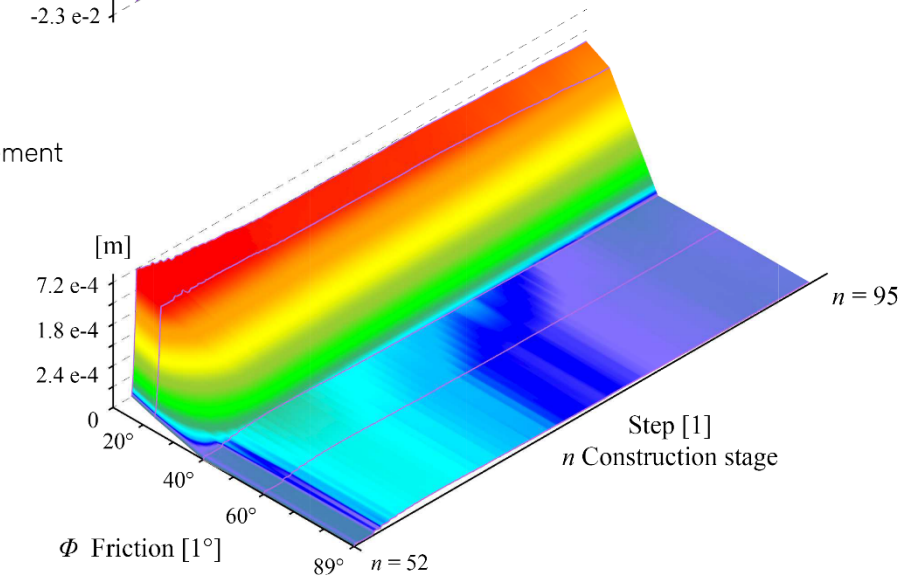

Course $i = 65$, Point A
Construction stages: $n = 95$
$10° < \Phi < 90°$

Z-Velocity

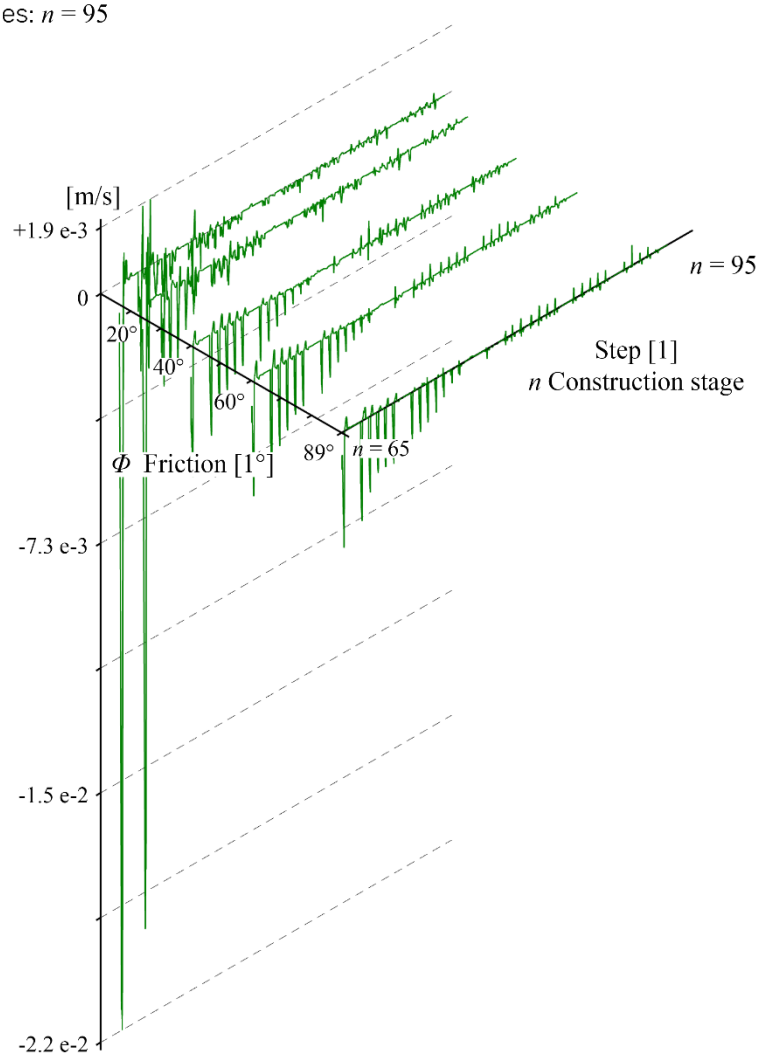

Displacement

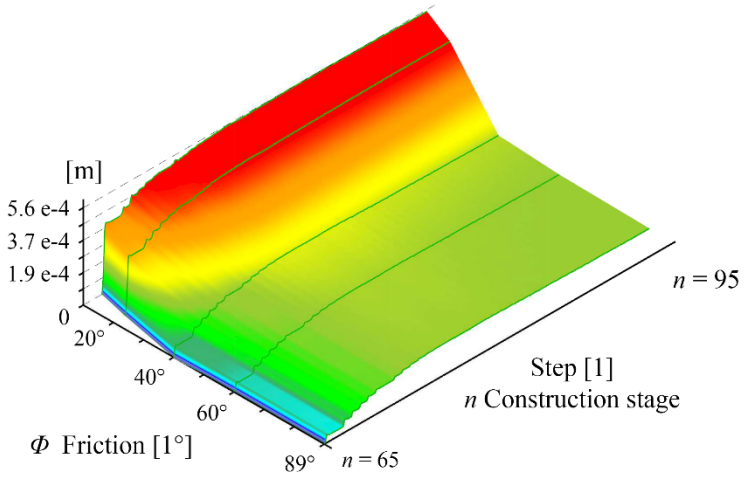

Course $i = 65$, Point B
Construction stages: $n = 95$
$10° < \Phi < 90°$

Z-Velocity

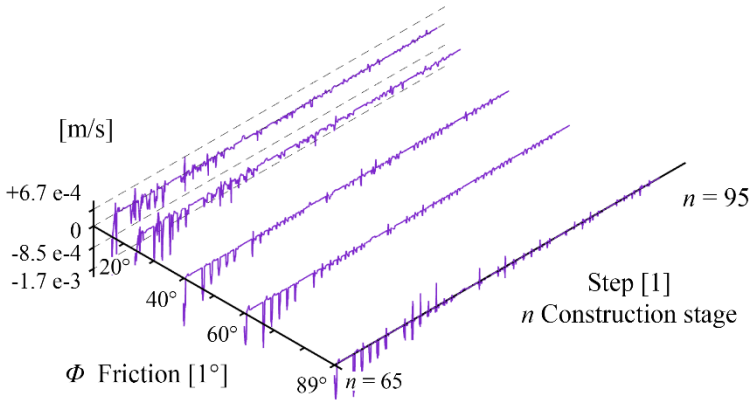

Displacement

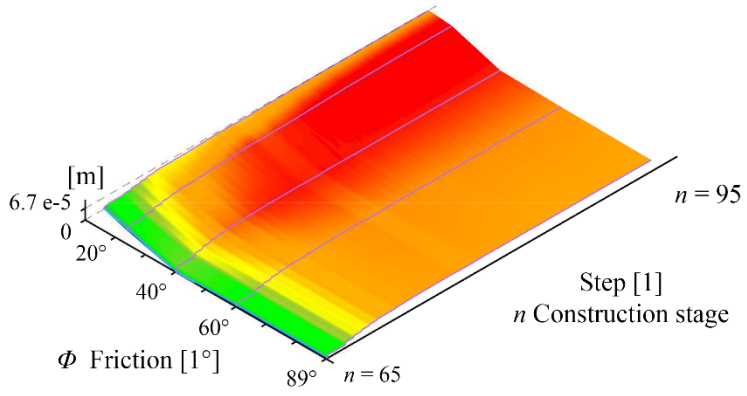

Course $i = 78$, Point A
Construction stages: $n = 95$
$10° < \Phi < 90°$

Z-Velocity

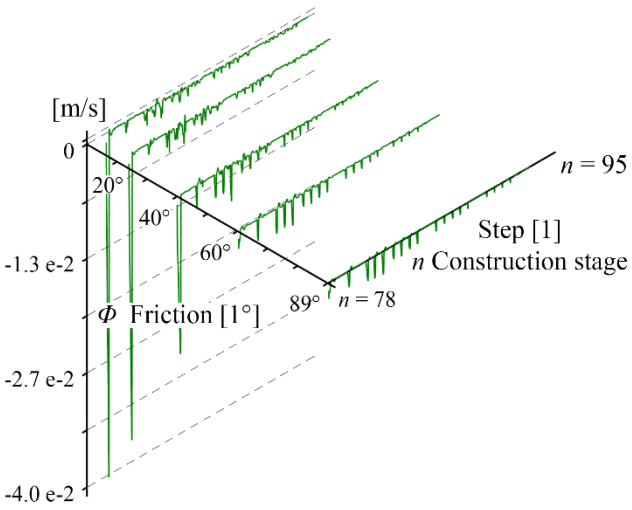

Displacement

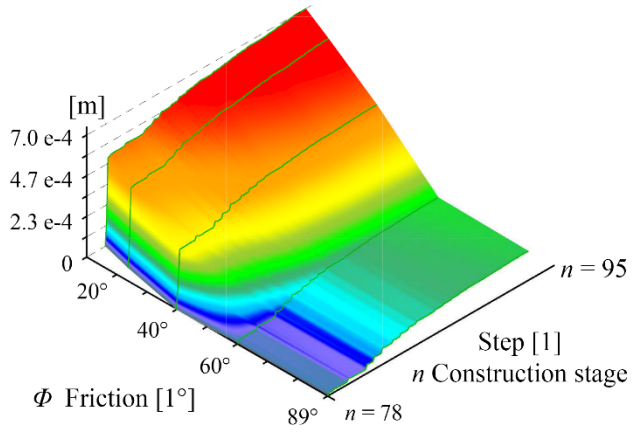

Course $i = 78$, Point B
Construction stages: $n = 95$
$10° < \Phi < 90°$

Z-Velocity

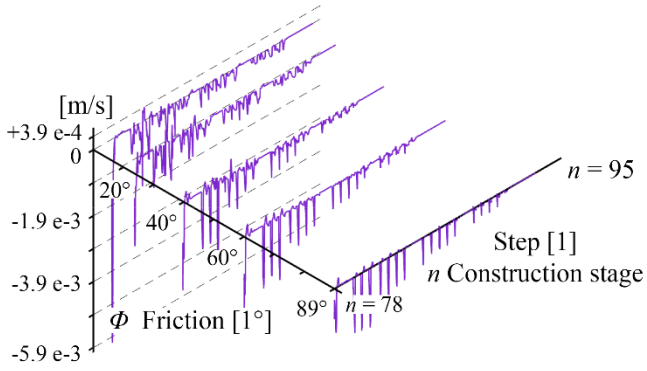

Displacement

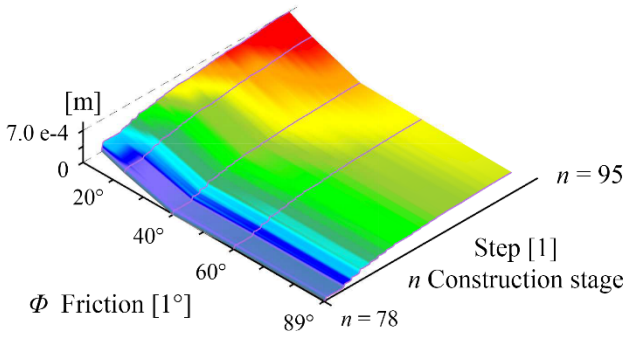

Hemispherical dome

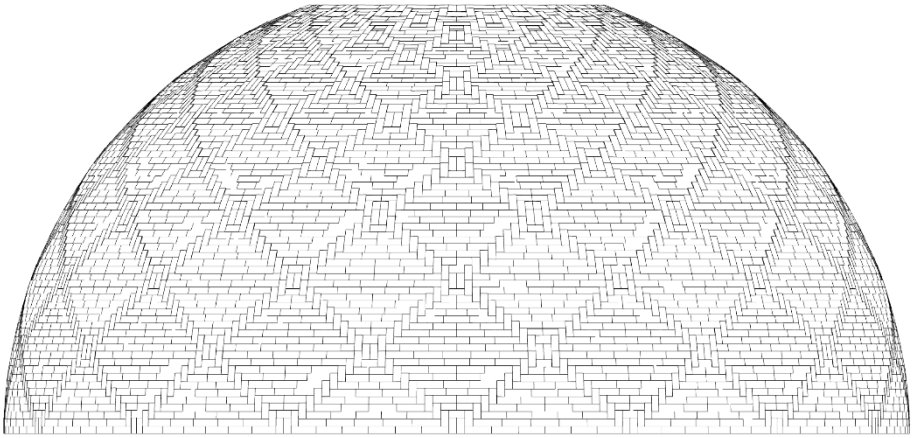

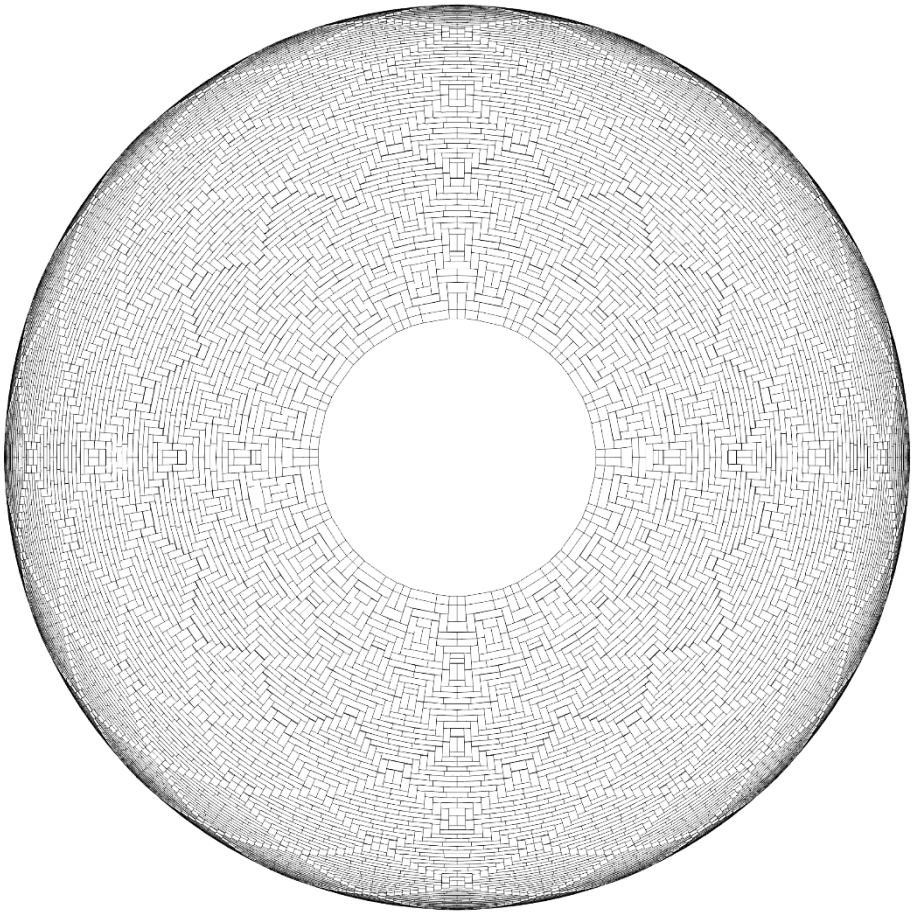

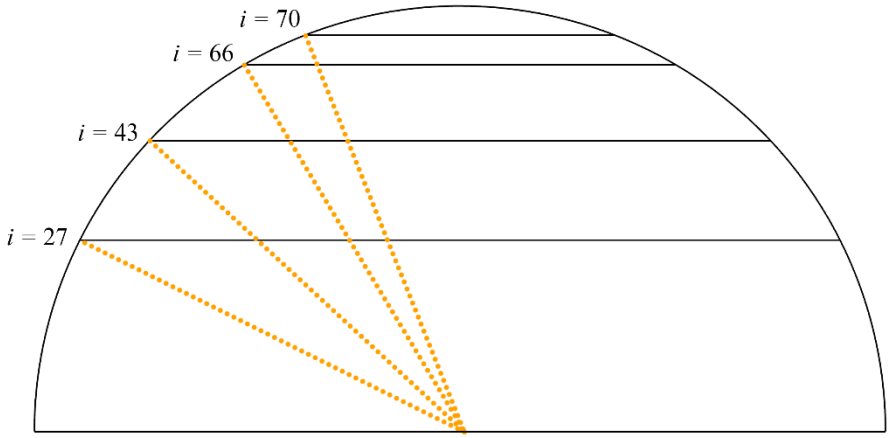

Key-section for analyses:
Courses analysed: i =27, 43, 66, 70

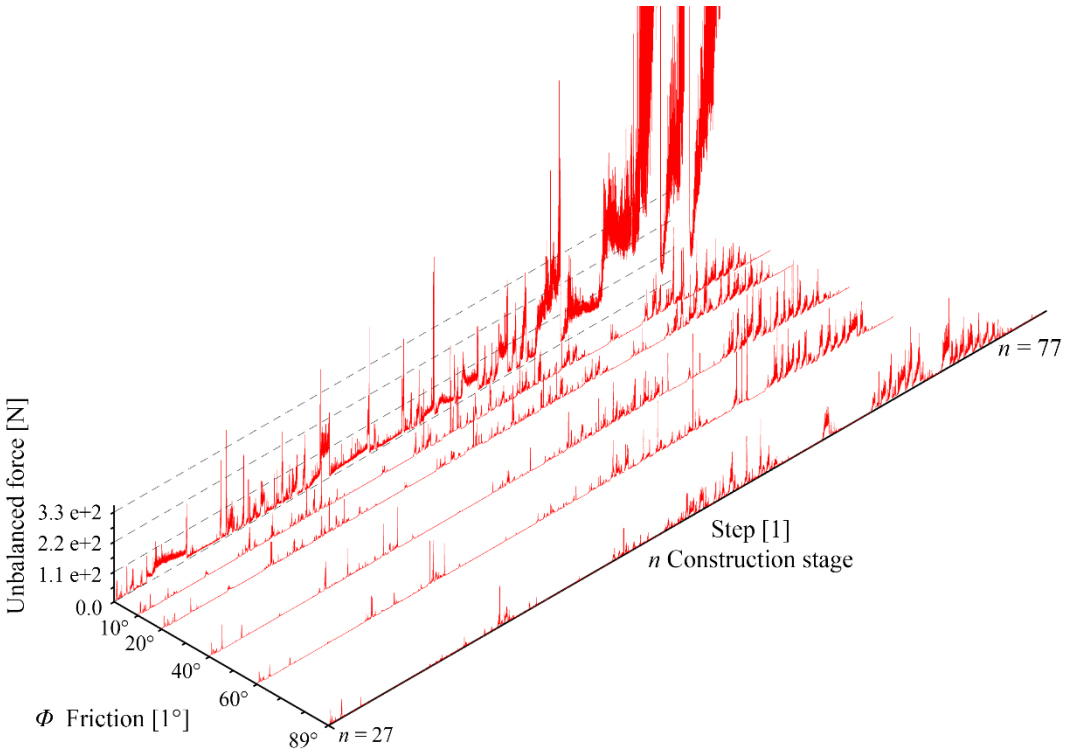

Unbalanced force Φ = 0°, 10°, 20°, 40°, 60°, 89°
Construction stage: n = 77

Course $i = 27$
Construction stages: $n = 77$
$10° < \Phi < 90°$

Z-Velocity

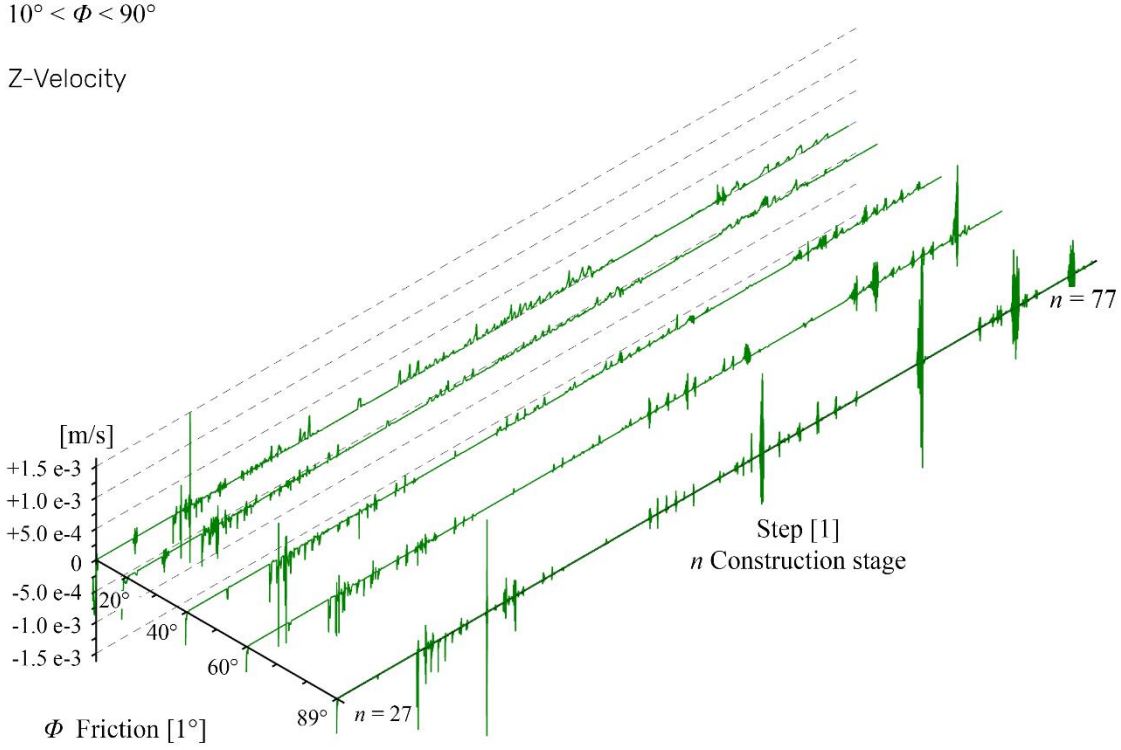

Displacement

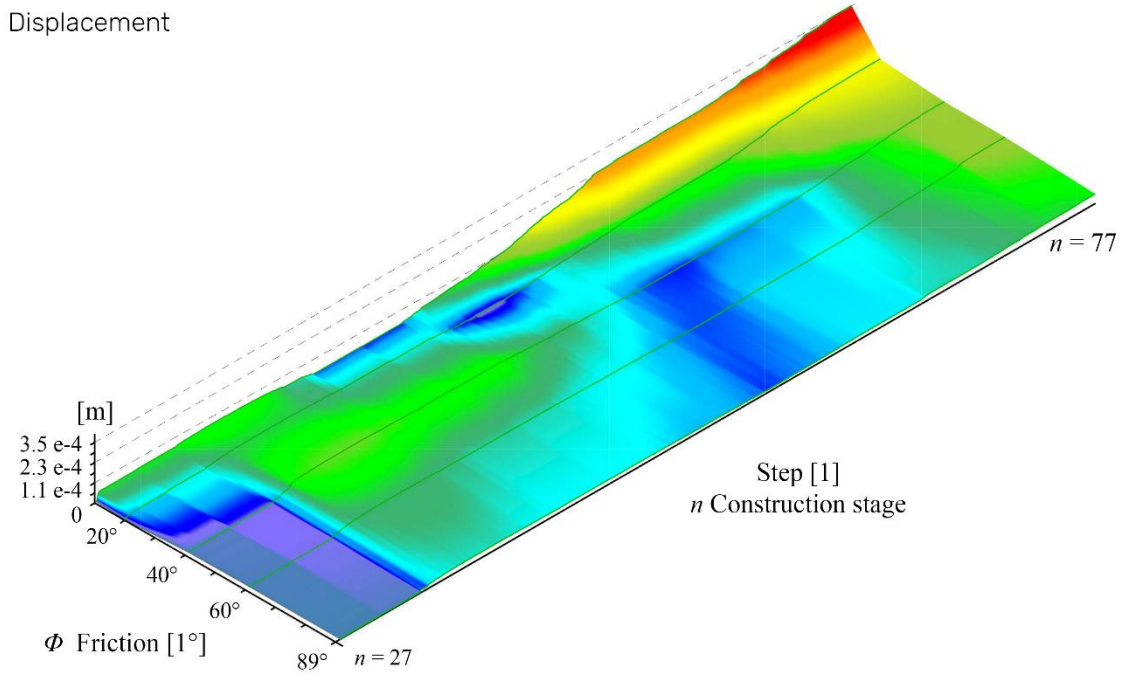

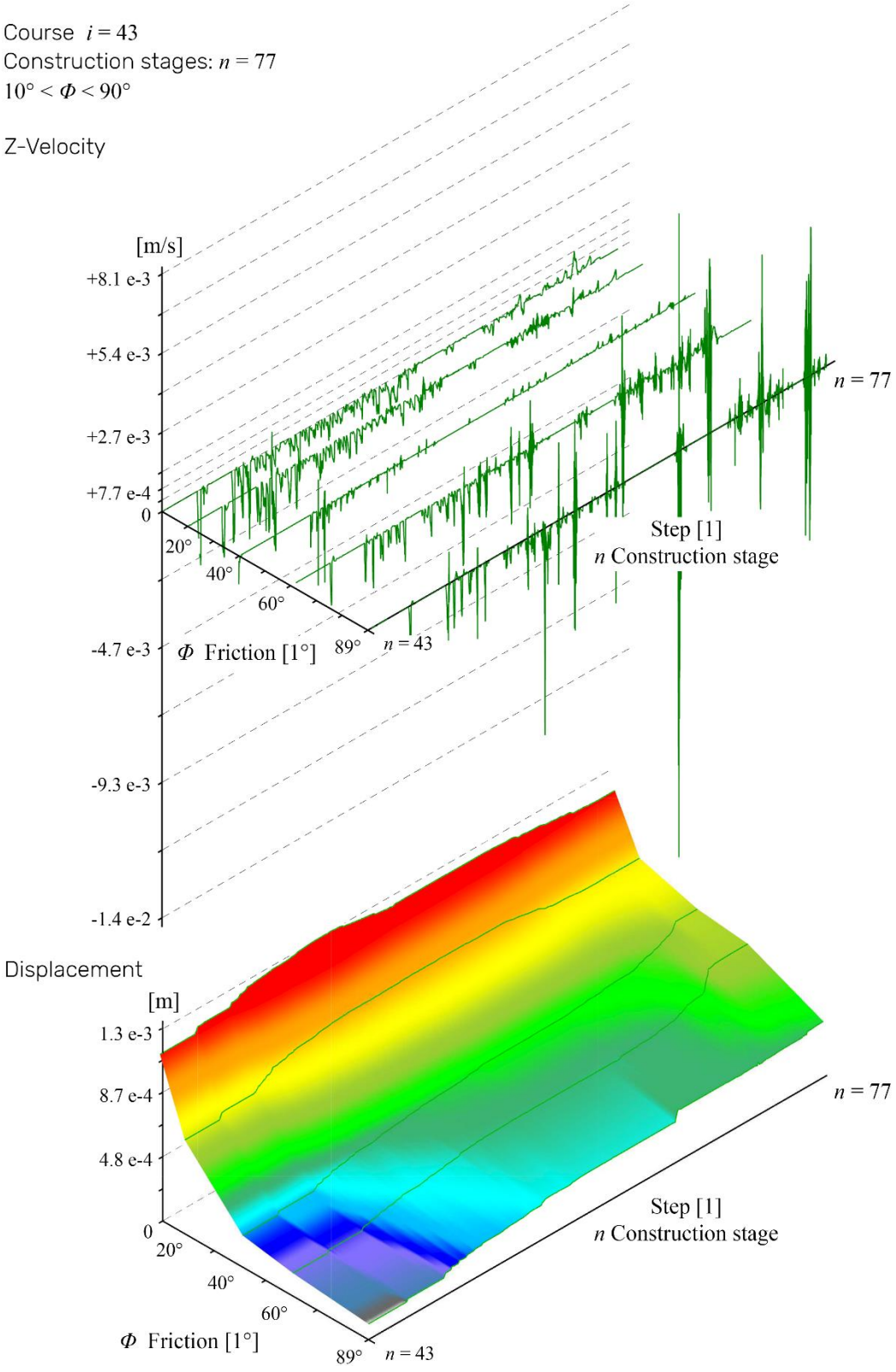
Course $i = 43$
Construction stages: $n = 77$
$10° < \Phi < 90°$
Z-Velocity
[m/s]
+8.1 e-3
+5.4 e-3
+2.7 e-3
+7.7 e-4
0
-4.7 e-3
-9.3 e-3
-1.4 e-2
20°
40°
60°
89°
Φ Friction [1°]
$n = 43$
$n = 77$
Step [1]
n Construction stage
Displacement
[m]
1.3 e-3
8.7 e-4
4.8 e-4
0
20°
40°
60°
89°
Φ Friction [1°]
$n = 43$
$n = 77$
Step [1]
n Construction stage

Course $i = 64$
Construction stages: $n = 77$
$10° < \Phi < 90°$

Z-Velocity

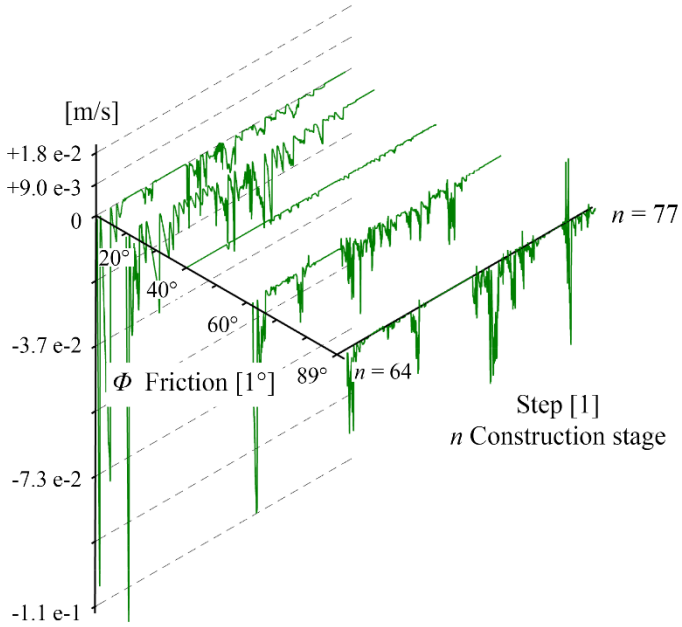

Displacement

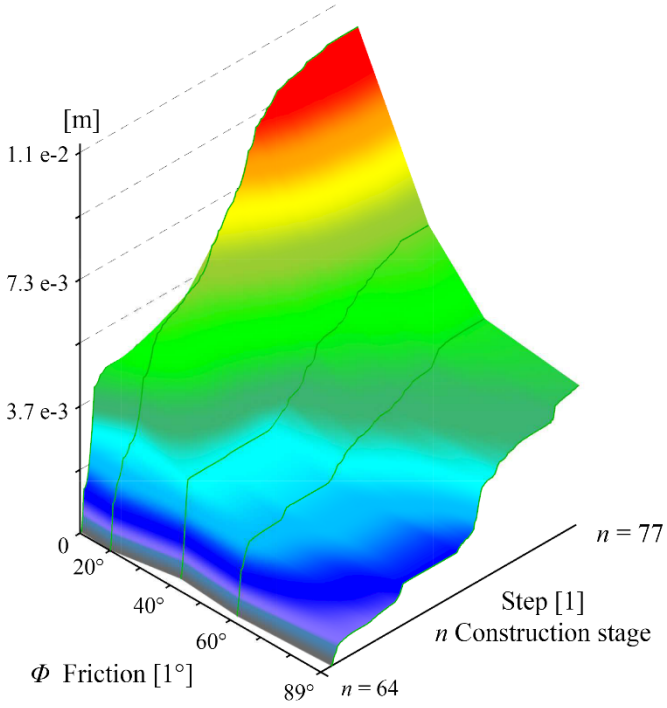

Course $i = 70$
Construction stages: $n = 77$
$10° < \Phi < 90°$

Z-Velocity

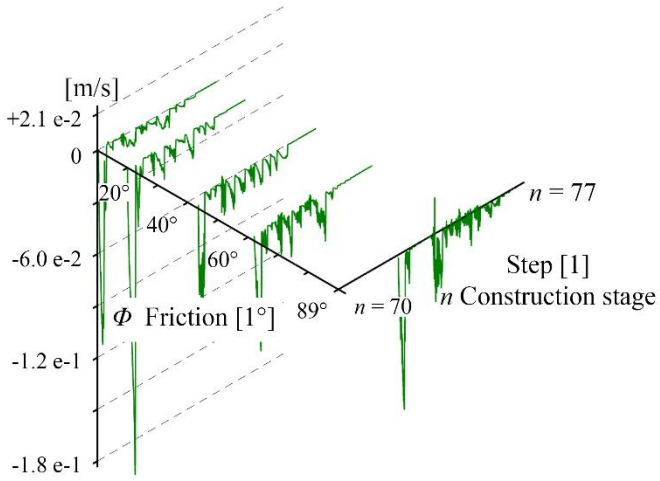

Displacement

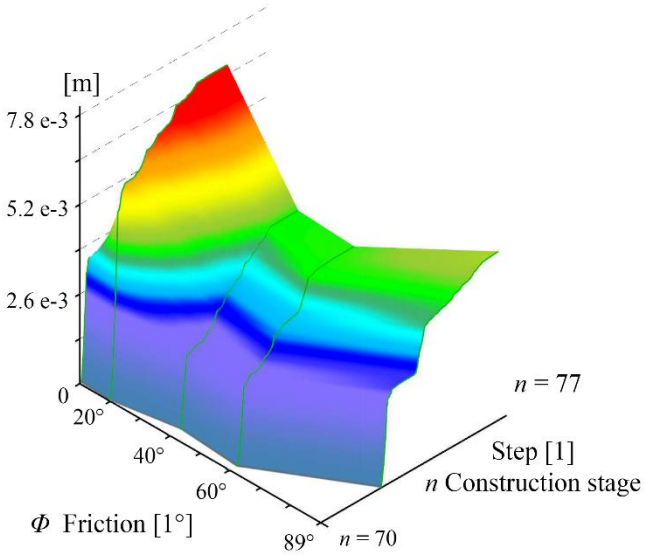

Appendix C

List of figures

List of tables

References

[1] P. Block, M. Rippmann, T. Van Mele, and D. Escobedo, “The Armadillo vault balancing computation and tradition craft,” in *Fabricate 2017*, JSTOR, Ed. 2017, pp. 286–293.

[2] J. Heyman, “The stone skeleton,” *Int. J. Solids Struct.*, vol. 2, pp. 249–279, 1966.

[3] M. Angelillo, L. Cardamone, and A. Fortunato, “A Numerical model for masonry-like structures,” *J. Mech. Mater. Struct.*, vol. 5, no. 4, pp. 583–615, 2010.

[4] A. Iannuzzo, F. De Serio, A. Gesualdo, G. Zuccaro, A. Fortunato, and M. Angelillo, “Crack patterns identification in masonry structures with a C° displacement energy method,” *Int. J. Mason. Res. Innov.*, vol. 3, no. 3, pp. 295–323, 2018.

[5] A. Tralli, C. Alessandri, and G. Milani, “Computational Methods for Masonry Vaults: A Review of Recent Results,” *Open Civ. Eng. J.*, vol. 8, pp. 272–287, 2014.

[6] A. Choisy, *L’art de bâtir chez les Romains*. Paris. Librairie générale de l’architecture et des travaux, 1873.

[7] S. F. Huerta, “The geometry and construction of Byzantine vaults: the fundamental contribution of Auguste Choisy,” in *Auguste Choisy (1841-1909): L’architecture et l’art de bâtir*, F. J. Girón Sierra and S. Huerta Fernández, Eds. Madrid, 2009, pp. 289–305.

[8] S. Andreani, A. Jyoti, and M. Bechthold, “Flowing Matter: Robotic Fabrication of Complex Ceramic Systems,” *SARC. Proc. Int. Symp. Autom. Robot. Constr.*, vol. 29, 2012.

[9] A. Menges *et al.*, “Robotic fabrication of stone assembly details,” in *Fabricate 2017*, 2019, pp. 106–113.

[10] S. Goessens, C. Mueller, and P. Latteur, “Feasibility study for drone-based masonry construction of real-scale structures,” *Autom. Constr.*, vol. 94, pp. 458–480, 2018.

[11] G. McKinsey, “Reinventing Construction. A Route to Higher Productivity. Vitattu 3.11. 2017,” 2017.

[12] N. Lepore, “Le volte in muratura: forma e struttura, equilibrio e analisi limite,” Roma Tre, 2018.

[13] S. H. Awad, *Concrete Formwork Svstems*. 1999.

[14] H. A. Rani, “The Impact of Construction Waste to The Environmental on Project Development in Aceh Road material View project Analytic Network Process Method View project,” *International J. Manag. Inf. Technol. Eng.*, vol. 5, pp. 1–8, 2017.

[15] S. F. Huerta, “Las bóvedas tabicadas en Alemania: la larga migración de una técnica

constructiva," in *Actas del Segundo Congreso Internacional Hispanoamericano, Noveno Nacional, de Historia de la Construcción*, Madrid, 2017, pp. 759–772.

[16] J. F. D. Dahmen and J. A. Ochsendorfs, "Earth masonry structures: Arches, vaults and domes," *Mod. Earth Build. Mater. Eng. Constr. Appl.*, pp. 427–460, 2012.

[17] I. J. Oppenheim, D. J. Gunaratnam, and R. H. Allen, "Limit State Analysis of Masonry Domes," *J. Struct. Eng.*, vol. 115, no. 4, pp. 868–882, Apr. 1989.

[18] M. Como, *Statics of Historic Masonry Constructions*, vol. 1. 2013.

[19] T. Michiels and S. Adriaenssens, "Form-finding algorithm for masonry arches subjected to in-plane earthquake loading," *Comput. Struct.*, vol. 195, pp. 85–98, Jan. 2018.

[20] L. C. Lancaster, *Innovative Vaulting in the Architecture of the Roman Empire: 1st to 4th Centuries CE*. Cambridge University Press, 2015.

[21] A. Bouet, *Les matériaux de construction en terre cuite dans les thermes de la Gaule Narbonnaise*. Ausonius Éditions, 2019.

[22] G. Mirabella Roberti and O. Spina, "Discrete element analysis on the Sardinian 'Nuaraghe,'" in *Strumas V International Symposium on Computer Methods in Structural Masonry*, 2001.

[23] S. El-Naggar, "Les voûtes dans l'architecture de l'Égypte ancienne," 1999.

[24] S. Storz, "Tonröhren im antiken Gewölbebau," in *Mainz: Philippe von Zabern*, 1994.

[25] R. Besenval, *Technologie de la voute dans l'orient ancient*. Paris, 1984.

[26] L. Davis, J. Ochsendorf, P. Block, and M. DeJong, "Tile vaulted systems for low-cost construction in Africa," *ATDF J.*, vol. 7, no. 1/2, pp. 4–13, 2010.

[27] D. Wendland, "Traditional vault construction without formwork: Masonry pattern and vault shape in the historical technical literature and in experimental studies," *Int. J. Archit. Herit.*, vol. 1, no. 4, pp. 311–365, 2007.

[28] B. Ward, Perkins; John, "Notes on the structure and building methods of early Byzantine Architecture," in *The Great Palace of the Byzantine emperors. Second Report., editado por D.T.Rice. Edimbourgh*, Edinburgh, Eds. D. Talbot Rice. , 1959, pp. 52–104.

[29] H. Fathy, *Architecture for the poor: an experiment in rural Egypt.* University of Chicago press, 2010.

[30] M. Angelillo, *Mechanics of masonry structures*. London, 2014.

[31] F. Ger y Lo´ bez, *Tratado de construcción civil*. Diputación, 1869.

[32] S. Olivier, A.; Storz, "Analyse et restitution d'un procédé de construction antique: réalisation d'une voûte d'arête sur coffrage perdu en tubes de terre cuite," in *Recherches archéologiques*

franco-tunisiennes à Bulla Regia , 1st ed., Beschaouch, A.; Hanoune, R.; Khanoussi, M.; Olivier, A.; Thébert, Y, 1983, pp. 11–127.

[33] R. J. A. Wilson, "Terracotta vaulting tubes (tubi fittili): on their origin and distribution," *J. Rom. Archaeol.*, vol. 5, pp. 97–129, 1992.

[34] S. Storz, "La tecnica edilizia romana e paleocristiana delle volte e cupole a tubi fittili," in *Lo specchio del cielo*, 1997, pp. 23–42.

[35] M. L. Stoppioni, "Con la terra e con il fuoco," *Fornaci romane nel Riminese*, 1993.

[36] G. D'ossat De Angelis, "Nuovi dati sulle volte costruite con vasi fittili," *Palladio*, vol. 5, 1941.

[37] G. Mirabella Roberti, N. Lombardini, and H. Faltehr, "Late Roman domes in clay tubes: historical and numerical study of San Vitale in Ravenna," in *Iass international Symposium*, 1955, vol. 2.

[38] J. Durm, "Die Baukunst der Etrusker," *Die Baukunst der Römer*, vol. 2, 1905.

[39] A. Almagro, "Bóvedas tabicadas en la Cartuja de Granada: el final de un proceso evolutivo," in *Actas del Simposio Internacional sobre Bóvedas Tabicadas*, 2011.

[40] A. Zaragozá. Catalán, "A propósito de las bóvedas de crucería y otras bóvedas medievales," in *Anales de Historia de l'arte*, Pubblicaciones Universidad Complutense de Madrid, Ed. Madrid, 2009, pp. 96–126.

[41] A. Zaragozá. Catalán, "Hacia una Historia de las Bóvedas Tabicadas," in *Construyendo Bóvedas Tabicadas*, 2011.

[42] I. M. Varela,Botella; Bevia, S.; Garcia, "Restauracion Catillo de la Atalya, dos fases," *Praxis Edilizia 10 anos con el Patrimonio Arquitectonico Resturacion*. Valencia, pp. 94–197, 2010.

[43] G. R. Collins, "The Transfer of Thin Masonry Vaulting from Spain to America," vol. 27, no. 3, pp. 176–201, 2018.

[44] J. Ochsendorf, *Guastavino vaulting: the art of structural tile*. Princeton Architectural Press, 201AD.

[45] C. Espie, *Manière de rendre toutes sortes d'édifices incombustibles*. Paris: Duchesne, 1754.

[46] M. H. Ramage, J. Ochsendorf, P. Rich, J. K. Bellamy, and P. Block, "Design and Construction of the Mapungubwe National Park Interpretive Centre , South Africa," pp. 14–23.

[47] Á. Truñó, *Construcción de bóvedas tabicadas.* Reverte, 2004.

[48] L. Moya Blanco, *Bóvedas tabicadas*. 1947.

[49] A. Choisy, *Histoire de l'Architecture*. Paris: G. Béranger, 1899.

[50] R. Guastavino, *Essay on the theory and history of cohesive construction applied especially to the timbrel vault*. Boston: Ticknor Co., 1892.

[51] L. Davis, M. Rippmann, T. Pawlofsky, and P. Block, "Innovative funicular tile vaulting: A prototype vault in Switzerland," *Struct. Eng.*, vol. 90, no. 11, pp. 46–56, 2012.

[52] D. Melonie, Bayl-Smith; Block, Philippe; Pigram, "Pass me the mixing bucket: The Ribbed Catalan studio as a design/research case study," *Brookes eJournal Learn. Teach.* , no. 8.1/2, 2016.

[53] H. Saalman, *Filippo Brunelleschi: The Cupola of Santa Maria del Fiore*. London: Zwemmer, 1980.

[54] S. Di Pasquale, *Brunelleschi: la costruzione della cupola di Santa Maria del Fiore*. 2002.

[55] F. Ottoni, "La lunga vicenda delle fabbriche cupolate. Note storiche sulla stabilità, tra dibattito e sperimentazione.," Università degli Studi di Parma. Dipartimento di Ingegneria Civile ed Architettura, 2009.

[56] A. Pizzigoni, "Brunelleschi.pdf." Zanichelli, p. 192, 1989.

[57] A. Pizzigoni, "Brunelleschi's Bricks," *J. Int. Assoc. Shell Spat. Struct.*, vol. 56, no. 2, pp. 137–156, 2015.

[58] G. Vasari, *Le vite dei più eccellenti pittori, scultori e architetti*, Vol.1. presso l'Ufficio Generale di Commissioni ed Annunzi, 1876.

[59] G. Zander, "Gli ottagoni di San Pietro riconosciute nel disegno Arch.Uff. N. 1330," *Palladio*, vol. 1, pp. 62–82, 1998.

[60] E. Galdieri, "Da Gerusalemme a Dakha: mille anni di cupole islamiche," in *Lo specchio del Cielo*, Caludia Conforti, Ed. MIlano: Electa, 1997, pp. 53–66.

[61] Shukur Askaro, *The Architecture of the Temurids*. Tashkent: San'at, 2009.

[62] S. Conti, Giuseppe; Guidelli, Sandra; Livi, "La spinapesce nel Rinascimento tra Filippo Brunelleschi, i Sangallo e Bernardo Buontale nella Grotta Grande del Giardino di Boboli: alcune considerazioni matematiche," *Bollettino della Società di Studi fiorentini*, Emmebi Edizioni, 2013.

[63] D. De Rosa, *Il pontificato di Vittore III: un riesame critico*. Aracne, 2008.

[64] M. S. Elsheikh, "Tracce di presenza arabo-musulmana in Toscana," *Plurilingual e-journal Lit. Relig. Hist. Stud.* , 2016.

[65] C. G. De Montauzan, *Les aqueducs antiques de Lyon: étude comparée d'archéologie romain*. E. Leroux, 1909.

[66] C. Gurrieri, Francesco; Acidini Luchinat, *La cattedrale di Santa Maria del Fiore a Firenze*,

Vol. 1. Giunti gruppo editoriale, 1994.

[67] "Ardesan Friday Mosque," 2013. [Online]. Available: http://www.selcuklumirasi.com/architecture-detail/ardestan-friday-mosque.

[68] V. Lanza, "La ventilazione naturale dei bādgir nell'architettura contemporanea. Il ruolo della tradizione nel condizionamento ad impatto zero: quattro esempi di ventilazione naturale nei Paesi del Golfo e in Occidente," Università Ca'Foscari Venezia, 2017.

[69] A. Pizzigoni, V. Paris, M. Pasta, M. Morandi, and A. Parsani, "Herringbone naked structure," in P*roceedings of the Iass international Symposium 2018. Creativity in Structural Design*, 2018, pp. 1–6.

[70] G. Conti, B. Sedili, and A. Trotta, "Le curve Lossodromiche in Architettura," *Chief Ed.*, vol. 65, no. 2, 2014.

[71] V. Paris and A. Pizzigoni, "La struttura nascosta," *Structural:Building engineering + Structural design*, pp. 1–15, 2016.

[72] A. Pizzigoni and V. Paris, "Herringbone, Gualandrino and Brunelleschi's Bricks," in *International Masonry Conference*, 2014, pp. 1–12.

[73] S. F. Huerta, "The analysis of masonry architecture: A historical approach: To the memory of professor Henry J. Cowan," *Archit. Sci. Rev.*, vol. 51, no. 4, pp. 297–328, 2008.

[74] K. Karl-Eugen, *The history of the theory of structures*. 2018.

[75] M. Corradi, *Edoardo Benvenuto: l'arte e la scienza del costruire*. Genova: Edizioni di Storia, Scienza e Tecnica &, 2008.

[76] J. Heyman, *Coulomb's memoir on statics: an essay in the history of civil engineering*. Imperial Collage Press, 1972.

[77] P. de La Hire, *Traité de mécanique, où l'on explique tout ce qui est nécessaire dans la pratique des Arts, et les proprietés des corps pesants lesquelles ont eu plus grand*. Paris: Imprimerie Royale, 1695.

[78] P. de La Hire, "Sur la construction des voûtes dans les édifices," 1712.

[79] B. F. de Belidor, *"La" science des ingenieurs dans la conduite des travaux de fortification et d'architecture civile*. Chez Charkes Antoine Jombert, 1739.

[80] P. Roca, M. Cervera, G. Gariup, and L. Pela', *Structural analysis of masonry historical constructions. Classical and advanced approaches*, vol. 17, no. 3. 2010.

[81] P. de T. Couplet, "Seconde partie de l'examen de la poussée des Voûtes," 173AD.

[82] S. F. Huerta, "Thomas Young's theory of the arch: thermal effects," in *Mechanics and architecture between episteme and techne*, 1st ed., A. Sinipoli, Ed. Roma, 2010.

[83] J. Weale, J. Hann, H. Moseley, R. Stevenson, and W. Hosking, *The Theory, practice, and architecture of bridges of stone, iron, timber, and wire: with examples on the principle of suspension*. 1843.

[84] H. Moseley, " L. On a new principle in statics, called the P rinciple of least P ressure ," *London, Edinburgh, Dublin Philos. Mag. J. Sci.*, vol. 3, no. 16, pp. 285–288, Oct. 1833.

[85] E. Méry, "Sur l'équilibre des voûtes en berceau," vol. 19, pp. 50–70, 1840.

[86] S. F. Huerta, "Mechanics of masonry vaults: The equilibrium approach," *3rd Int. Semin. Hist. Constr. Guimarães, Port.*, no. February, pp. 47–70, 2001.

[87] H. T. Eddy, *Researches in graphical statics*. D.Van Nostrand Publisher, 1878.

[88] E. Benvenuto, M. Corradi, A. Becchi, and F. Foce, *La scienza delle costruzioni e il suo sviluppo storico*. Edizioni di storia e letteratura, 2010.

[89] S. F. Huerta, "The analysis of masonry architecture: A historical approach: To the memory of professor Henry J. Cowan," *Archit. Sci. Rev.*, vol. 51, no. 4, pp. 297–328, 2008.

[90] G. Ungewitter, "Lehrbuch der gotischen Konstruktionen," 1892.

[91] D. C. Drucker, "A more fundamental approach to plastic stress-strain relations," in *Proc. of 1st US National Congress of Applied Mechanics*, 1*951*.

[92] A. Kooharian, "Limit analysis of voussoir (segmental) and concrete archs," J*ounar Proceedings*, *1952*, vol. 49, no. 12.

[93] W. Prager, "An Introduction to Plasticity. Addison Wessley," 1959.

[94] P. Block, M. Dejong, and J. Ochsendorf, "As hangs the flexible line: Equilibrium of masonry arches," in *Nexus Network Journal*, 2006, vol. 8, no. 2, pp. 13–24.

[95] M. Angelillo, P. B. Lourenço, and G. Milani, "Masonry behaviour and modelling," in *CISM International Centre for Mechanical Sciences, Courses and Lectures*, vol. 551, Springer International Publishing, 2014, pp. 1–26.

[96] R. Hart, P. A. Cundall, and J. Lemos, "Formulation of a three-dimensional distinct element model-Part II. Mechanical calculations for motion and interaction of a system composed of many polyhedral blocks," *Int. J. Rock Mech. Min. Sci.*, vol. 25, no. 3, pp. 117–125, 1988.

[97] Cundall. P. A, "Formulation of a three-dimensional distinct element model—Part I. A scheme to detect and represent contacts in a system composed of many polyhedral blocks," *Int. J. Rock Mech. Min. Sci. Geomech.*, vol. 25, no. 3, pp. 107–116, 1988.

[98] V. Sarhosis, et al., *Computational modeling of masonry structures using the discrete element method*. IGI Global 2016.

[99] *Manual, Theory and Background*. Minneapolis, Minnesota, USA: Itasca Consulting Group. Inc.

[100] A. Fraddosio, N. Lepore, and M. D. Piccioni, "Lower Bound Limit Analysis of Masonry Vaults Under General Load Conditions," *Rilem Bookseries*, vol. 18, pp. 1090–1098, 2019.

[101] J. Heyman, *Structural analysis: a historical approach*. Cambridge University Press, 2010.

[102] J. Heyman, "On shell solutions for masonry domes," *Int. J. Solids Struct.*, vol. 3, no. 2, pp. 227–241, 1967.

[103] W. H. Barlow, “On the existence (pratically) of the line of equal horizontal thrust in arches, and the mode ofdeterminf it by geomerical construction.,” *Minutes Proc. Inst. Civ. Eng.*, vol. 5, no. 1846, pp. 162–172, 1846.

[104] D. D’Ayala and C. Casapulla, “Limit state analysis of hemispherical domes with finite friction,” *Hist. Constr. possibilities Numer. Exp. Tech.*, no. 1977, pp. 617–626, 2001.

[105] B. Cipriani and W. Lau, “Construction Techniques in Medieval Cairo: the Domes of Mamluk Mausolea (1250 AD-1517A. D.),” *Second Int. Congr. Constr. Hist.*, pp. 695–716, 2006.

[106] A. Romano and J. A. Ochsendorf, “The mechanics of Gothic masonry arches,” *Int. J. Archit. Herit.*, vol. 4, no. 1, pp. 59–82, 2010.

[107] D. Ferretti and E. Coisson, “A New Numerical Approach to the Structural Analysis of Masonry Vaults”, *Key Engineering Material*, vol. 747, pp52-59, Trans Tech Publications Ltd, 2017.

[108] J. McInerney and M. J. Dejong, “Discrete Element Modeling of Groin Vault Displacement Capacity,” *Int. J. Archit. Herit.*, vol. 9, no. 8, pp. 1037–1049, 2015.

[109] I. N. Psycharis, J. V Lemos, D. Y. Papastamatiou, and C. Zambas, “Numerical study of the seismic behaviour of a part of the Parthenon Pronaos,” *Earthq. Eng. Struct. Dyn.*, vol. 32, no. January 2002, pp. 2063–2084, 2003.

[110] Ž. Smoljanović, Hrvoje; Živaljić, Nikolina; Nikolić, “A combined finite-discrete element analysis of dry stone masonry structures,” *Eng. Struct. Elsevier*, vol. 52, pp. 89–100, 2013.

[111] J. Simon and K. Bagi, “Discrete element analysis of the minimum thickness of oval masonry domes,” *Int. J. Archit. Herit.*, vol. 10, no. 4, pp. 457–475, 2016.

[112] B. S. A. Tatone and G. Grasselli, “A calibration procedure for two-dimensional laboratory-scale hybrid finite-discrete element simulations.”

[113] A. Munjiza and K. R. F. Andrews, “Penalty function method for combined finite-discrete element systems comprising large number of separate bodies,” *Int. J. Numer. Methods Eng.*, vol. 49, no. 11, pp. 1377–1396, Dec. 2000.

[114] B. Valentina, R. Gianni, and T. Alessandro, “A non-smooth-contact-dynamics analysis of Brunelleschi’s cupola: an octagonal vault or a circular dome?,” *Mecc. Elsevier*, pp. 1–23, 2019.

[115] I. Caliò, M. Marletta, and B. Pantò, “A new discrete element model for the evaluation of the seismic behaviour of unreinforced masonry buildings,” *Eng. Struct. Elsevier*, vol. 40, pp. 327–338, 2012.

[116] M. Ricci, *Il genio di Filippo Brunelleschi : e la costruzione della Cupola di Santa Maria del Fiore*. Sillabe, 2014.

[117] L. B. Alberti, *De re aedificatoria*. Firenze, 1443.

[118] M. Haines, “Myth and mangement in the construction of brunelleschi’s cupola,” *I Tatti Stud. Ital. Renaiss.*, vol. 14/15, pp. 47–101, Jan. 2011.

[119] M. Ricci, *L’accusa di Giovanni di Gherardo Gherardi a Filippo Brunelleschi: spiegazione integrale della pergamena, dei disegni e relativi contenuti tecnici*. Firenze: Salimbeni, 1987.

[120] M. Haines, “Gli anni della cupola,” 2015. [Online]. Available: http://duomo.mpiwg-berlin.mpg.de/.

[121] M. Viganò, “L’architettura militare nell’età di Leonardo.‘Guerre milanesi’ e diffusione del bastione in Italia e in Europa,” in *Atti del Convegno*, 2007.

[122] G. Giovannoni, *Antonio da Sangallo, il Giovane*. Tipografia regionale, 1959.

[123] P. Portoghesi, *Dizionario enciclopedico di architettura e urbanistica*. Roma: Istituto editoriale romano.

[124] G. Da Sangallo and L. Zdekauer, “Il taccuino senese di Giuliano da San Gallo: 49 facsimili di disegni d’architettura, scultura ed arte applicata,” 1902.

[125] A. Pizzigoni and V. PAris, “Il dispositivo a spinapesce: attualità e futuro della tecnologia costruttiva brunelleschiana,” *Costruire in laterizio CIL*, 2018. [Online]. Available: http://www.laterizio.it/cil/storia-e-restauro/482-il-dispositivo-a-spinapesce-attualita-e-futuro-della-tecnologia-costruttiva-brunelleschiana.html. [Accessed: 09-Mar-2020].

[126] R. Docci, Mario; Migliari, “La costruzione della spinapesce nella copertura della sala ottagonale di Simon Mago nella fabbrica di San Pietro,” *Palladio*, vol. 3, pp. 61–72, 1989.

[127] P. Sanpaolesi, *Brunelleschi*. Milano: Club del Libro, 1962.

[128] G. Breccola, *La Chiesa di Santa Maria in Montedoro, Montefiascone*. Montefiascone, 2000.

[129] A. Pizzigoni, V. Paris, and G. Ruscica, “Herringbone technique: truth and history of a cutting-edge technology,” in *Proceedings of the Iass international Symposium 2018. Creativity in Structural Design*, 2018, pp. 1–8.

[130] C. Ragghianti, *Filippo Brunelleschi: un uomo, un universo*. Vallecchi, 1977.

[131] S. Rebora, “Scoperto il modello della Cupola del Brunelleschi? A Firenze c’è aria di scoop, attorno ai lavori per l’ampliamento del Museo dell’Opera del Duomo | Artribune,” *Artribune*, 2012. [Online]. Available: https://www.artribune.com/tribnews/2012/12/scoperto-il-modello-della-cupola-del-brunelleschi-a-firenze-ce-aria-di-scoop-attorno-ai-lavori-per-lampliamento-del-museo-dellopera-del-duomo/. [Accessed: 19-Oct-2019].

[132] M. Rippmann, P. B.-P. of *Iass international Symposium* 2011, “Digital Stereotomy: Voussoir geometry for freeform masonry-like vaults informed by structural and fabrication constraints,” *block.arch.ethz.ch*.

[133] P. Block, T. Van Mele, A. Liew, M. DeJong, D. Escobedo, and J. Ochsendorf, “Structural design, fabrication and construction of the Armadillo vault,” *Struct. Eng.*, vol. 96, no. 5, pp. 10–20, 2018.

[134] D. V. Oliveira, P. B. Lourenço, and C. Lemos, “Geometric issues and ultimate load capacity of masonry arch bridges from the northwest Iberian Peninsula,” *Engineering structures*, no.32, vol. 12, pp.3955-65, 2010.

[135] M. Angelillo and A. Fortunato, “Equilibrium of Masonry Vaults,” *Novel Approaches in civil engineering*, Springer, 2004, pp. 105–111.

[136] G. Milani and P. B. Lourenço, "3D non-linear behavior of masonry arch bridges," *Comput. Struct.*, vol. 110–111, pp. 133–150, Nov. 2012.

[137] M. Como, "A static analysis of the Brunelleschi's Dome in Florence," in *Symposium of the International Association for Shell and Spatial Structures (50th. 2009. Valencia). Evolution and Trends in Design, Analysis and Construction of Shell and Spatial Structures : Proceedings.*, 2009, pp. 1661–1674.

[138] A. Giuffrè, *Letture sulla meccanica delle murature storiche*. Aracne Ed.,1991.

[139] L. Coppola, *Concretum*. McGraw-Hill, 2007.

[140] W. W. . Lau, "Equilibrium analysis of masonry domes," B.S., Civil Engineering Michigan State University, 2006.

[141] J. Heyman, "'Gothic' Construction in Ancient Greece," *J. Soc. Archit. Hist.*, vol. 31, no. 1, pp. 3–9, 1972.

[142] J. Zessin, W. Lau, and J. Ochsendorf, "Equilibrium of cracked masonry domes," *Proc. Inst. Civ. Eng. - Eng. Comput. Mech.*, vol. 163, no. 3, pp. 135–145, 2010.

[143] E. Çaktı, Ö. Saygılı, J. J. V. Lemos, C. S. Oliveira, C. O.-E. Structures, and undefined 2016, "Discrete element modeling of a scaled masonry structure and its validation," *Eng. Struct.*, vol. 126, pp. 224–236, 2016.

[144] D. L. Fang, "Assessing the stability of unreinforced masonry arches and vaults: a comparison of analytical and numerical strategies," *Int Juornal of Heritage*, 2018.

[145] W. David, *Lassaulx und der Gewölbebau mit selbsttragenden Mauerschichten: Neumittelalterliche Architektur um 1825-1848*. Verlag , Micheal Imhof, 2008.

[146] T. Bock, "Concept of building system for robotization," *Int. Symp. Autom. Robot. Constr.*, 1987.

[147] T. Bock and T. Linner, *Robotic Industrialization*. Cambridge University Press, 2015.

[148] J. N. Richardson, S. Adriaenssens, R. Filomeno Coelho, and P. Bouillard, "Coupled form-finding and grid optimization approach for single layer grid shells," *Eng. Struct.*, vol. 52, pp. 230–239, 2013.

[149] S. Adriaenssens, P. Block, D. Veenendaal, and C. Williams, *Shell structures for architecture: form finding and optimization*. 2014.

[150] D. Dragoni, *Antichità e Reiguardevolezza della venerabil compagnia della SS. Annunziata d'Arezzo, e della sua chiesa altrimenti detta dipoi di S. Maria delle Lagrime*. Nella stamperida di Gio: Batifta Secchi, 1759.

[151] A. Schiavo, "Documentazione. La Madonna di San Biagio a Montepulciano (1518-45)," *Boll. del Cent. di Stud. di Stor. dell'Architettura*, vol. vi, pp. 33–50, 1952.

[152] F. Gurrieri and P. Mazzoni, *La Fortezza da Basso: un monumento per la città*. Ponte alle Grazie, 1990.

[153] J. Heyman, “Hemingbrough spire,” *Struct. repair Maint. Hist. Build. Gen. Stud. Mater. Anal.*, vol. 1, pp. 12–22, 1991.